MOBILE ROBOT GUIDANCE

A thesis presented to the faculty of the Graduate School of
Western Carolina University in partial fulfillment of the
requirements for the degree of Master of Science in Technology.

By

Oscar Gamez

Director: Dr. Paul Yanik
Associate Professor
School of Engineering and Technology

Committee Members: Dr. Martin Tanaka, School of Engineering and Technology
Dr. Peter Tay, School of Engineering and Technology
Dr. Ellen Sigler, Department of Psychology

July 2018

Quiciera didicar esta obra a mis padres.

ACKNOWLEDGEMENTS

I would like to acknowledge my fellow graduate students: Reza Farsad Asadi, Pranoy Kumar Singha Roy, Jairo Nevarez, Kaleb Frizzell, and Trevor Parrish. Your assistance is greatly appreciated. There are two individuals from the undergraduate Psychology major I would like to thank for their hard work and dedication, Jordan Privette, and Sara Young. I would also like to show gratitude towards my thesis advisor Dr. Paul Yanik and my committee members: Dr. Peter Tay, Dr. Martin Tanaka, and Dr. Ellen Sigler for being instrumental in the completion of this endeavor.

TABLE OF CONTENTS

LIST OF TABLES

LIST OF FIGURES

ABSTRACT

MOBILE ROBOT GUIDANCE

Oscar Gamez, M.S.T.

Western Carolina University (July 2018)

Director: Dr. Paul Yanik

Assistive robotics is an increasingly growing field that has many applications. In an assisted living setting, there may be instances in which patients experience compromised mobility, and are therefore left either temporarily or permanently restricted to wheelchairs or beds. The utilization of assistive robotics in these settings could revolutionize treatment for immobile individuals by promoting effective patient-environment interaction and increase the independence and overall morale of affected individuals.

Currently, there are two primary classes of assistive robots: service robots, and social robots. Service robots assist with tasks that individuals would normally complete themselves, but are unable to complete due to impairment or temporary restriction. Assistive social robots include companion robots, which stimulate mental activity and, intellectually engages its users. Current service robots may have depth sensors and visual recognition software integrated into one self-contained unit. The depth sensors are used for obstacle avoidance. Vision systems may be used for many applications including obstacle avoidance, gesture recognition, or object recognition. Gestures may be used by the unit as commands to move in the indicated direction.

Assistive mobile robots have included devices such as laser pointers or vision systems to determine a user's object of interest and where it is located. Others have used video cameras for gesture recognition as stated above. Approaches to mobile robot guidance involving these devices may be difficult for individuals with impaired manual dexterity to use. If the individual is immobile, it would be difficult to operate the mentioned devices.

The objective of this research was to integrate a method that allowed the user to command a robotic agent to traverse to an object of interest by utilizing eye gaze. This approach allowed the individual to command the robot with eyesight through the use of a head-worn gaze tracking device. Once the object was recognized, the robot was given the coordinates retrieved from the gaze tracker. The unit then proceeded to the object of interest by utilizing multiple sensors to avoid obstacles.

In this research, the participant was asked to don an eye gaze tracker head worn device. The device gathered multiple points in the x, y, and z coordinate planes. MATLAB was used to determine the accuracy of the collected data, as well as the means to determine a set of x, y, and z coordinates needed as input for the mobile robot. After analyzing the results, it was determined that the eye gaze tracker could provide x and y coordinates that could be utilized as inputs for the mobile robot to get the object of interest. The z coordinate was determined to be unreliable as it would either be too short or overshoot from the object of interest.

CHAPTER 1: INTRODUCTION

1.1 Overview

Assisted living and hospital care share several common qualities. One commonality is that future residents in these settings will increase as the Baby Boom generation continues to come into the age of retirement. This means the need for caretakers will grow. With this in mind, consideration of the circumstances where an individual is confined to a chair or bed due to injury or disability is warranted. This situation can be difficult for the individuals as well as the caretakers. There may be times when individuals need assistance such as object retrieval, where the user may feel it is too bothersome to involve the caretaker. A proposed possible solution to this issue would utilize the eye gaze tracking device and a mobile robot. In the envisioned system, a person dons the eye gaze tracker and looks at an object of interest. The gaze tracker software will produce 3-Dimensional (3D) coordinates, which can be used as a goal point for the mobile robot. The robot will accept the 3D coordinates and proceed to the object of interest.

In this research, an autonomous mobile robot, which allows the manual input of coordinates gathered from a head worn eye gaze tracker was utilized. The collected data from the head worn device was filtered and verified to be within an acceptable range of the target object through a MATLAB script that outputs the coordinates. Ultrasonic sensors were used for obstacle avoidance.

1.2 Objective of the Study

For this research, the objective was to determine whether gaze data could be used to guide an assistive robot. The x, y, and z coordinates produced by an eye gaze head worn device were studied to see if they could be used to guide a mobile robot. This project involved the implementation of an autonomous robot and eye gaze tracking glasses.

1.3 Outline

This thesis is divided into six chapters. Chapter 2 is a review of literature pertaining to eye gaze tracking and assistive mobile robots. Chapter 3 presents the methodology which explains in more detail the experimentation conducted. Chapter 4 contains results from the robot test as well as the results from the gaze tracker. Chapter 5 is the Discussion where the validity, quality,and usefulness of the results are examined. Chapter 6 discusses future work and the conclusion.

CHAPTER 2: LITERATURE REVIEW

Assistive robotics is a field with increasing interest. This is due in part to robots being used to assist individuals in a multitude of settings. Current models can be categorized into three different sections: social, fixed based, and autonomous. Some assistive robots are used for therapy. Mataric [1] and Tapus [2] used a P2-DX by Mobile Robots to test patients' willingness to be around an autonomous unit. The results from the studies in [1] and [2] showed that the patients welcomed the autonomous device.

2.1 P3-DX

The Pioneer model P3-DX has been used in a variety of research environments. Espinosa *et al.* [3] had a 2009 P3-DX used for teleoperations. Do *et al.* [4] used voice commands to instruct a P3-DX to navigate to a location of interest. Gu *et al.* [5] the researchers explored a technique that used two laser pointers as a method to indicate the point of interest for a P3-DX.

2.2 Teleoperation and P3-DX

For the teleoperated P3-DX project, Espinosa *et al.* [3] chose to modify the P3-DX. They decided to upgrade their model since the hardware it came with was thought to be insufficient for their research purpose. The team added a VIA EPIA EN1500G mini-ITX motherboard as well as a WLI-TX4-G54HP wireless bridge (Ethernet Converter). With the modifications, the group was able to teleoperate the P3-DX. The results showed the difference with respect to the wired and wireless connection. The data demonstrated that during a local (wired) operation, the device has velocity. Also, the data showed that when the robot is teleoperated, and has a five percent packet dropout, the unit does not maintain its path.

2.3 Laser Pointer and P3-DX

There are many methods to control a mobile unit. Gu *et al.* [5] explored a method that used real-time localization for indoor service robots based on cameras and lasers. The researchers utilized an upward fisheye camera and secured it to the robot. Also, researchers had a red and green laser, which were utilized to flash a point onto the ceiling. The researchers placed the two points at an equal depth. They used a SICK 100 laser rangefinder and used it as ground truth for their method. The researchers had favorable results with localization accuracy.

2.4 Voice Command and P3-DX

Do *et al.* [4] experimented with voice recognition software and a P3-DX. Their experiment showed that it is possible to have a robot estimate the sound source position as well as recognize human speech. The researchers used Robot Operating System (ROS) as the interface for the robot and the sensors. For their auditory hardware researchers used a NI USB-9234 Data Acquisition (DAQ) and 4 NI G.R.A.S. IEPE microphones. Researchers used an open source audition software HARK for data collection. Their research showed that human and robot collaboration can facilitate non-voice recognition while maintaining human privacy.

2.5 Eye Gaze Tracking

Most techniques to perform eye gaze tracking utilize stereoscopic cameras. These methods typically use two cameras mounted on the autonomous unit. Atienza *et al.* [6–10] used the stereoscopic depth data and fixed world coordinates to perform real-time camera recalibration. Researchers used eye gaze and head pose to calculate gaze point, while the user is trying to move his fixation point on a monitor.

Gaze tracking can be accomplished by many methods. Nguyen *et al.* [11] used a three step approach. In the first step, they used an object detection method based on Haar-like features to detect the eye. Next, researchers used the Lucas-Kanade approach, which utilized

a set of pyramid representations to first detect the eye, and then track the eye. Finally the authors used a Gaussian process to find the function relationship between the eye of the user and the point on the screen where the user is looking. This method allowed the user to be free of any head wear. The problem, researchers concluded, was that it required the subject to be constantly stable or the predictions would be wrong.

Bulling *et al.* [12] looked at a variety of eye gaze glasses. The researchers observed a multitude of eye gaze trackers available in 2010. Some models they reviewed included the Mobile Eye by Applied Science Laboratories and iView X HED by SensoMotoric Instruments. Researchers described the possible uses for these devices to be multimodal interaction and eye-based context inference, as well as cognition-aware user interfaces.

Zhiwei Zhu and Qiang Ji [13] researched eye gaze tracking techniques under natural head movement. The researchers used one camera and one IR LED per eye to examine the glint. They tested seven participants that did not wear glasses. The work showed the accuracy in the x and y coordinates. The researchers collected data at five depths: 280 mm, 320 mm, 370 mm, 390 mm, and 440 mm. Their results for x were: 5.02 mm, 7.20 mm, 9.74 mm, 12.47 mm, 19.60 mm respectively. For y their results were: 6.40 mm, 6.93 mm, 13.24 mm, 17.30 mm, 24.32 mm respectively.

Lee *et al.* [14] researched 3D gaze tracking methods using Purkinje images on the optical eye model and the pupil. A Purkinje image is the illuminative reflection on the surface of the cornea. The researchers used one camera and one IR LED per eye to examine the glint. They tested 15 participants. The work showed the accuracy in the z coordinate. The researchers tested at five depths: 100 mm, 200 mm, 300 mm, 400 mm, and 500 mm. Their results for z were: 33 mm, 117 mm, 141 mm, 136 mm, 167 mm respectively.

2.6 Conclusion

Based on the research mentioned above, the P3-DX mobile unit is a very versatile research agent. This robotic platform can be programmed to travel autonomously and it can also be

fitted with multiple sensors such as SONAR, laser rangefinder, and RGB cameras. Lasers and voice command have been used to give the P3-DX a go-to-goal destination. For this research, eye gaze tracking was used as a mean to retrieve coordinates that were later used to indicate the go-to-goal destination. Eye gaze tracking was chosen as a novel format that could be a supportive device for assistive robotics. It can be a possible aid to individuals with limited manual dexterity as well as those temporarily or permanently restricted to a wheel chair or a bed.

CHAPTER 3: METHODOLOGY

3.1 Identification of Hardware and Software

For this research, the objective was to determine whether gaze data could be used to guide an assistive robot. To test for the objective a P3-DX Mobile Robot and the head worn tracking device, the Tobii Pro Glasses 2, were used. The tracking device was used to retrieve 3D coordinates for the object of interest. The mobile agent was used as a mean to get to the object of interest.

The Pioneer 3-DX (P3-DX), shown in Figure 3.1a, is a versatile research platform that has been designed for indoor use. It is a three-wheeled rugged robot equipped with 500-tick wheel encoders and front facing SONAR. The model available has eight ultrasonic sensors, a laser range finder, and a 7-axis Cyton robot arm. Figure 3.1b shows the robot's arm length when extended. It has the Mamba EBX-37 Dual Core 2.26 GHz motherboard integrated in the body of the robot. An 802.11 a/b/g Wi-Fi wireless adapter is also on board [15].

The P3-DX, shown in Figure 3.1a, also has an Inertial Measurement Unit (IMU) to correct for inaccuracies, such as wheel slippage. The ultrasonic (SONAR) sensors have a range from 152 mm to 4876 mm (approximately 6 inches to 16 feet) and are set to a left-to-right firing pattern. The laser range finder is a SICK LMS-100 with a range from 500 mm to 20000 mm (1 foot 8 inches to 65 feet). The Cyton robot arm is an Epsilon 300 with 7 degrees of freedom and a reach of 480 mm. It has a payload of 300 g (about 0.66 lbs) at full range and 350 g (about 0.77 lbs) at mid-range.

Advanced Robotics Interface for Applications (ARIA) is the language used to control the autonomous robot P3-DX. It is a C++ based language that also has object oriented capabilities. ARIA is the higher level language utilized to write the commands used by the P3-DX but it needs Linux or bash level viewer to run the compiled code. Geany, a GUI text

editor with basic IDE features, was utilized. This software allowed the C++ to be viewed, edited, and troubleshooted.

(a)

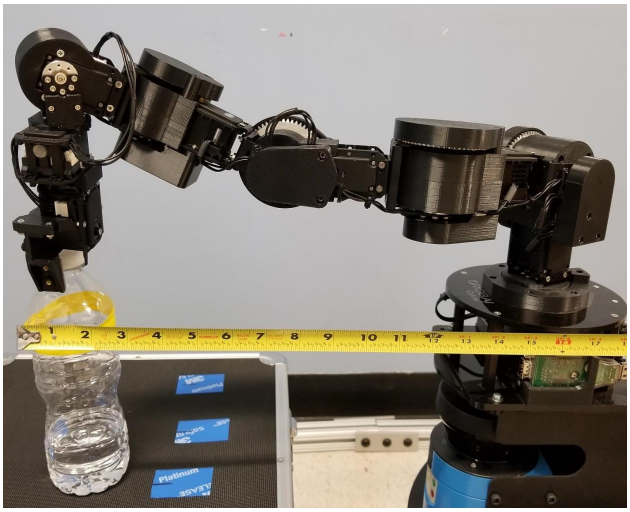

(b)

Figure 3.1: (a) P3-DX with LASER rangefinder and 7-axis Cyton robot arm (b) Extended robot arm

The Tobii Pro Glasses 2, seen in Figure 3.2, are eye gaze tracking devices capable of generating 3D gaze coordinates. The glasses have a full HD wide angle scene camera, microphone, gyroscope and accelerometer, and two cameras per eye. Tobii Pro Glasses Controller is the interface used to access the glasses' capabilities such as recording, calibrating, and live viewing. MATLAB R2015a, a high level programming language, was used to filter the collected data.

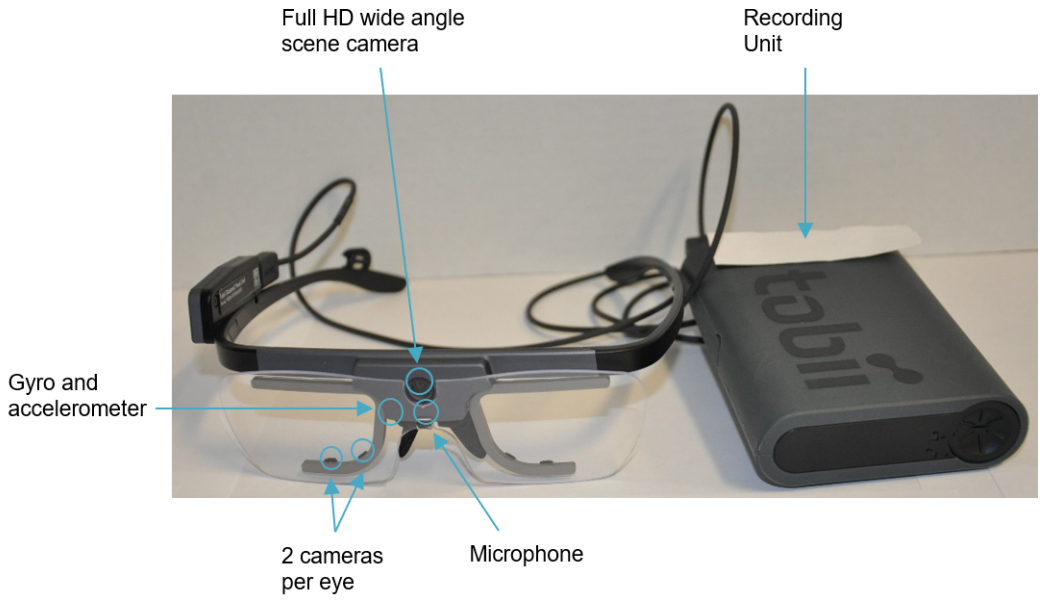

Figure 3.2: Tobii Pro Glasses 2

The head worn device has an HD camera, which samples the data at 50 Hz. This means it records 50 points per second. The participant was asked to keep their head still while looking at the target of interest for 10 seconds. The collected data for each coordinate was 500 samples. For this reason, the mean of the head-word device data was taken using equation (3.1) [16].

$$\mu = \frac{1}{N}\sum_{i=1}^{N} A_i \tag{3.1}$$

Where A is the variable vector, N is the number of scalar observations and μ is the average of the collected data. For this research, A is either the x, y, or z coordinates and N is the number of samples taken.

To test the precision of data along each axis the standard deviation of the collected data was taken. Equation (3.2) [17] was utilized to determine the precision.

$$S = \sqrt{\frac{1}{N-1}\sum_{i=1}^{N}|A_i - \mu|^2} \tag{3.2}$$

In this equation, S is the standard deviation which equals the square root of the variance and μ is the mean of A_i. The remaining variable N is the number of samples taken.

To test the collected data for each plane, a box and whisker plot was generated for each participant. To test the accuracy of the depth values, an ellipse and straight line path plot was generated. The ellipse is a visual representation of when the target is within two standard deviations of the mean. Equations (3.3 and 3.4) were used to generate the x and y values needed to generate the ellipse for the ellipse and straight line path plots. To generate the x values, equation (3.3) was used and to generate the y values, equation (3.4) was used.

In (3.3), $Ellipse_x$ represents the generated x values needed to produce the ellipse, where S_x is the standard deviation for the x values needed to produce the radius in the x axis and μ_x is the mean of the x values needed to produce the center of the ellipse.

$$Ellipse_x = 2S_x * cos(\theta) + \mu_x \tag{3.3}$$

In (3.4), $Ellipse_z$ represents the generated z values needed to produce the ellipse, where S_z is the standard deviation for the z values needed to produce the radius in the z axis and μ_z is the mean of the z values needed to produce the center of the ellipse.

$$Ellipse_z = 2S_z * sin(\theta) + \mu_z \tag{3.4}$$

3.2 Experimental Setup and Description

For this research, the experiment was set up to test the accuracy of the 3D coordinates produced by the gaze tracker. To accomplish this task an Institutional Review Board(IRB) approval was obtained. An informed consent form was also generated. The consent form was reviewed and signed by every participant before testing. A space with dimensions (1981 mm $\times$ 2438 mm) was used. The space had few windows and was utilized to minimize the extra external light source. The participant was asked to sit in a chair and maintain a stationary posture for the duration of each depth test. There were three test depths, which are shown in Table 3.1. The participants were asked to stare at the object of interest. The object of interest was a water bottle. The water bottle had the following dimensions: radius 32 mm and height 203 mm. Figure 3.3 shows the x plane values and Figure 3.4 shows the y plane values. The bottle was centered on top of a box with dimensions (406 mm $\times$ 330 mm $\times$ 305 mm). Figure 3.5 shows the test scenario.

Table 3.1: Eye Gaze Tested Depths

Distance (mm)
1524
2134
3048

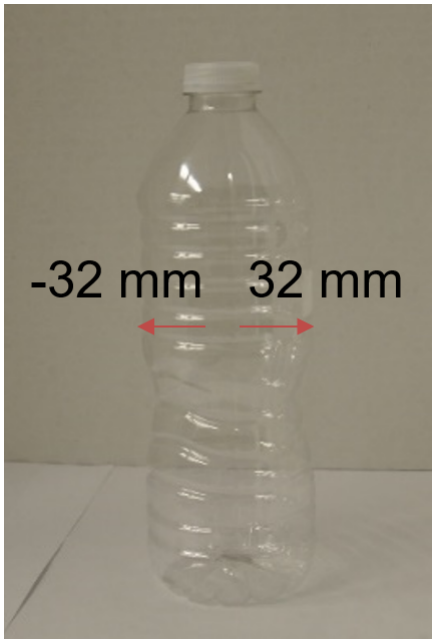

Figure 3.3: Radius for water bottle

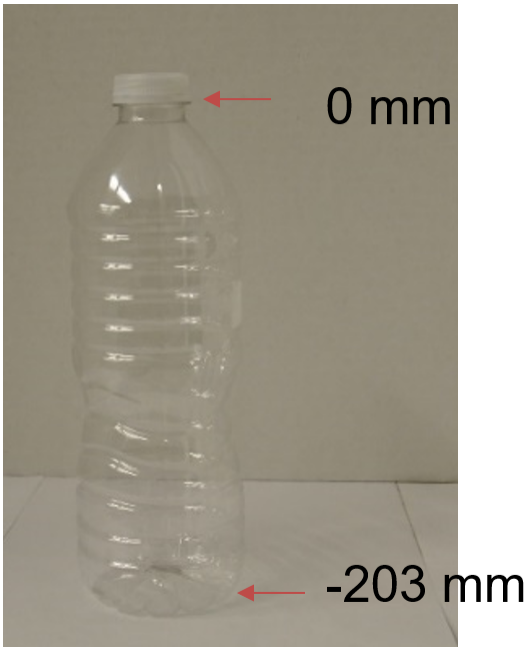

Figure 3.4: Height for water bottle

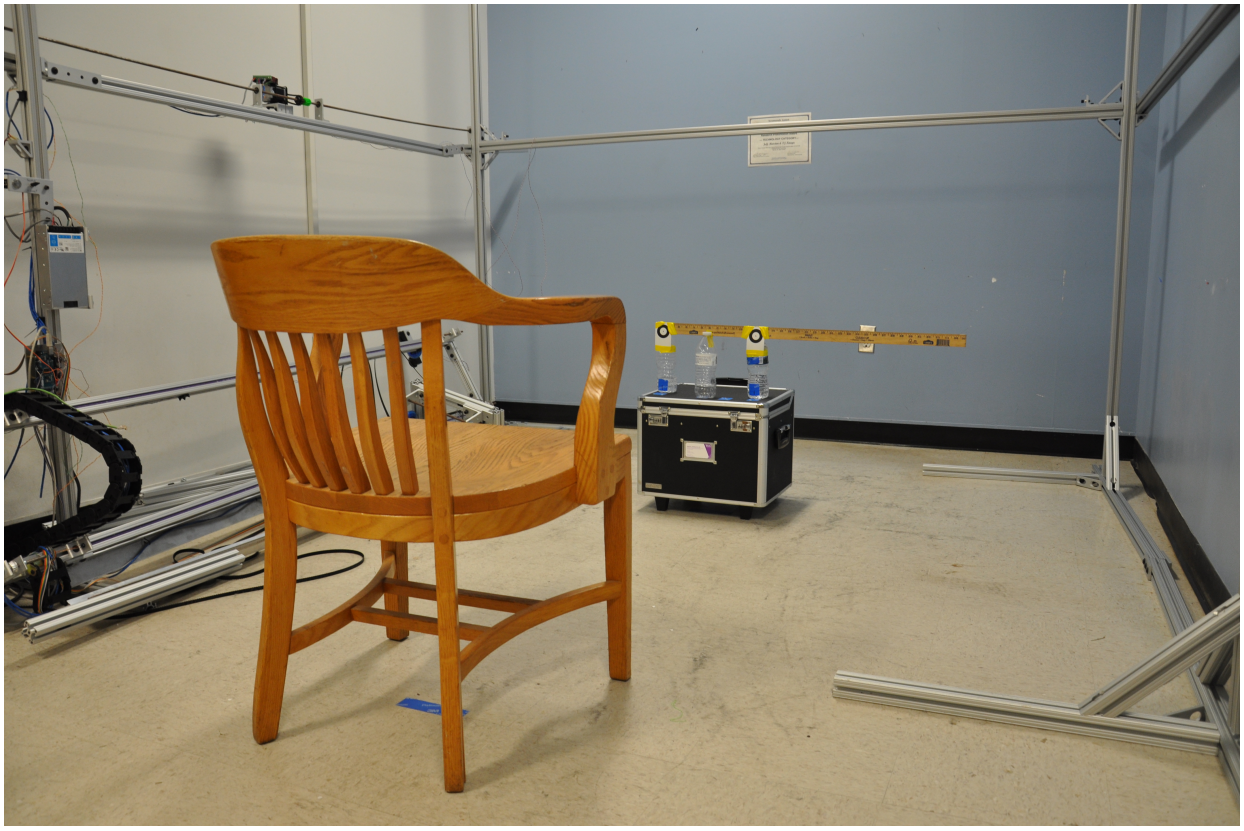

Figure 3.5: Eye Gaze tracking test setup

A yellow piece of electrical tape was placed at the center between both bottles at a distance of 153 mm from either bottle and a third bottle was placed behind the electrical tape. The third bottle was behind to give the participant a larger target to focus on during testing. Figure 3.6 shows how the assessment was taken and Figure 3.7 shows how a participant wears the gaze tracking device.

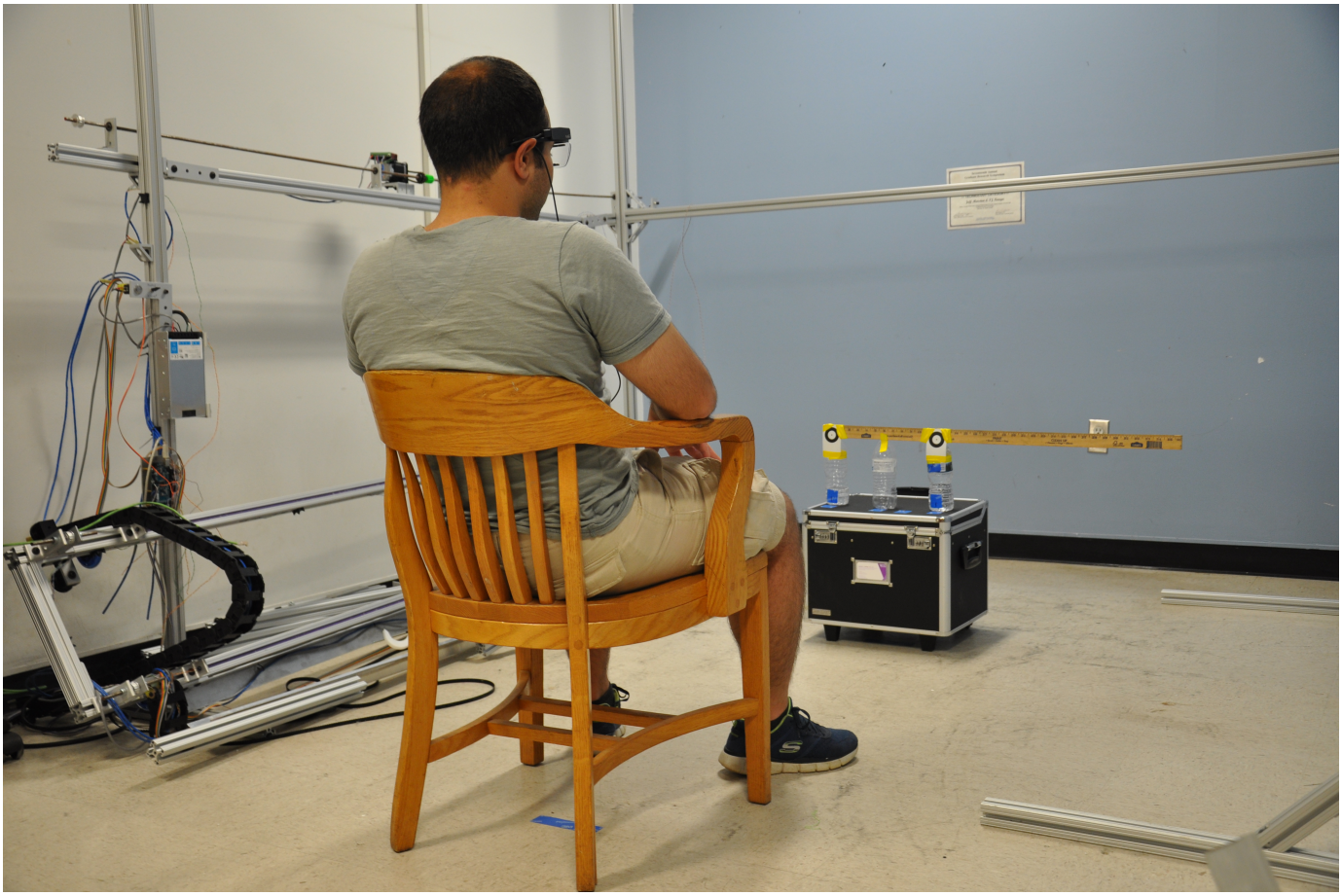

Figure 3.6: Eye Gaze tracking test

Figure 3.7: Eye Gaze tracking device donned

To process the collected data, first the folders, which are automatically generated by the Tobii controller software, are copied. The recordings folder was opened and then the segments folder which is inside the recordings folder. Folder number 1 is then opened. The livedata.json file is then selected and then using a compression application the files are extracted from the .json file. The .json file contians the coordinates in a compressed format. Once the .json file is extracted, an application developed by [18] is used. This software converts .json files into comma separated .txt files. After the files are converted they are imported into MATLAB. The combined x, y, and z data is then saved. The mean value for the x, y, and z coordinates is calculated for each participant by using (3.1). To test for accuracy an ellipse and straight line path was created, as well as a box and whisker plot.

To test the functionality of the developed algorithm the mobile unit was initially programmed to go to a goal that was straight ahead of it and without any obstacles. The mobile unit was tested at three different depths which were 1524 mm, 2134 mm, and 3048 mm. Figure 3.8 shows the initial programmed path. After completing the initial tests at the

three different depths the next step was to introduce obstacles. Obstacles were introduced at halfway points from the three mentioned tested depths. A box with dimensions (635 mm $\times$ 203 mm $\times$ 152 mm) was used as an obstacle. Figure 3.9 shows the box that was utilized as an obstacle.

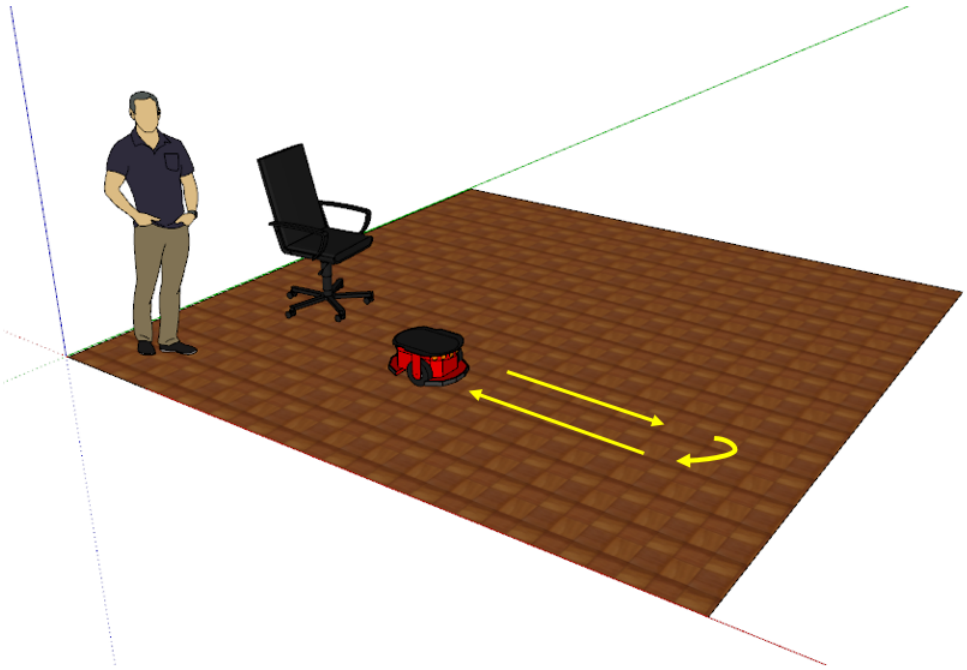

Figure 3.8: Initial setup for P3-DX

Figure 3.9: Obstacle used to test obstacle avoidance

The final test was to have the mobile robot go to the goal and avoid obstacles. This was accomplished by placing the robot at a marked location and then having it move to a target destination. The coordinates that were extracted from the Tobii Pro Glasses 2 where manually coded into the P3-DX. The target destination was set at different depths, which are displayed in 3.1. There was an obstacle placed halfway between the start and the end goal. This was completed for every distance in 3.1.

CHAPTER 4: RESULTS

In this chapter there are three sections. Each section contains two figures for each participant an ellipse and straight line path plot and a box and whisker plot. A table with the standard deviation of the x, y, and z coordinates was created to show the accuracy of each coordinate. As well as a table with the mean of the x, y, and z coordinates useful for trend analysis.

4.1 Results for 1524 mm testing

4.1.1 Ellipse and straight line path and box and whisker plots for testing at 1524 mm

In this section the data collected for seven participants at a distance of 1524 mm from the object of interest will be discussed. Figures 4.1a-4.7b show the results for each of the seven participants at 1524 mm.

Figure 4.1a shows a red dotted ellipse which encapsulates about 95 % of the collected data. The red dot in the center of the ellipse is the mean for the collected points. It can be noted that it is about 6 mm in the x axis. In this figure it can be seen that the data points follow the straight line path. This is an indication that participant maintained a steady poster and the glasses where donned correctly.

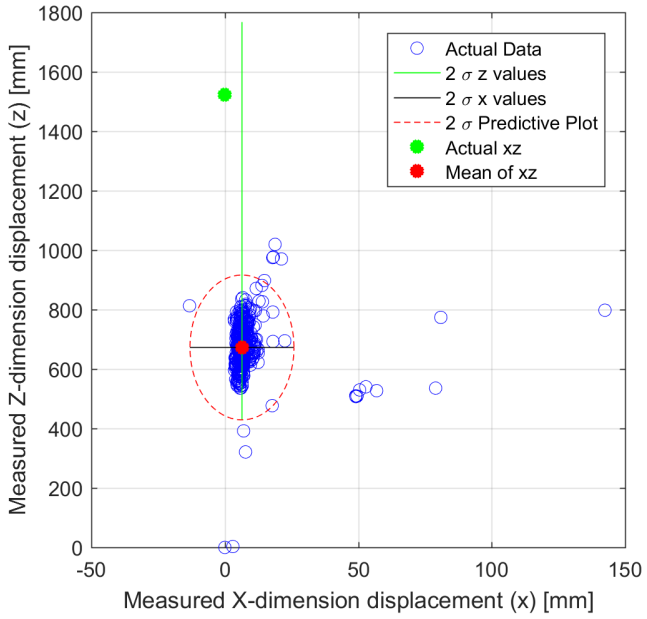

(a)

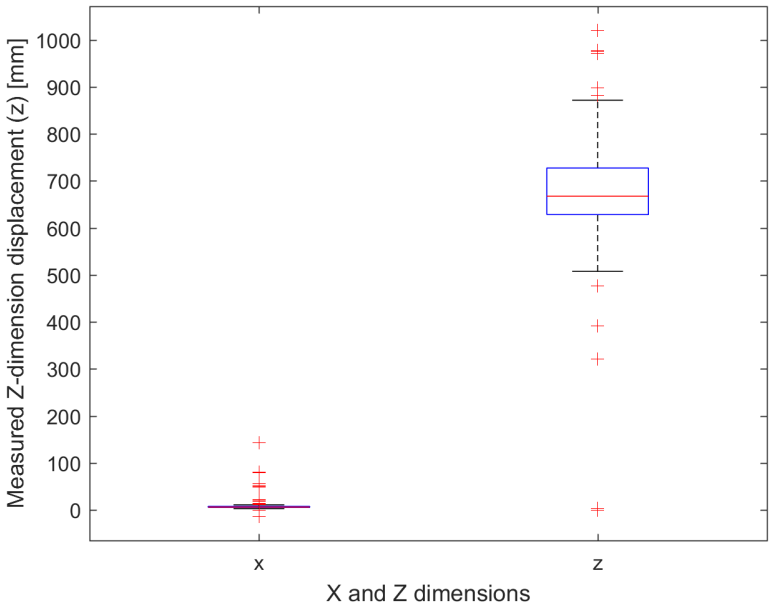

(b)

Figure 4.1: (a) Ellipse and straight line path for Participant 1 at 1524 mm. Here it can be seen that mean of the xz-coordinate is approximately 900 mm from the expected target. (b) Box and whisker plot for Participant 1 at 1524 mm from the object of interest. It can be noted that the x coordinate has very little variance while the z coordinate is approximately 900 mm from the point of interest correlating with the ellipse and straight line path.

Figure 4.2a shows the collected data in a tight grouping forming a slanted line. Now recall that the object of interest for all testing was located directly in front of the participant. In order to create a line that has a slant to the right, the glasses would have had to have been slightly tilted to the right. This could happen by having the chair slightly to left or the participant not seated centered. There is a small grouping outside the ellipse. It is considered an anomaly because it indicates the participant seeing something at about 15 meters. The spaced used for testing was only 1981 mm $\times$ 2438 mm. This could be caused by a the delay from pressing the stop record button and the transmission actually stopping.

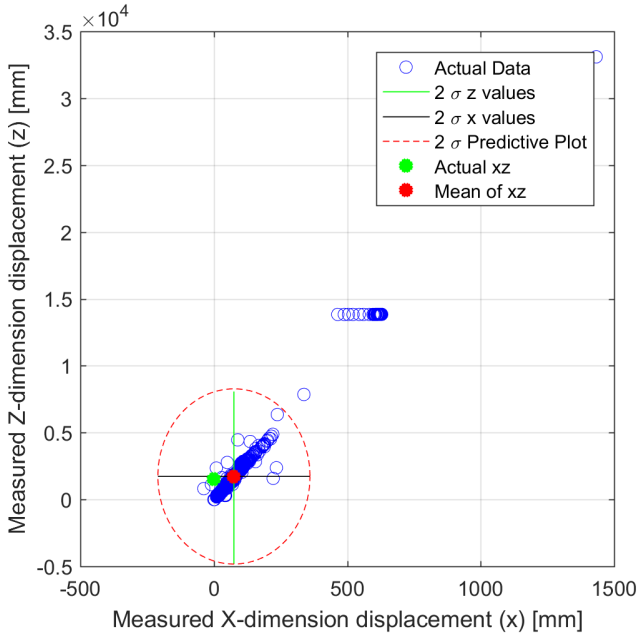

(a)

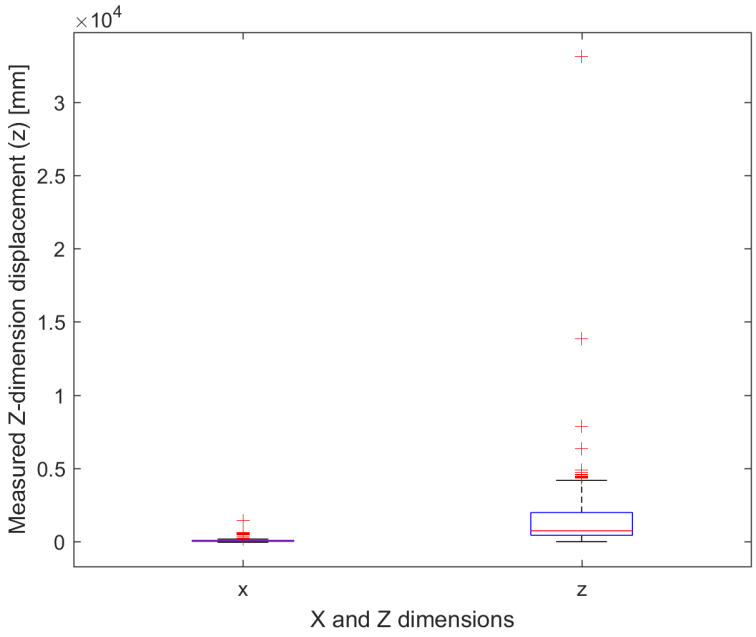

(b)

Figure 4.2: (a) Ellipse and straight line path for Participant 2 at 1524 mm. Here it can be seen that mean of the xz-coordinate is approximately next to the expected target. (b) Box and whisker plot for Participant 2 at 1524 mm from the object of interest. It can be noted that the x coordinate has very little variance while the z coordinate is approximately 2000 mm which would indicate an overshoot.

Figure 4.3a shows the collected data in an expanded grouping forming a cloud of points. The object of interest for all testing was located directly in front of the participant. If Figure A.3 in Appendix A shows the 3D rendering of what the participant was seeing. It shows a tight group of data wiggling in space. Considering both figures the cloud would be formed because y values are not present in the 2D plot.

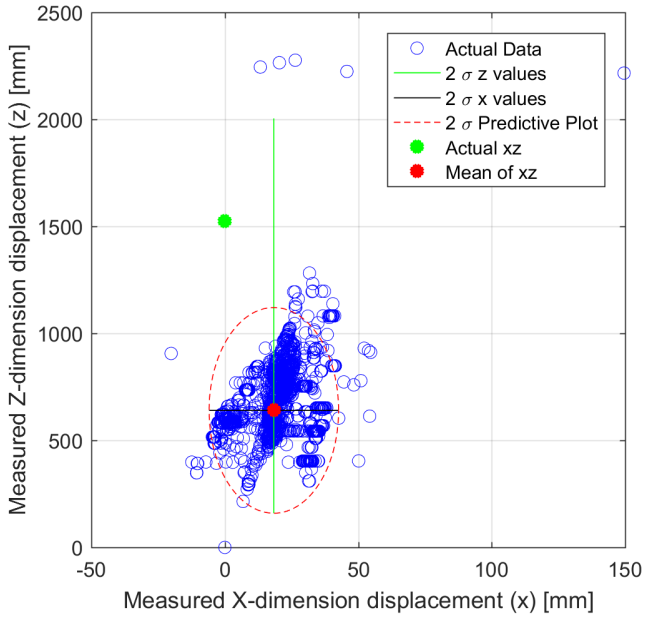

(a)

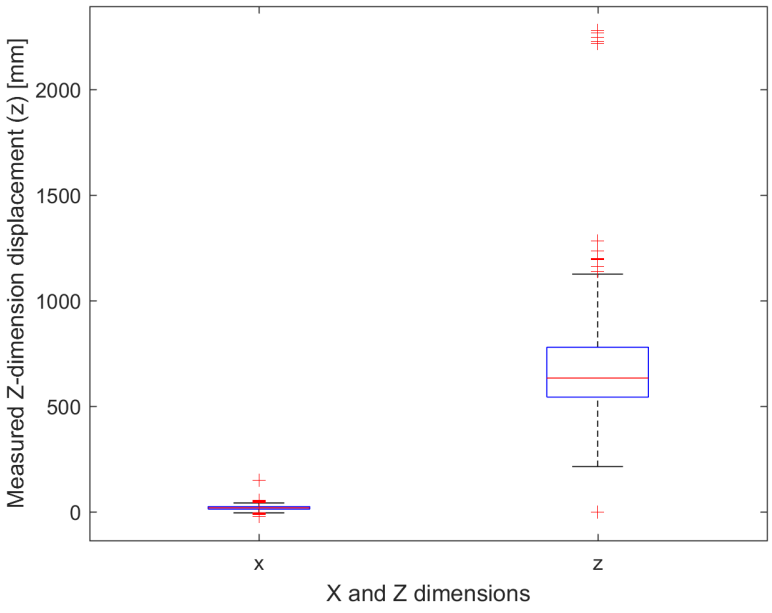

(b)

Figure 4.3: (a) Ellipse and straight line path for Participant 3 at 1524 mm. Here it can be seen that mean of the xz-coordinate is approximately 900 mm from the expected target in the z plane. (b) Box and whisker plot for Participant 3 at 1524 mm from the object of interest. It can be noted that the x coordinate has very little variance while the z coordinate is approximately 900 mm from the point of interest.

Figure 4.4a shows the collected data in a tight grouping forming a slanted line. In order to create a line that has a slant to the left the glasses would have been slightly tilted to the left. This could happen by having the chair slightly to the right or the participant not seated centered. There is a small grouping outside the ellipse. It is considered an anomaly because it indicates the participant seeing something at about 50 meters. The spaced used for testing was only 1981 mm $\times$ 2438 mm. This could be caused by a disturbance in the room.

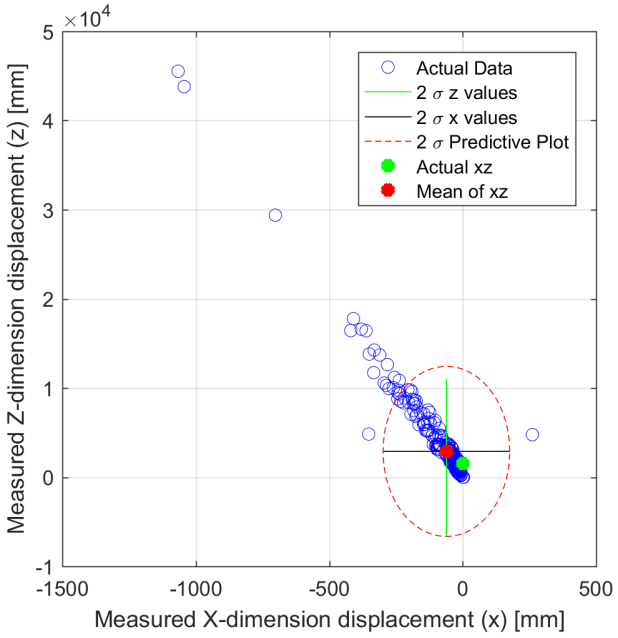

(a)

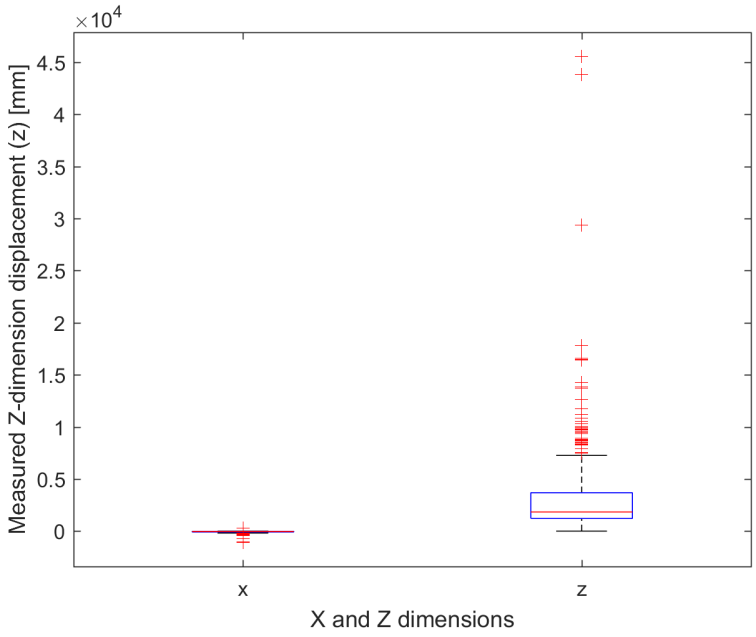

(b)

Figure 4.4: (a) Ellipse and straight line path for Participant 4 at 1524 mm. Here it can be seen that mean of the xz-coordinate is approximately 1500 mm from the expected target in the z plane. (b) Box and whisker plot for Participant 4 at 1524 mm from the object of interest. It can be noted that the x coordinate has very little variance while the z coordinate is approximately 1500 mm from the point of interest.

Figure 4.5a shows the collected data in tight grouping with a slight slant to the right. This could have been caused by either the participant or the chair not being centered with respect to the object of interest. The major anomaly is that the readings start at about 2 meters in the z axis. This could be caused by hardware error.

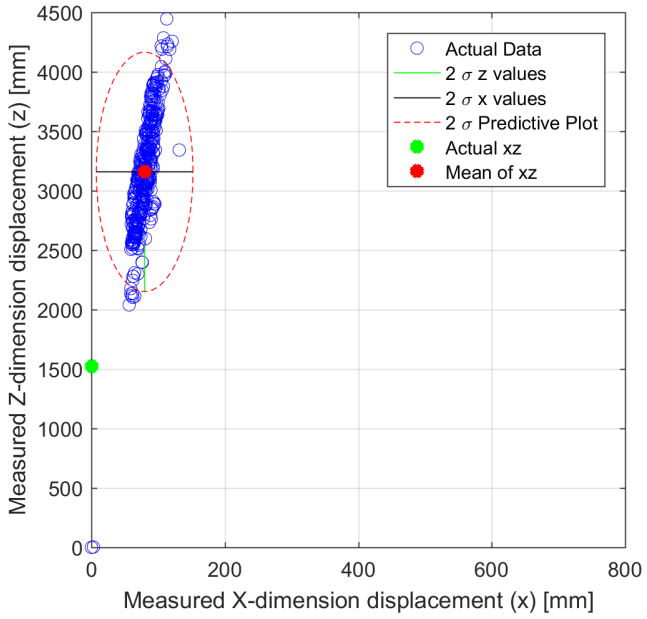

(a)

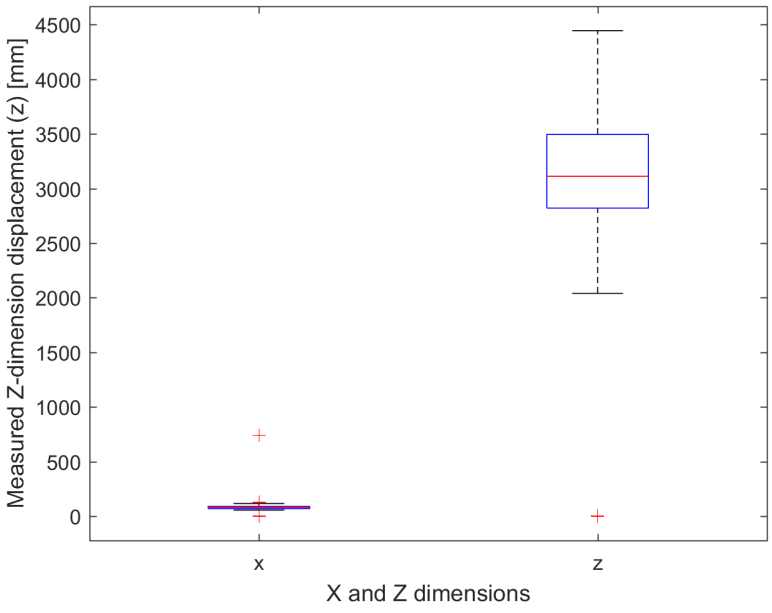

(b)

Figure 4.5: (a) Ellipse and straight line path for Participant 5 at 1524 mm. Here it can be seen that mean of the xz-coordinate is approximately 1500 mm from the expected target in the z plane. (b) Box and whisker plot for Participant 5 at 1524 mm from the object of interest. It can be noted that the x coordinate has very little variance while the z coordinate is approximately 1500 mm from the point of interest.

Figure 4.6a shows a red dotted ellipse which encapsulates about 95 % of the collected data. The red dot in the center of the ellipse is the mean for the collected points. It can be noted that it is about -6 mm in the x axis. In this figure it can be seen that the data points follow the straight line path. This is an indication that the participant maintained a steady posture and the glasses where donned correctly. Figure 4.6b shows that the x values had very little variance considering it shows a reading of about zero. The z values show the mean is about 700 mm. This is about 800 mm off from target. As mentioned before the use of another sensor such as a Kinect or a Lidar would allow for object recognition and possibly a better outcome.

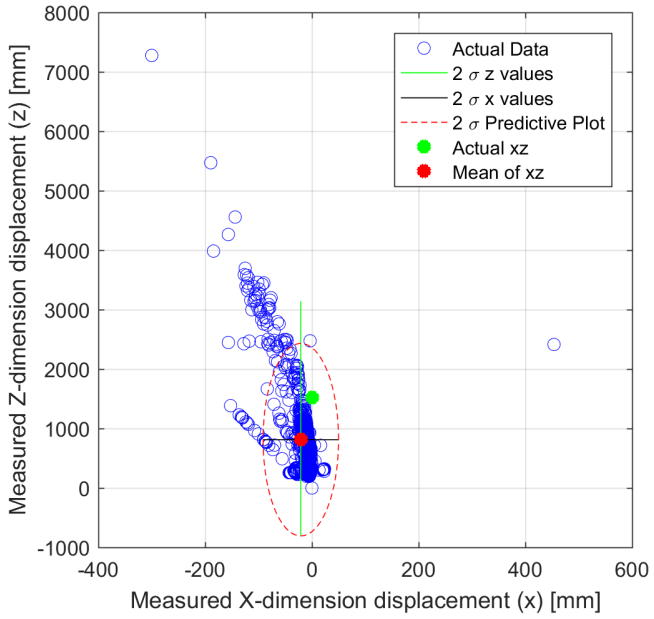

(a)

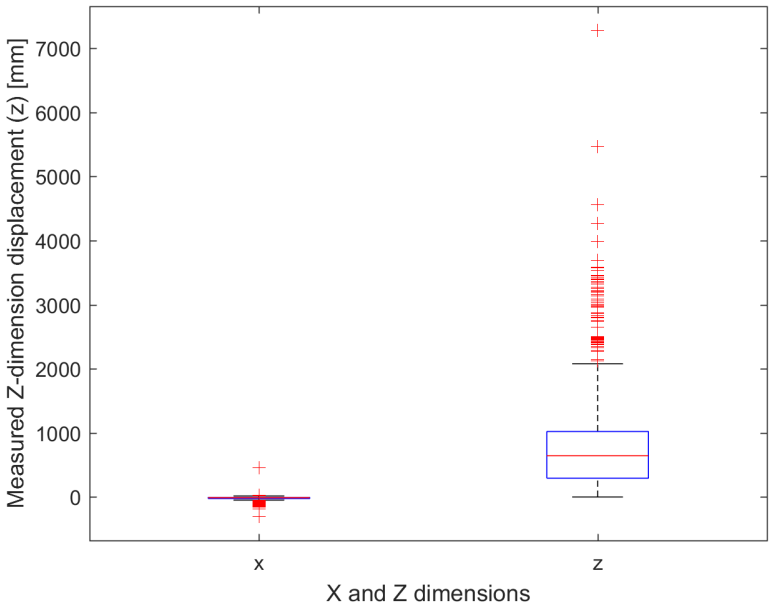

(b)

Figure 4.6: (a) Ellipse and straight line path for Participant 6 at 1524 mm. Here it can be seen that mean of the xz-coordinate is approximately 700 mm from the expected target in the z plane. (b) Box and whisker plot for Participant 6 at 1524 mm from the object of interest. It can be noted that the x coordinate has very little variance while the z coordinate is approximately 700 mm from the point of interest.

Figure 4.7a shows a red dotted ellipse which encapsulates about 95 % of the collected data. The red dot in the center of the ellipse is the mean for the collected points. It can be noted that it is about -10 mm in the x axis. In this figure it can be seen that the data points follow the straight line path. This is an indication that participant maintained a steady posture and the glasses where donned correctly. Figure 4.7b shows that the x values has very little variance as it shows a reading of about zero. The z values show the mean to be about 1100 mm. This is about 400 mm off from target. As mentioned before the use of another sensor such as a Kinect or a Lidar would allow for object recognition and possibly a better outcome.

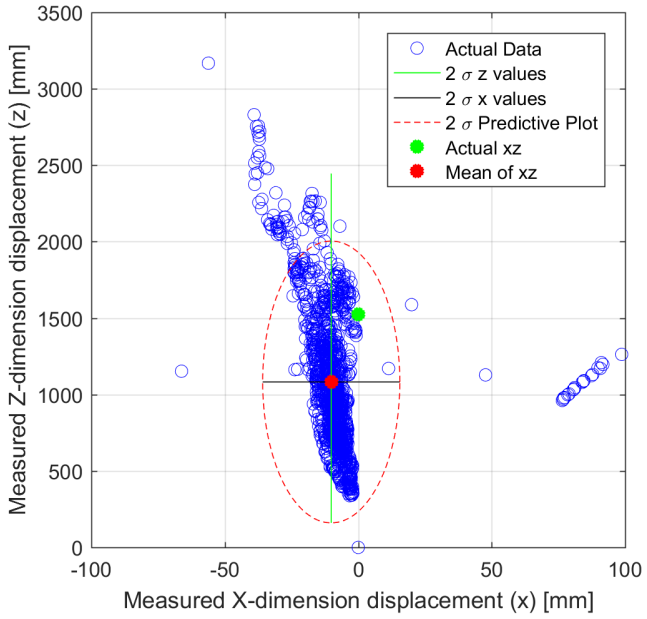

(a)

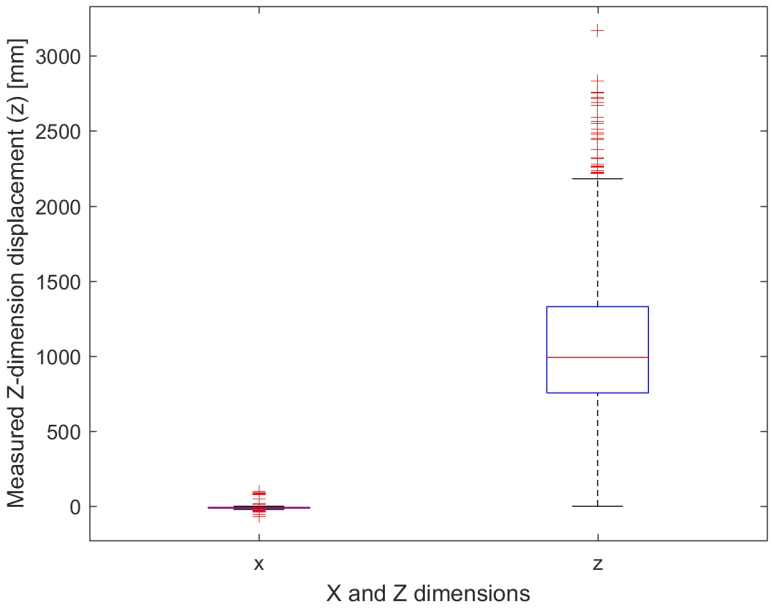

(b)

Figure 4.7: (a) Ellipse and straight line path for Participant 7 at 1524 mm. Here it can be seen that mean of the xz-coordinate is approximately 500 mm from the expected target in the z plane. (b) Box and whisker plot for Participant 7 at 1524 mm from the object of interest. It can be noted that the x coordinate has very little variance while the z coordinate is approximately 500 mm from the point of interest.

4.1.2 Tables for standard deviation and mean

The Tobii software yielded 3 coordinates for each participant. To test for precision the standard deviation of each coordinate plane for each participant was taken. Below are the results gathered from seven participants where the object of interest was at 1524 mm distance from the participant.

In Table 4.1, it can be noted that Participant 4 has a reading in the y-coordinate that is considered an anomaly. The standard deviation is 875 indicating the participant was looking at something with a different height than the object of interest. The 3D rendering Figure A.4 in Appendix A shows that the participant had their head tilted down and then looking up. This tilt appears to have caused the head worn device to show readings for and obstacle that is about 6 meters in the y axis and about 15 meters in the z axis.

Table 4.1: Standard deviation for data at 1524 mm

Participant	x-coordinate (mm)	y-coordinate (mm)	z-coordinate (mm)
1	2	5	70
2	124	249	2879
3	11	32	213
4	67	875	2524
5	11	21	401
6	26	158	706
7	9	80	435
Average	36	203	1033

The mean for the x coordinate is represented in Table 4.2. In this case the initial coordinates were expected to be zero. With the 3D parameters of the water bottle taken into consideration a -32 to 32 mm tolerance can be used. With the tolerance added to the mean it would allow a broader indication of the location of the object of interest.

Table 4.2: x-coordinate accuracy of object of interest at 1524 mm from participant

Participant	x mean (mm)	error after tolerance (mm)	% error after tolerance
1	6	0	0
2	75	43	134
3	18	0	0
4	-61	29	90
5	80	48	150
6	-21	0	0
7	-10	0	0
Global Average	39	17	54

The mean for the y coordinate is represented in Table 4.3. In this case the initial coordinates were expected to be zero. With the 3D parameters of the water bottle taken into consideration a 0 to -203 mm tolerance can be used. The tolerance would take in to account the height of the object of interest allowing for more retrieval points.

Table 4.3: y-coordinate accuracy of object of interest at 1524 mm from participant

Participant	y mean (mm)	error after tolerance (mm)	% error after tolerance
1	-9	0	0
2	-173	0	0
3	-97	0	0
4	976	774	381
5	-199	0	0
6	153	0	0
7	171	0	0
Global Average	254	110	54

For the z values shown in Table 4.4 the robotic arm shown in Figure 3.1b was taken into consideration. It has a length of 355 mm (14 in) as measured in the figure. With this consideration the results show some improvement.

Table 4.4: z-coordinate accuracy of object of interest at 1524 mm from participant

Participant	z mean (mm)	error after tolerance (mm)	% error after tolerance
1	673	496	33
2	1728	0	0
3	640	529	35
4	2898	1019	67
5	3159	1280	84
6	812	357	23
7	1082	87	6
Global Average	1571	614	40

4.2 Results for 2134 mm testing

4.2.1 Ellipse and straight line path and box and whisker plots and for testing at 2134 mm

Each section contains two figures for each participant. An ellipse and straight line path plot and a box and whisker plot. Figures 4.8a-4.14b show the results for each of the seven participants at 2134 mm. The ellipse and straight line path plot was chosen because it can display the collected data points within two standard deviations. The box and whisker plot was used because it provides a visual representation of the collected data points that are within one standard deviation.

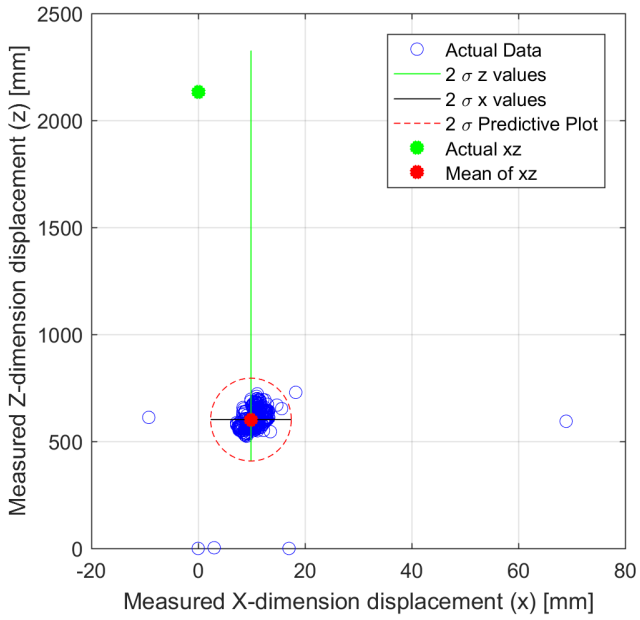

(a)

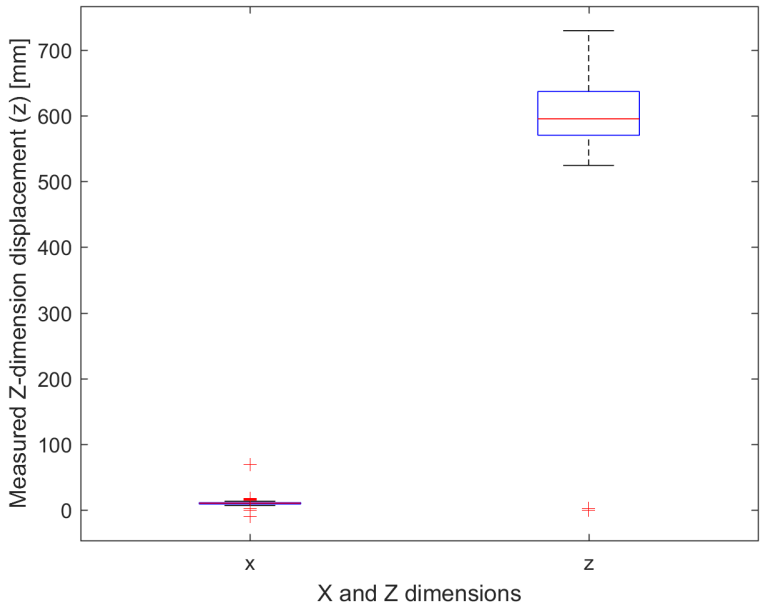

(b)

Figure 4.8: (a) Ellipse and straight line path for Participant 1 at 2134 mm. Here it can be seen that the mean of the xz-coordinate is approximately 1500 mm from the expected target in the z plane. (b) Box and whisker plot for Participant 1 at 2134 mm from the object of interest. It can be noted that the x coordinate has very little variance while the z coordinate is approximately 1500 mm from the point of interest.

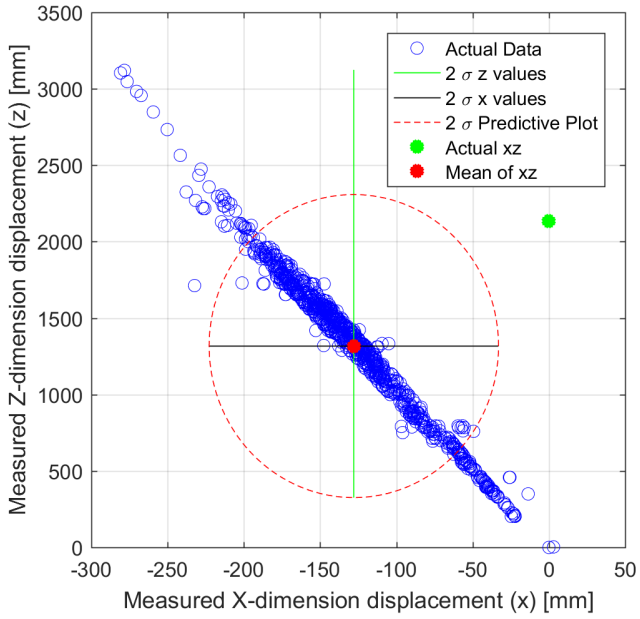

(a)

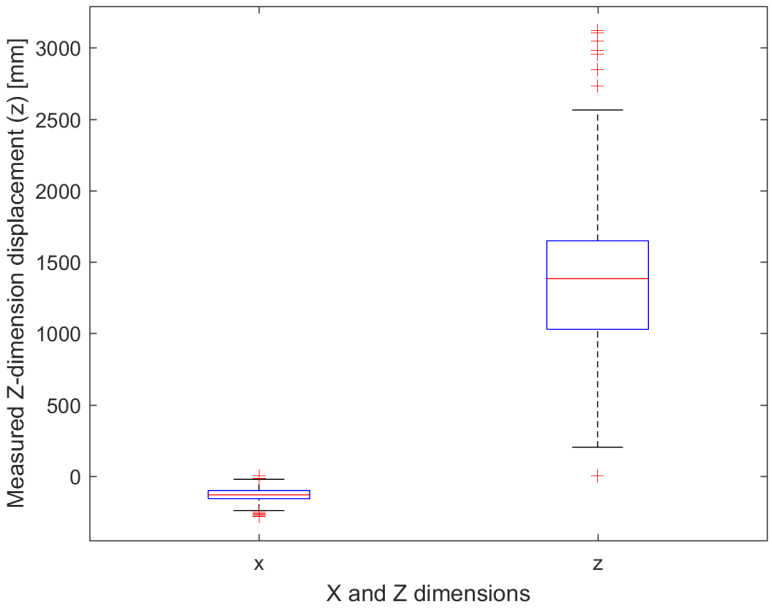

(b)

Figure 4.9: (a) Ellipse and straight line path for Participant 2 at 2134 mm. Here it can be seen that the mean of the xz-coordinate is approximately 800 mm from the expected target in the z plane. (b) Box and whisker plot for Participant 2 at 2134 mm from the object of interest. It can be noted that the x coordinate has very little variance while the z coordinate is approximately 800 mm from the point of interest.

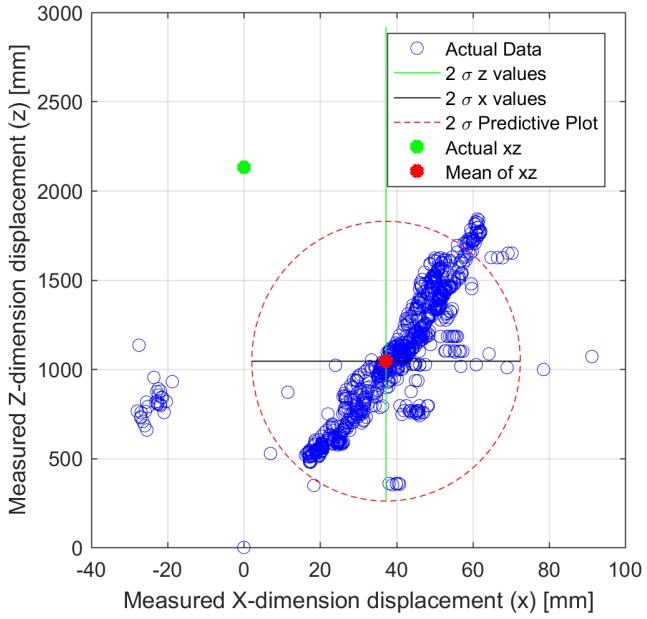

(a)

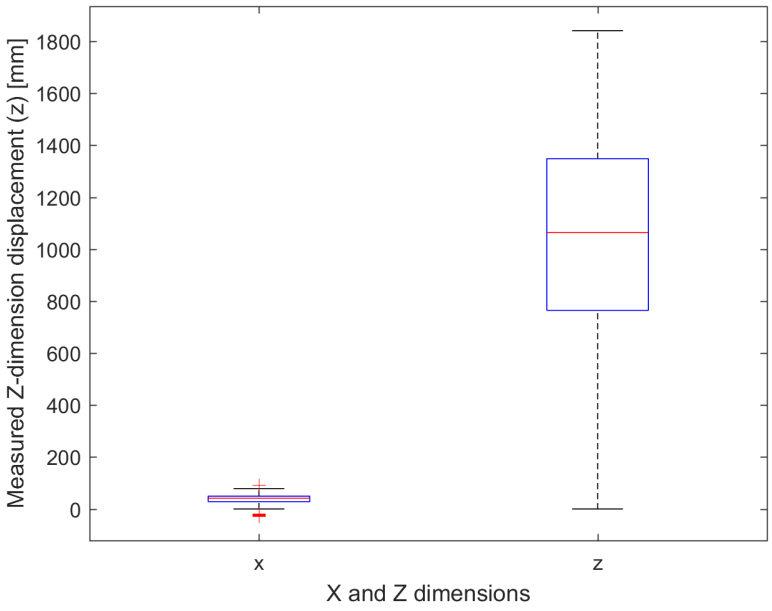

(b)

Figure 4.10: (a) Ellipse and straight line path for Participant 3 at 2134 mm. Here it can be seen that the mean of the xz-coordinate is approximately 1100 mm from the expected target in the z plane. (b) Box and whisker plot for Participant 3 at 2134 mm from the object of interest. It can be noted that the x coordinate has very little variance while the z coordinate is approximately 1100 mm from the point of interest.

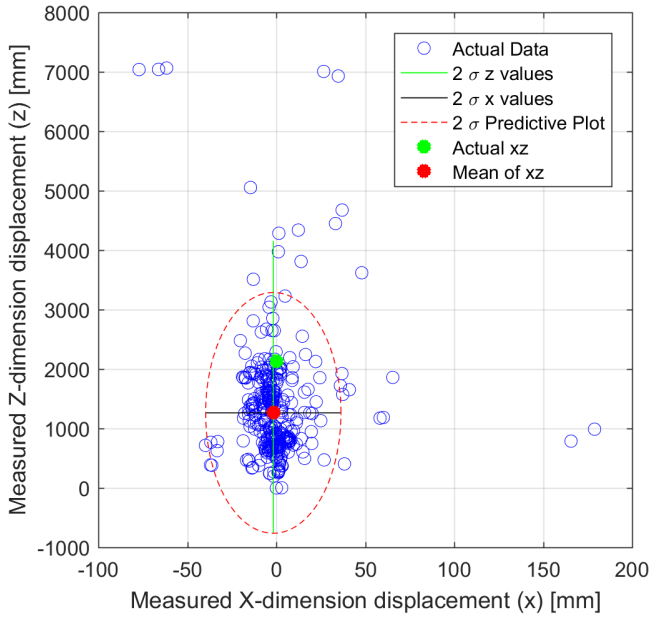

(a)

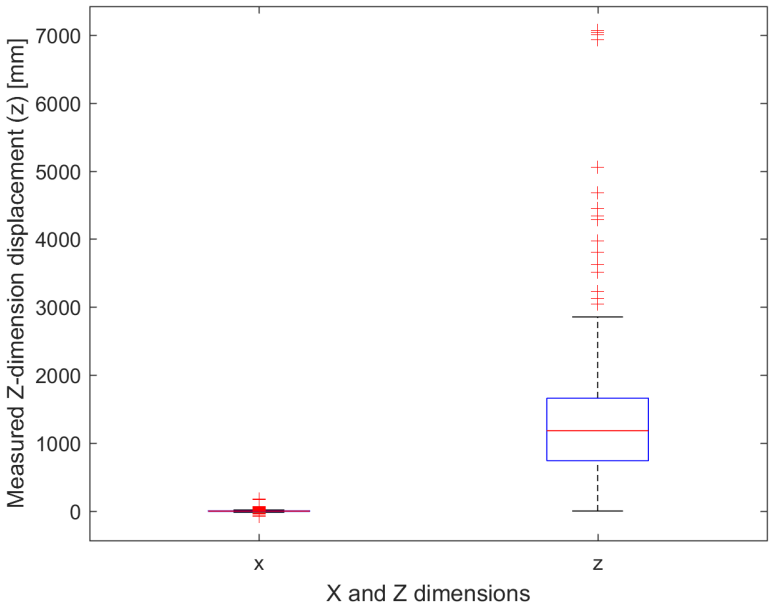

(b)

Figure 4.11: (a) Ellipse and straight line path for Participant 4 at 2134 mm. Here it can be seen that the mean of the xz-coordinate is approximately 900 mm from the expected target in the z plane. (b) Box and whisker plot for Participant 4 at 2134 mm from the object of interest. It can be noted that the x coordinate has very little variance while the z coordinate is approximately 900 mm from the point of interest.

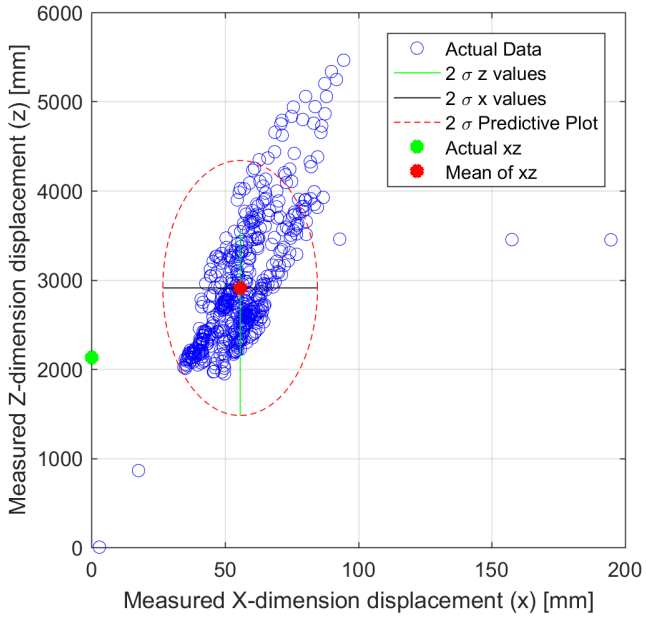

(a)

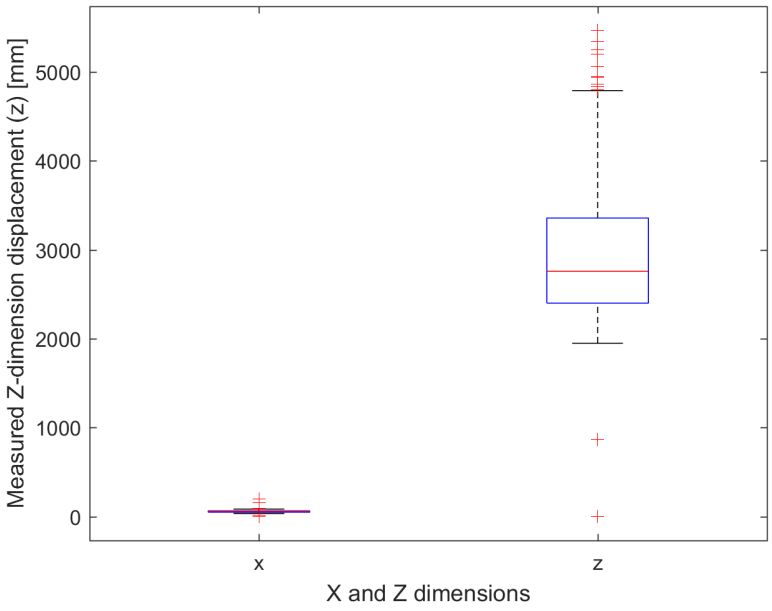

(b)

Figure 4.12: (a) Ellipse and straight line path for Participant 5 at 2134 mm. Here it can be seen that the mean of the xz-coordinate is approximately 800 mm from the expected target in the z plane. (b) Box and whisker plot for Participant 5 at 2134 mm from the object of interest. It can be noted that the x coordinate has very little variance while the z coordinate is approximately 800 mm from the point of interest.

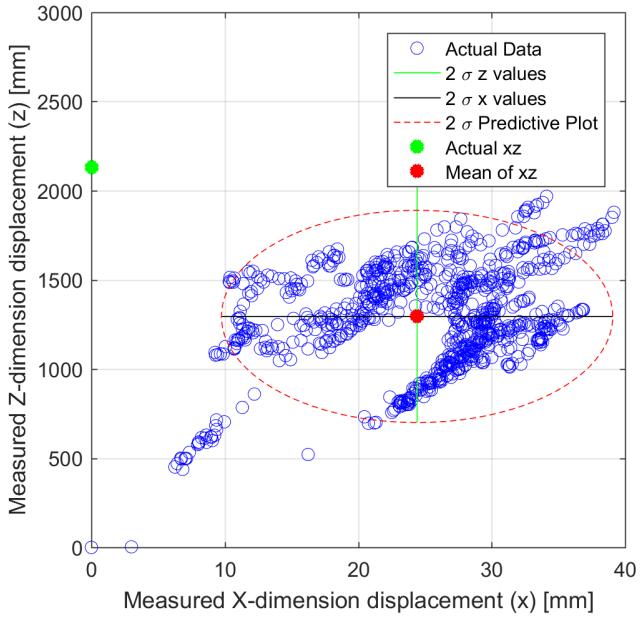

(a)

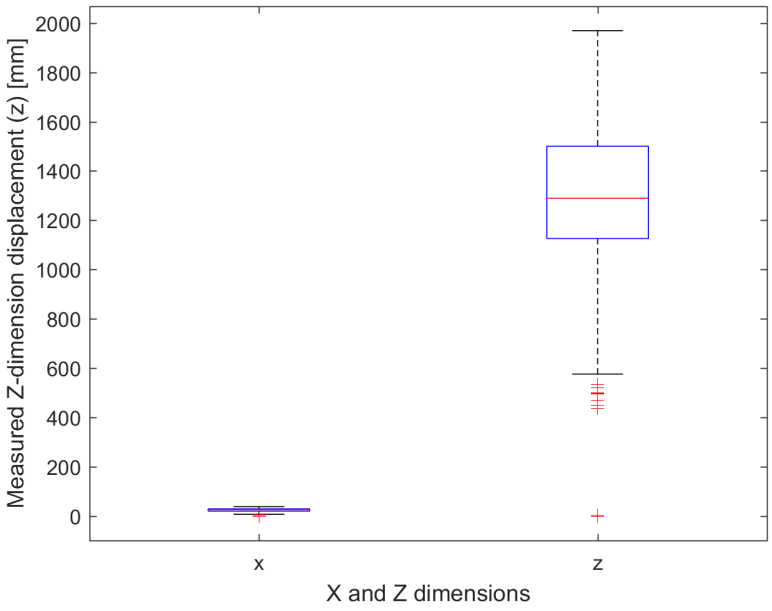

(b)

Figure 4.13: (a) Ellipse and straight line path for participant 6 at 2134 mm. Here it can be seen that mean of the xz-coordinate is approximately 900 mm from the expected target in the z plane. (b) Box and whisker plot for Participant 6 at 2134 mm from the object of interest. It can be noted that the x coordinate has very little variance while the z coordinate is approximately 900 mm from the point of interest.

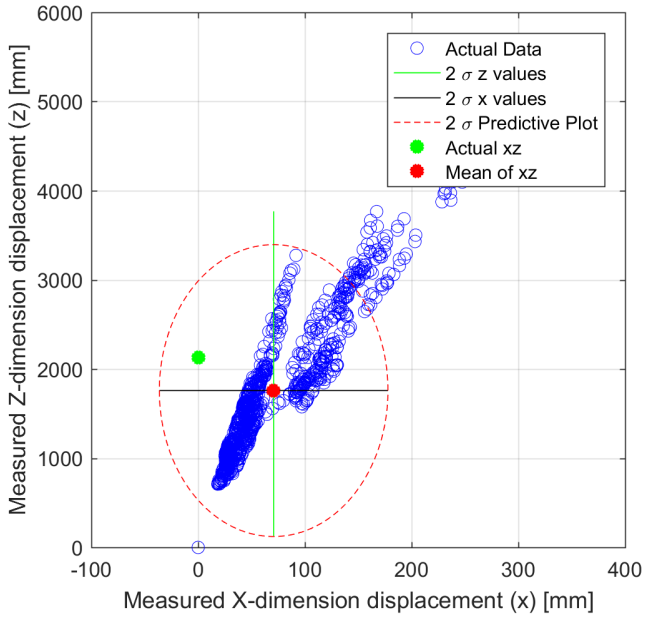

(a)

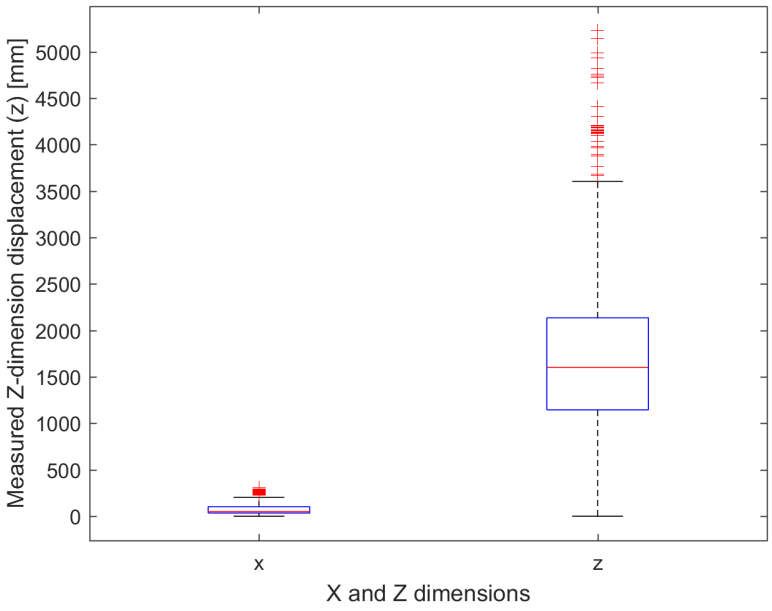

(b)

Figure 4.14: (a) Ellipse and straight line path for Participant 7 at 2134 mm. Here it can be seen that mean of the xz-coordinate is approximately 400 mm from the expected target in the z plane. (b) Box and whisker plot for Participant 7 at 2134 mm from the object of interest. It can be noted that the x coordinate has very little variance while the z coordinate is approximately 400 mm from the point of interest.

4.2.2 Tables for standard deviation and mean

The Tobii software yielded three coordinates for each participant. To test for precision the standard deviation of each coordinate plane for each participant was taken. Below are the results gathered from seven participants having the object of interest at 2134 mm from them.

In Table 4.5, it can be noted that Participant 4 has a reading in the y-coordinate that is considered an anomaly. The standard deviation is 186 mm indicating the participant was looking at something with a different height than the object of interest. The 3D rendering Figure A.11 in Appendix A shows that the participant had their head tilted down and then looking up. This tilt appears to have caused the head worn device to show readings for and obstacle that is about 500 mm in the y axis and about 4000 mm in the z axis..

Table 4.5: Standard deviation for data at 2134 mm

Participant	x-coordinate (mm)	y-coordinate (mm)	z-coordinate (mm)
1	1	5	39
2	43	29	453
3	16	29	372
4	9	186	639
5	11	10	625
6	6	33	268
7	49	120	755
Global Average	19	59	450

Table 4.6, shows the x mean for seven participants. The tolerance in this table is -32 mm to 32 mm. This tolerance comes from the radius of the object of interest. If the tolerance is taken into account it can be noted the robot would be able to arrive at expected goal.

Table 4.6: x-coordinate accuracy of object of interest at 2134 mm from participant

Participant	x mean (mm)	error after tolerance (mm)	% error after tolerance
1	10	0	0
2	128	96	300
3	37	5	17
4	-2	0	0
5	56	24	74
6	24	0	0
7	71	39	121
Global Average	46	23	73

As mentioned before the mean value for the y coordinate was generated. For this average the coordinates were gathered where the object of interest was 2134 mm from the participant. Table 4.7 shows the collected data. In this table the tolerance is 203 mm, which comes the height of the object of interest. If the tolerance is taken into consideration then it allows for more retrieval points.

Table 4.7: y-coordinate accuracy of object of interest at 2134 mm from participant

Participant	y mean (mm)	error after tolerance (mm)	% error after tolerance
1	2	0	0
2	63	0	0
3	97	0	0
4	331	128	63
5	92	0	0
6	139	0	0
7	303	100	49
Global Average	147	33	16

Table 4.8, shows the z mean for data collected at 2134 mm for seven participants. The tolerance in this table comes from the 7-axis robot arm (3.1b) which has a measured reach of about 355 mm. If the tolerance is taken into consideration then z error decreases and one value will be close to the expected target.

Table 4.8: z-coordinate accuracy of object of interest at 2134 mm from participant

Participant	z mean (mm)	error after tolerance (mm)	% error after tolerance
1	602	1177	77
2	1317	462	30
3	1044	735	48
4	1263	516	34
5	2910	421	28
6	1295	484	32
7	1759	20	1
Global Average	1456	632	41

4.3 Results for 3048 mm testing

4.3.1 Ellipse and straight line path and box and whisker plots for testing at 3048 mm

Each section contains two figures for each participant. An ellipse and straight line path plot and a box and whisker plot. Figures 4.15a-4.21b show results for each of the seven participants at 3048 mm. The ellipse and straight line path plot was chosen because it can display the collected data points within two standard deviations. The box and whisker plot was used because it provides a visual representation of the collected data points that are within one standard deviation.

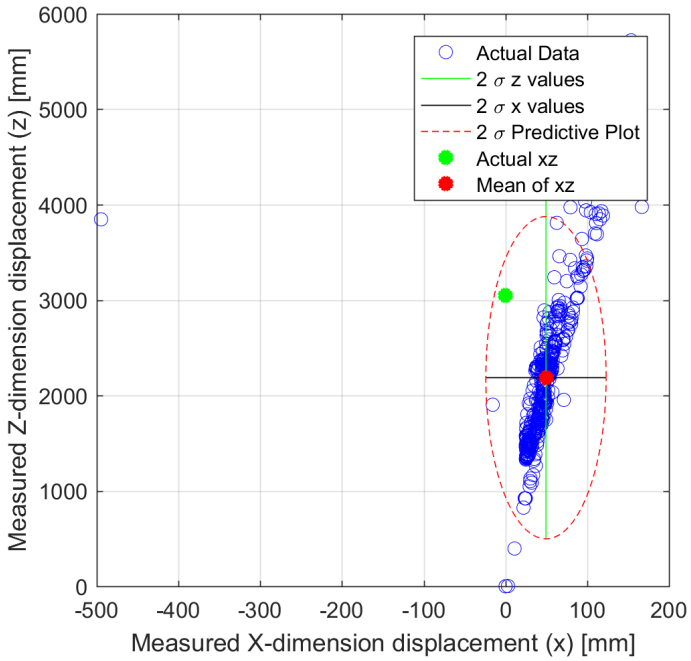

(a)

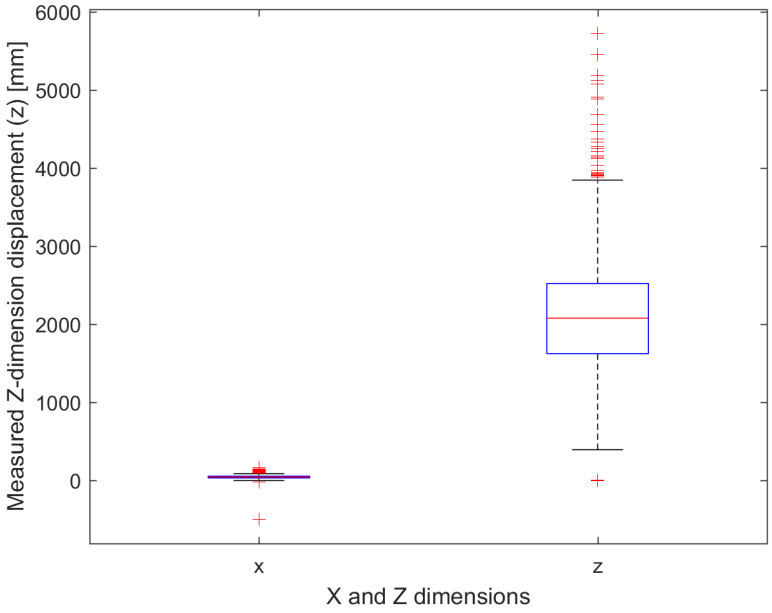

(b)

Figure 4.15: (a) Ellipse and straight line path for Participant 1 at 3048 mm. Here it can be seen that the mean of xz is approximately 900 mm from the expected target in the z plane. (b) Box and whisker plot for Participant 1 at 3048 mm from the object of interest. It can be noted that the x coordinate has very little variance while the z coordinate is approximately 900 mm from the point of interest.

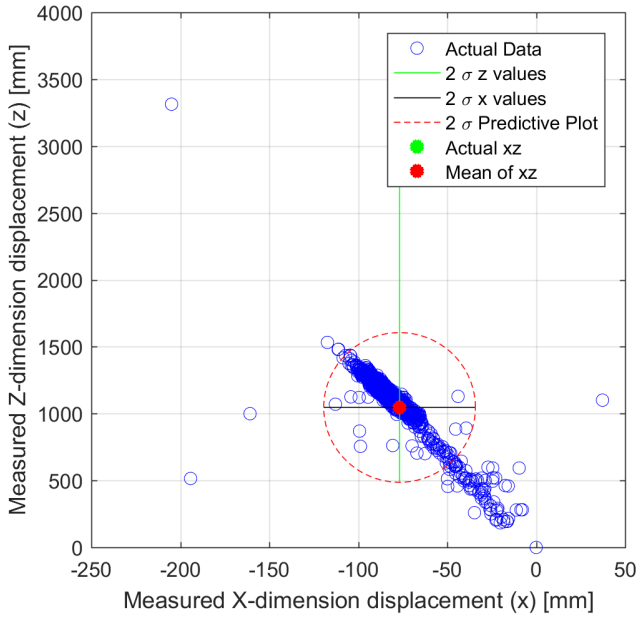

(a)

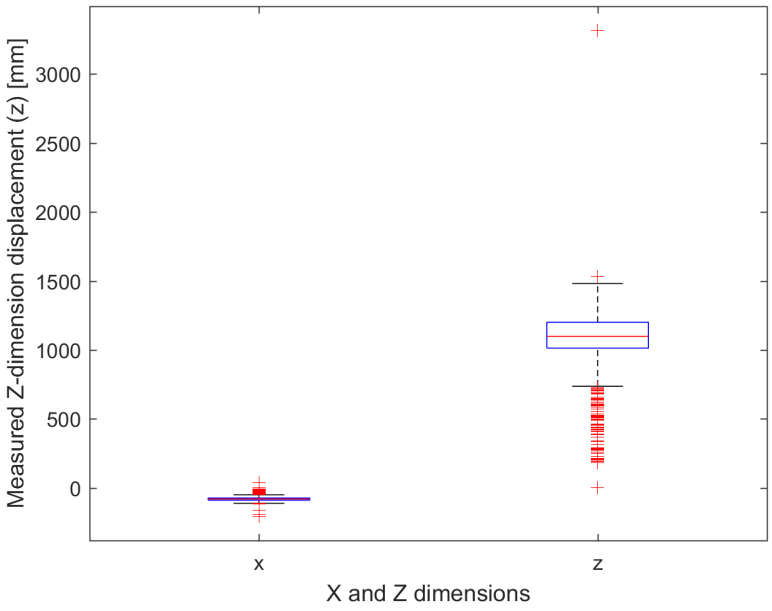

(b)

Figure 4.16: (a) Ellipse and straight line path for Participant 2 at 3048 mm. Here it can be seen that the mean of the xz-coordinate is approximately 2000 mm from the expected target in the z plane. (b) Box and whisker plot for Participant 2 at 3048 mm from the object of interest. It can be noted that the x coordinate has very little variance while the z coordinate is approximately 2000 mm from the point of interest.

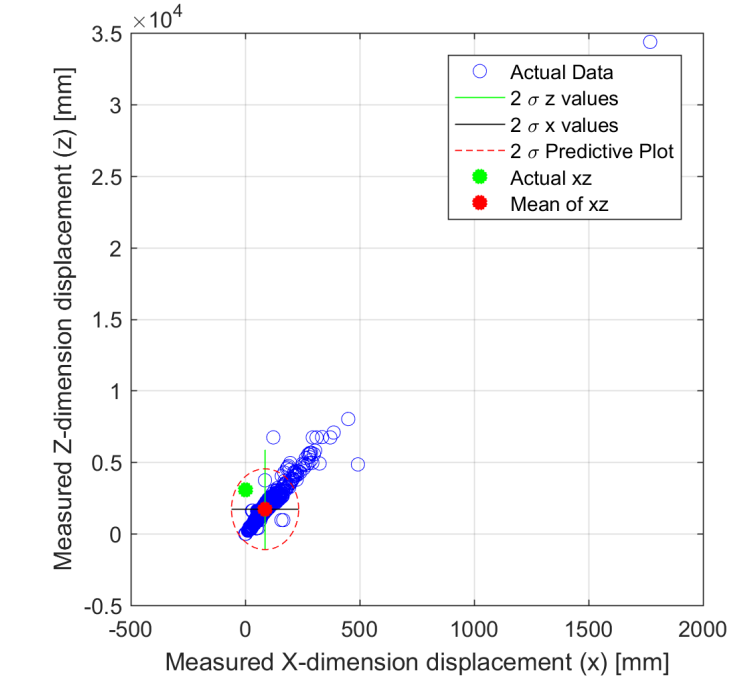

(a)

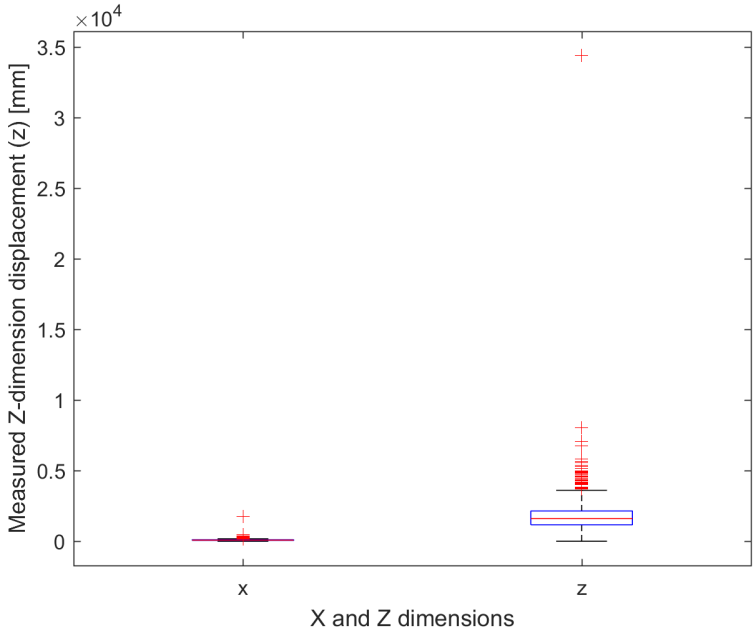

(b)

Figure 4.17: (a) Ellipse and straight line path for Participant 3 at 3048 mm. Here it can be seen that mean of the xz-coordinate is approximately 1300 mm from the expected target in the z plane. (b) Box and whisker plot for Participant 3 at 3048 mm from the object of interest. It can be noted that the x coordinate has very little variance while the z coordinate is approximately 1300 mm from the point of interest.

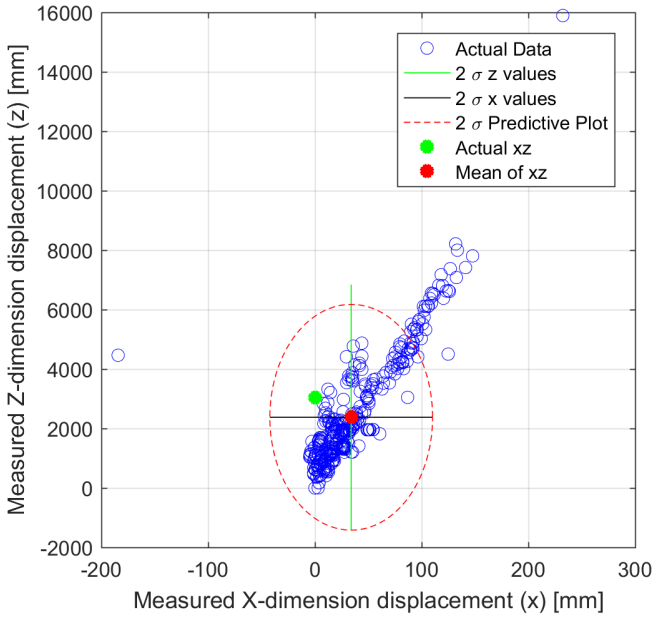

(a)

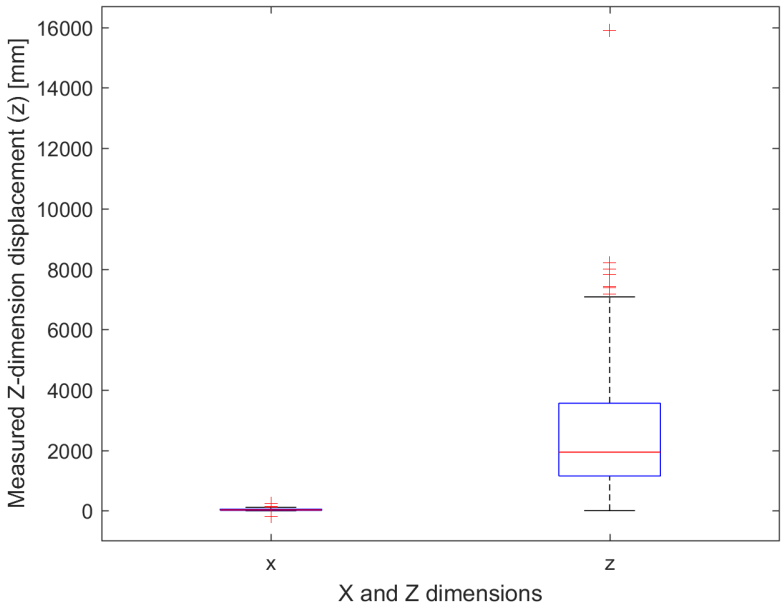

(b)

Figure 4.18: (a) Ellipse and straight line path for Participant 4 at 3048 mm. Here it can be seen that the mean of the xz-coordinate is approximately 2400 mm from the expected target in the z plane. (b) Box and whisker plot for Participant 4 at 3048 mm from the object of interest. It can be noted that the x coordinate has very little variance while the z coordinate is approximately 2400 mm from the point of interest.

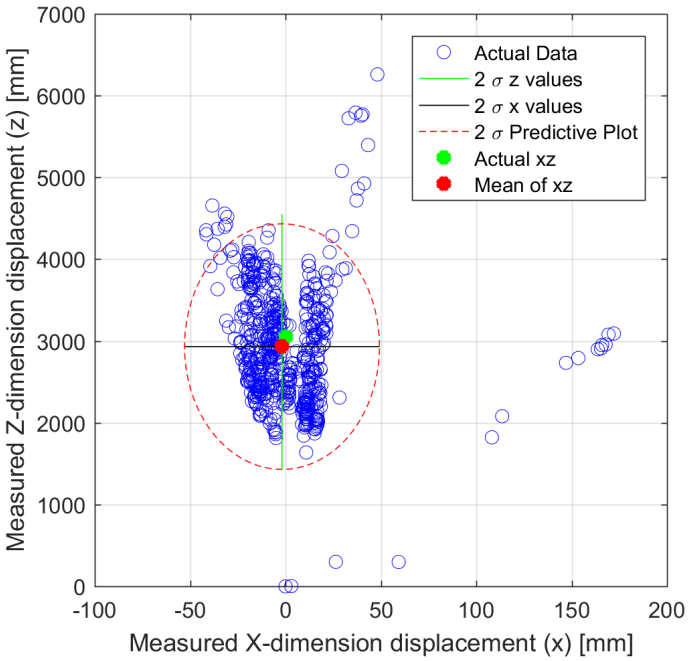

(a)

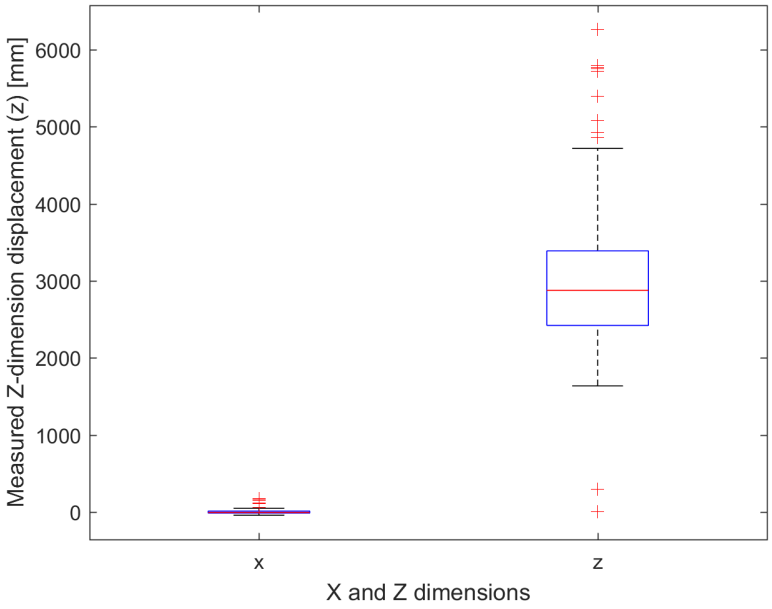

(b)

Figure 4.19: (a) Ellipse and straight line path for Participant 5 at 3048 mm. Here it can be seen that the mean of the xz-coordinate is approximately 1400 mm from the expected target in the z plane. (b) Box and whisker plot for Participant 5 at 3048 mm from the object of interest. It can be noted that the x coordinate has very little variance while the z coordinate is approximately 1400 mm from the point of interest.

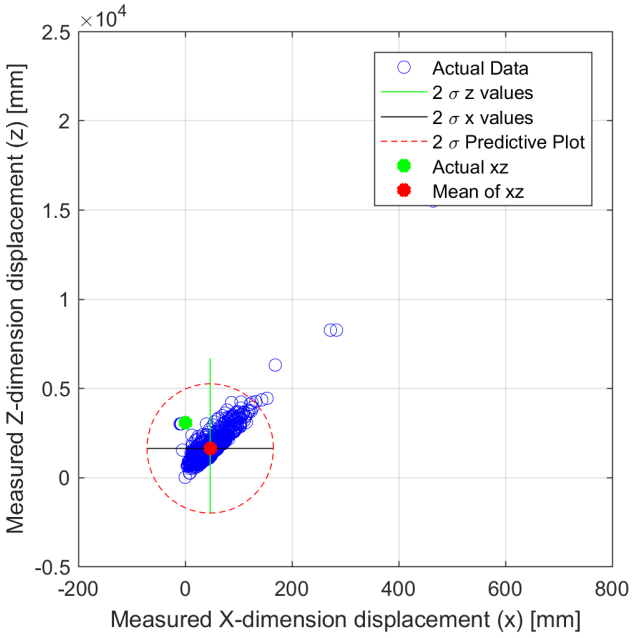

(a)

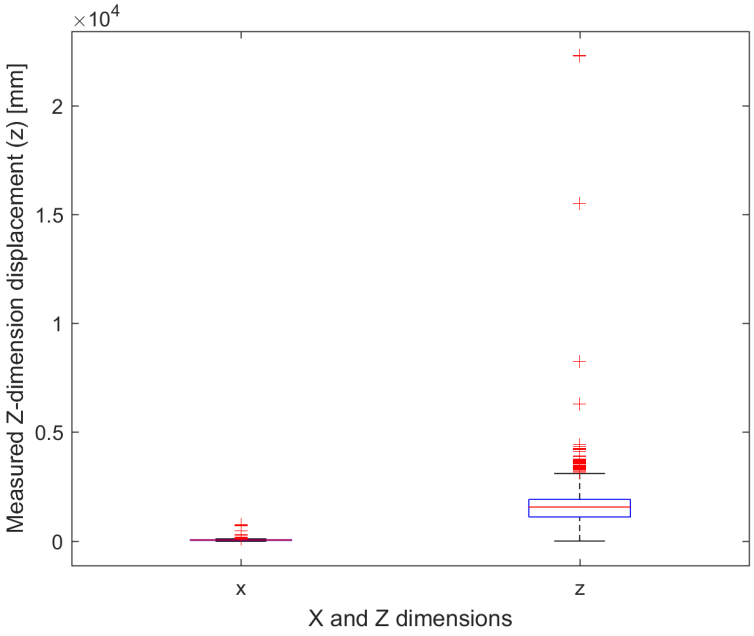

(b)

Figure 4.20: (a) Ellipse and straight line path for Participant 6 at 3048 mm. Here it can be seen that the mean of the xz-coordinate is approximately 100 mm from the expected target in the z plane. (b) Box and whisker plot for Participant 6 at 3048 mm from the object of interest. It can be noted that the x coordinate has very little variance while the z coordinate is approximately 100 mm from the point of interest.

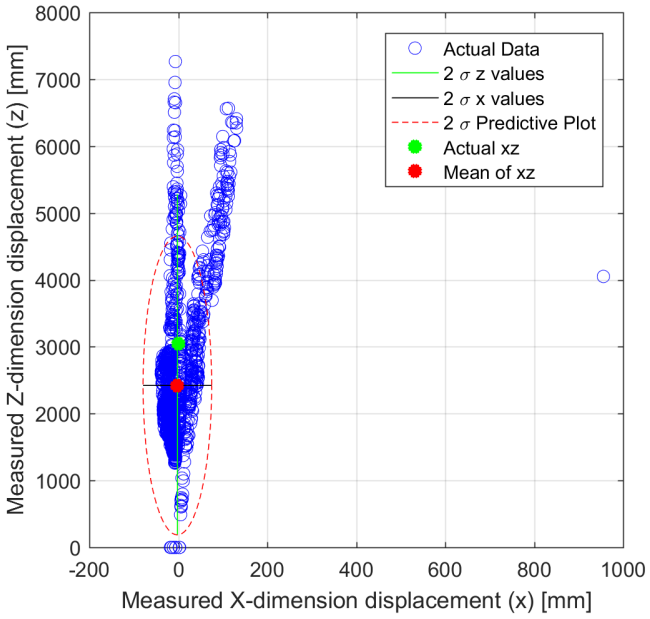

(a)

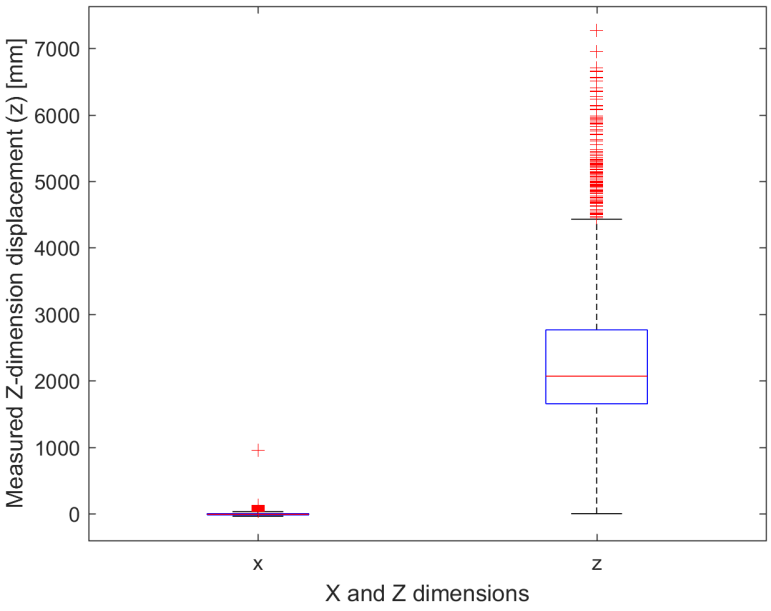

(b)

Figure 4.21: (a) Ellipse and straight line path for Participant 7 at 3048 mm. Here it can be seen that the mean of the xz-coordinate is approximately 600 mm from the expected target in the z plane. (b) Box and whisker plot for Participant 7 at 3048 mm from the object of interest. It can be noted that the x coordinate has very little variance while the z coordinate is approximately 600 mm from the point of interest.

4.3.2 Tables for standard deviation and mean

The Tobii software yielded three coordinates for each participant. To test for precision the standard deviation of each coordinate plane for each participant was taken. Below are the results gathered from seven participants 3048 mm from the object of interest.

In Table 4.9 it can be noted that Participant 4 had the most difficult time concentrating on the object of interest.

Table 4.9: Standard deviation for data at 3048 mm

Participant	x-coordinate (mm)	y-coordinate (mm)	z-coordinate (mm)
1	21	70	696
2	19	16	255
3	44	27	871
4	31	512	1570
5	15	23	612
6	22	149	690
7	29	251	1061
Global Average	26	150	454

Table 4.10 shows the mean value for the x coordinate of the collected data at 3048 mm. The tolerance in this table comes from the radius of the object of interest. It is -32 mm to 32 mm and when the tolerance is considered it allows for a broader target area, which as the table shows, would allow the target point to be reached more often.

Table 4.10: x-coordinate accuracy of object of interest at 3048 mm from participant

Participant	x mean (mm)	error after tolerance (mm)	% error after tolerance
1	50	18	55
2	77	45	140
3	87	55	171
4	34	2	6
5	2	0	0
6	47	15	47
7	2	0	0
Global Average	43	19	60

As mentioned before, the mean value for the y coordinate was generated. For this average the coordinates were gathered where the object of interest was 3048 mm from the participant. Table 4.11 shows the collected data. In this table the tolerance is 203 mm, which comes from the height of the object of interest. If the tolerance is taken into consideration then it allows for more retrieval points.

Table 4.11: y-coordinate accuracy of object of interest at 3048 mm from participant

Participant	y mean (mm)	error after tolerance (mm)	% error after tolerance
1	171	0	0
2	33	0	0
3	39	0	0
4	775	572	282
5	70	0	0
6	309	106	52
7	476	273	135
Global Average	267	136	67

Table 4.12, shows the z mean for data collected at 3048 mm for seven participants. The tolerance in this table comes from the 7-axis robot arm (3.1b), which has a measured reach of about 355 mm. If the tolerance is taken into consideration, then the z error decreases and one value will be close to the expected target.

Table 4.12: z-coordinate accuracy of object of interest at 3048 mm from participant

Participant	z mean (mm)	error after tolerance (mm)	% error after tolerance
1	2187	506	17
2	1047	1646	54
3	1717	976	32
4	669	2024	66
5	1617	1077	35
6	2931	0	0
7	2421	272	9
Global Average	1798	1038	34

4.4 Mobile robot guidance

In this section the robot mobile guidance will be observed. The mean of the collected 3D coordinates were separated into three tables, one for each coordinate. Table 4.13 shows the absolute value for the x mean for each of the seven participants at each of the three depths. It can be noted that for the x mean there was variance at all three depths. When the x mean was given as an input to the robot and the z mean remained a constant, it would still arrive to the target. The x value did not vary enough to cause the robot to go off target. The z mean had the greatest affect on the robot traveling to a goal. It was found that the robot had about a 100 mm tolerance.

Figures 4.22-4.25 were taken from videos which show the robot moving to the given input coordinates from Tables 4.13 and 4.15. The director of this thesis will have the videos.

Table 4.13: x mean at 1524 mm, 2134 mm, 3048 mm

x mean at 1524 mm	x mean at 2134 mm	x mean at 3048 mm
6	2	2
10	10	2
18	24	34
21	37	47
61	56	50
75	71	77
80	128	87

Table 4.14 shows the absolute value for the y mean for each of the seven participants at each of the three depths. It can be noted that for the y mean there was variance at all three depths. For this mean it was observed that as the target was moved further away the y mean got worse.

Table 4.14: y mean at 1524 mm, 2134 mm, 3048 mm

y mean at 1524 mm	y mean at 2134 mm	y mean at 3048 mm
9	2	33
97	63	39
153	92	70
171	97	171
173	139	309
199	303	476
977	331	775

Table 4.15 shows the absolute value for the z mean for each of the seven participants at each of the three depths. It can be noted that for the z mean there was variance at all three depths. When the z mean was given as an input to the robot and the x mean remained a constant it would arrive to the given input.

Table 4.15: z mean at 1524 mm, 2134 mm, 3048 mm

z mean at 1524 mm	z mean at 2134 mm	z mean at 3048 mm
640	602	669
673	1044	1047
812	1263	1617
1082	1295	1717
1728	1317	2187
2898	1759	2421
3159	2910	2931

Figures 4.22-4.25 show the robot moving from the starting point to the given input and then back to the origin. It can be noted that in Figure 4.22b the robot stopped short of the expected target. The given input was from Participant 1 at a distance of 1524 mm from the object of interest. The input was 6 for the x-coordinate and 672 for the z-coordinate which can be found in Tables 4.2 and 4.4.

Figure 4.22 shows the mobile robot at the start position as well as the position for the given coordinates. The robot stopped at 600 mm. The robot has an internal tolerance of 100 mm so it did not stop at 672 mm.

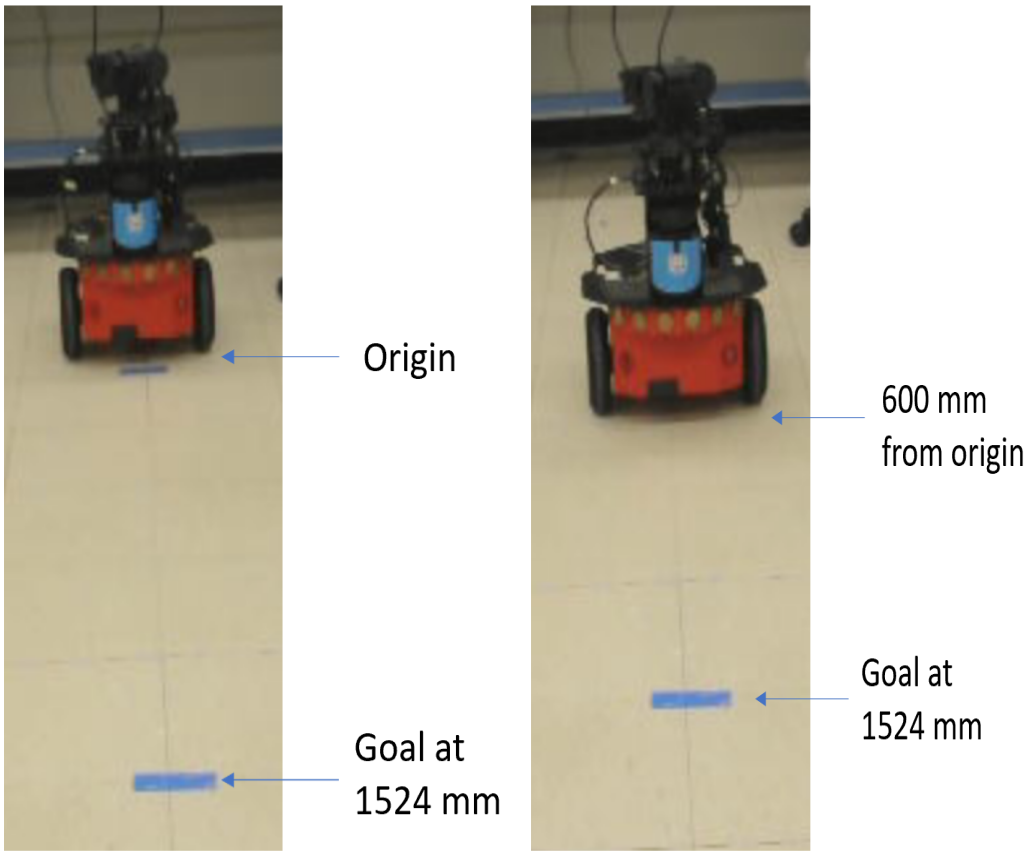

(a) Start location for coordinates from Participant 1

(b) Traveled distance using coordinates from Participant 1

Figure 4.22: Robot travel to coordinates from Participant 1 at 1524 mm

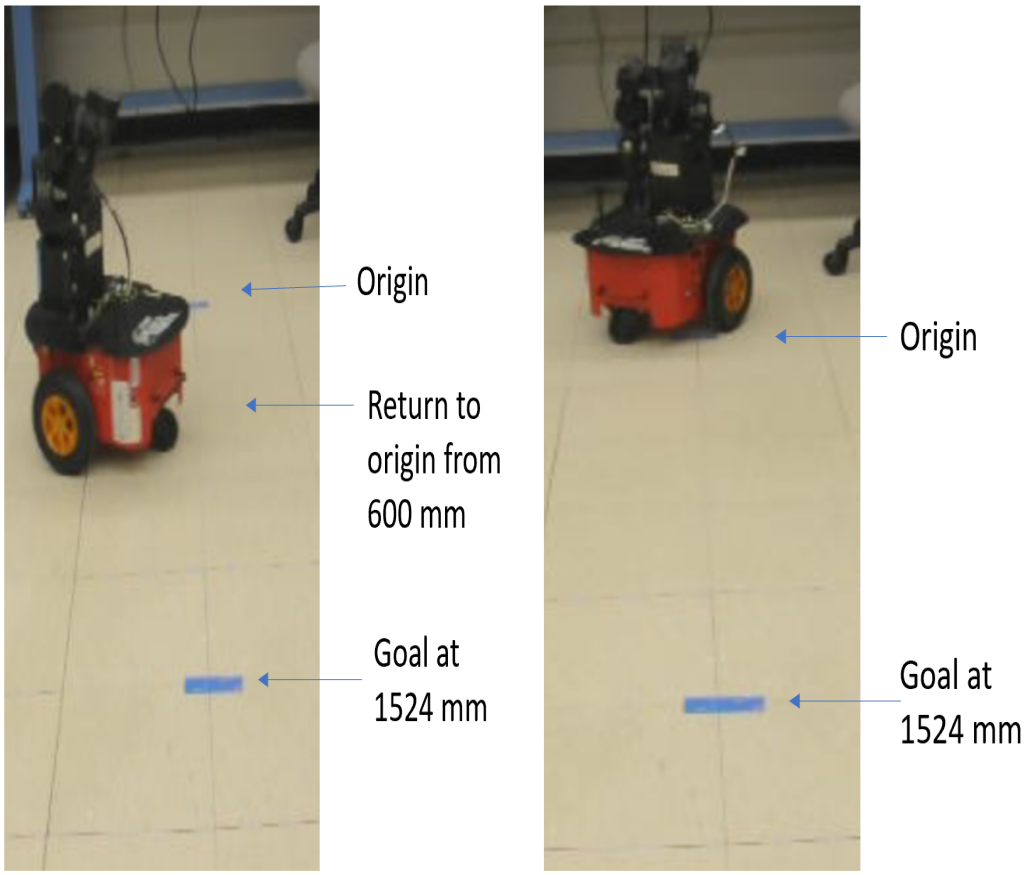

(a) Start of return to origin for coordinates from Participant 1

(b) Returned to origin using coordinates from Participant 1

Figure 4.23: Robot return to origin from coordinates from Participant 1 at 1524 mm

Figure 4.23 shows the mobile robot at the 600 mm position on the return path to the origin.

Figure 4.24a shows the mobile robot at the start position and Figure 4.24b the position for the coordinates from Participant 2. In this case the robot went over the expected 1524 mm. It traveled to the 1700 mm given coordinates.

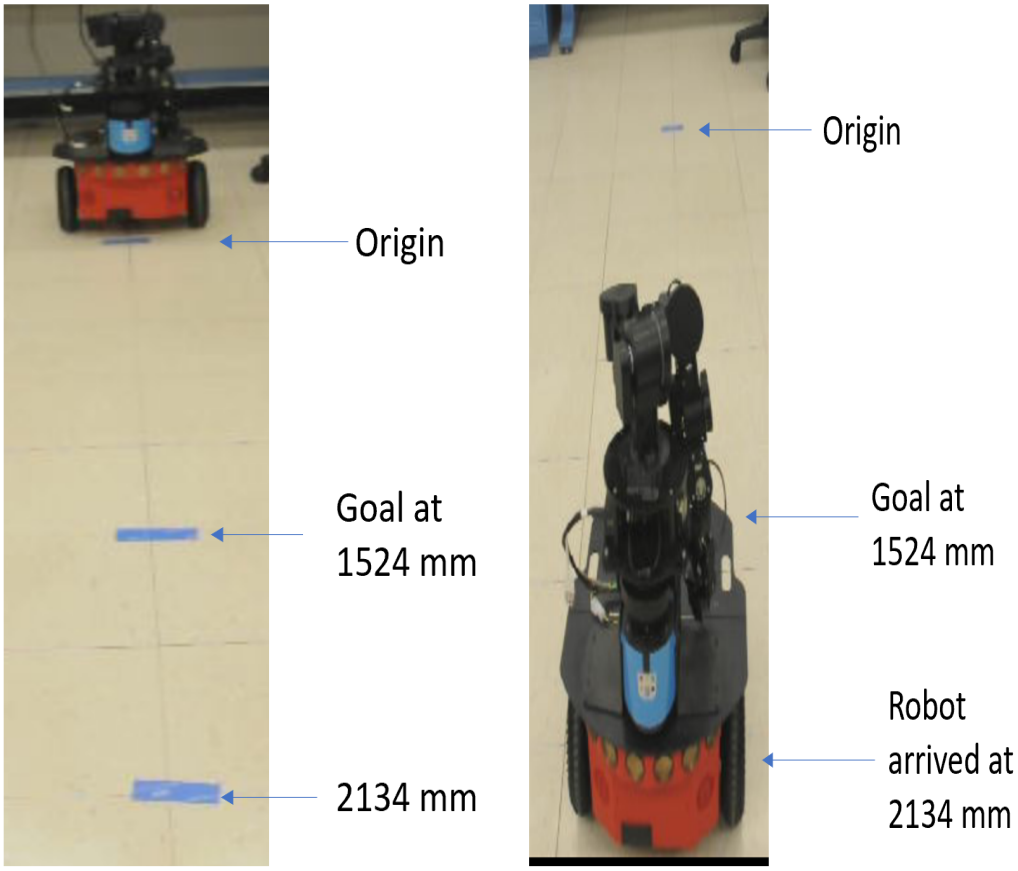

(a) Start location for coordinates from Participant 2

(b) Traveled distance using coordinates from Participant 2

Figure 4.24: Robot travel to coordinates from Participant 2

Figure 4.25 shows the mobile robot on the return path to the origin from the 1700 mm position.

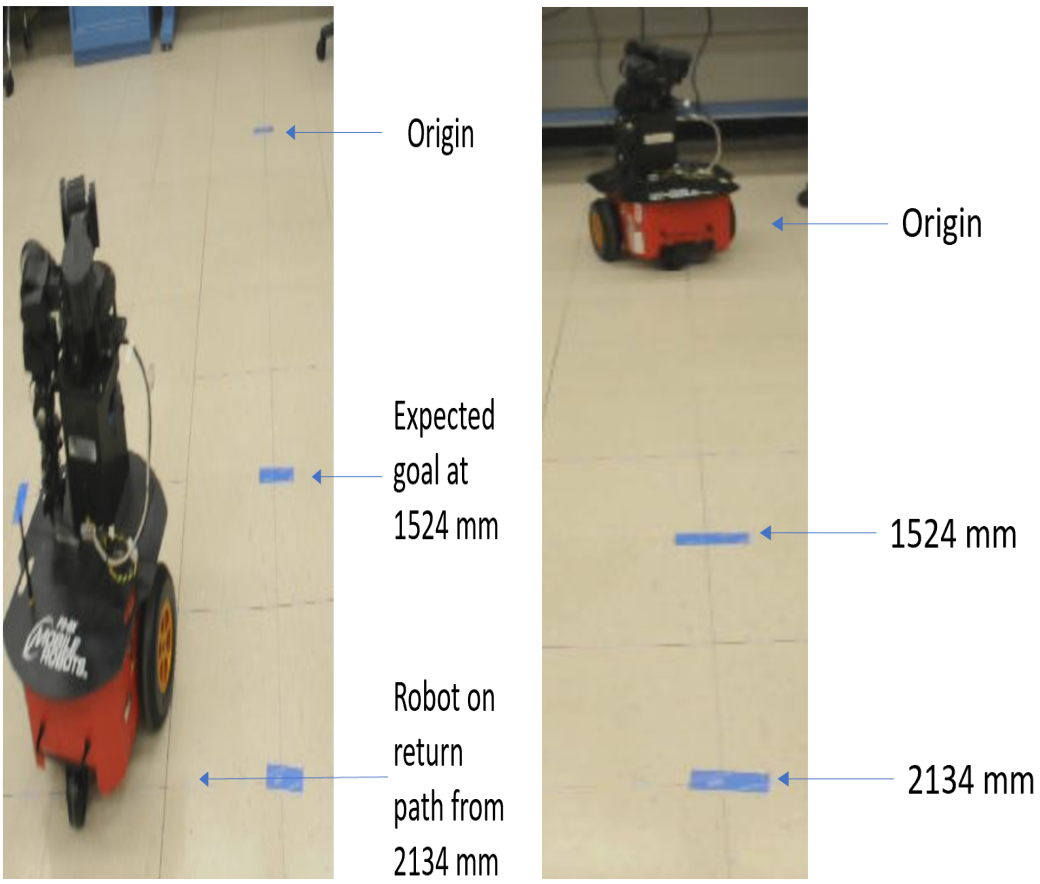

(a) Start location for return to origin from coordinates from Participant 2

(b) Returned to origin using coordinates from Participant 2

Figure 4.25: Robot return to origin from coordinates from Participant 2 at 1524 mm

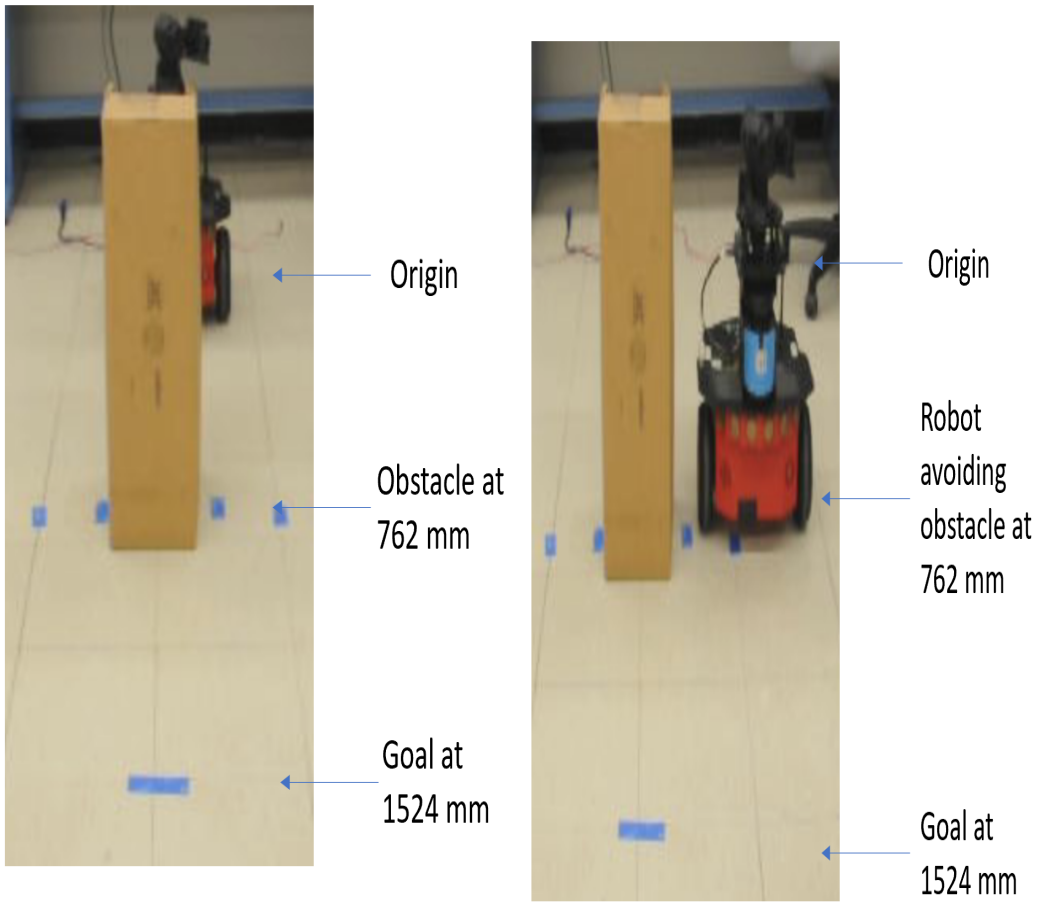

(a) Start location for obstacle avoidance test

(b) Location after obstacle avoidance

Figure 4.26: Start location for obstacle avoidance using ideal coordinates of 0 mm for the x-coordinate and 1524mm for the z-coordinate

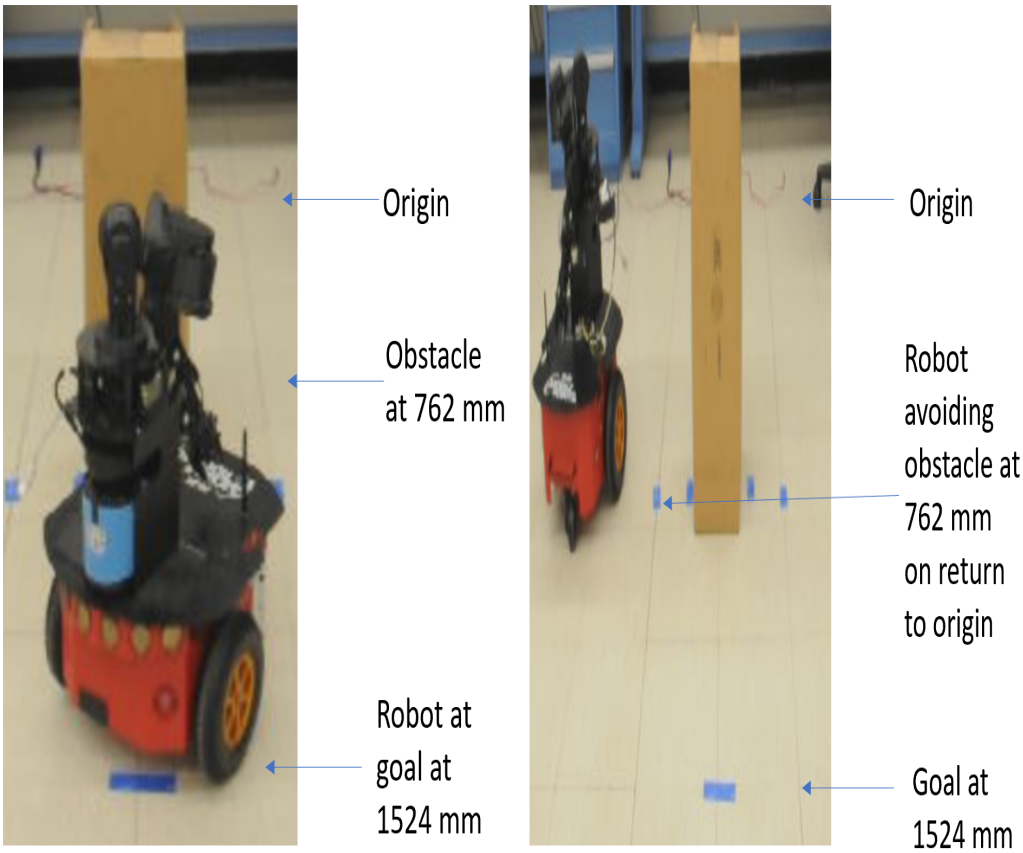

(a) Robot at goal (b) Returned to origin avoiding obstacle

Figure 4.27: Robot return to origin from 1524 mm (using ideal coordinates of 0 mm for x-coordinate and 1524 mm for z-coordinate)

Figures 4.26-4.28 shows the mobile robot starting at the origin and traveling to the goal at 1524 mm. The robot is able to avoid one obstacle and reach the goal. On the return path to the origin from the 1524 mm the robot again avoids the obstacle as it returns the origin. Testing showed that it could avoid multiple obstacles. It was tested with as many as three obstacles. The director of this thesis has the videos.

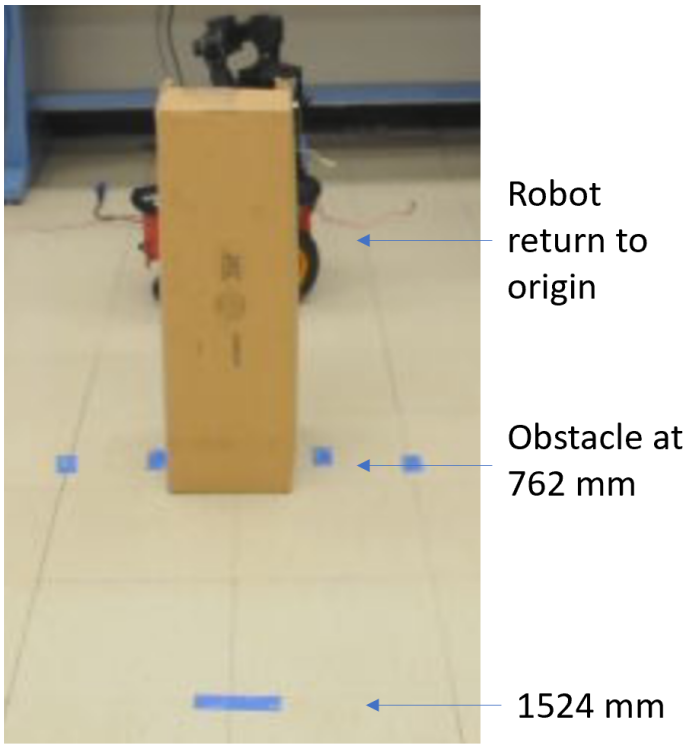

Figure 4.28: Robot at origin from 1524 mm (using ideal coordinates of 0 mm for x-coordinate and 1524 mm for z-coordinate)

CHAPTER 5: DISCUSSION

This chapter is divided into three sections: Data Analysis, Comparison with previous research, and a Summary. The Data Analysis section will discuss the findings in more detail. The Comparison section will have a comprehensive description between this research and previous work by [13] and [14]. In the Summary both the data analysis and the comparison will be summarized.

5.1 Data Analysis

In this section the data will be discussed in more detail. The discussion will commence with the ellipse and straight line path plot which were generated in order to show that even though the variation in the z-coordinate is great, the ellipse and straight line path can be used to get to the object of interest. The straight line path shows how the point of interest could be reached if the straight line path was to be used in conjunction with another sensor. Using the straight line path, will allow the use of a third device, such as a laser range finder or depth camera like the Kinect. The ellipse is a visual representation of when the target is within two standard deviations of the mean. If the robot arm length is considered then the ellipse and straight line path plots show that at 1524 mm and at 2134 mm the mobile robot would be within reach of the goal 57 % of the time. At 3048 mm the robot would be within reach of the target 86 % of the time.

The box and whisker plot was used to analyze the x and z coordinates. The x and z coordinates were used to guide the mobile robot to the point of interest. The box and whisker plot shows how the x-coordinate has a second quartile at or near zero for every instance. The z-coordinate varies more dramatically, and therefore, an ellipse and straight line path plot was generated that could serve as a visual representation of when the target is within two standard deviations of the mean.

The 3D plots are a visual representation of the collected data. Two dots were used

to represent the data: a green dot for the expected coordinates and a red dot for the mean of the collected data. The 3D plot can be used to see the participants eye gaze path.

The three different plots are used as a visual representation of the collected data at 1524 mm from the object of interest. Tables 4.2-4.4 show the mean for the x, y, and z coordinates. For the x mean at 1524 mm it can observed that there is a deviation of 6 mm to as much as 80 mm. For this research a bottle with a radius of 32 mm was utilized as the object of interest for all participants. If the radius of the bottle is used as a tolerance then four out of the seven, or about 57 % of mean values, would be on target. The remaining three mean values have deviations ranging from 29 mm to 48 mm.

Some participants exhibited interesting results in terms of gaze variance. These were participant 2, 4 and 5. Results for these individuals are discussed below.

Participant 2 had an x mean value of 75 mm, which means that it is 43 mm outside of tolerance. After reviewing Figures A.2, 4.2a, and Table 4.2, it can be determined that the participant was looking at the top of the bottle with their head tilted downward. This can be seen in Figure A.2 where the collected data points in the y axis go from about -1250 mm to 0 mm indicating the participant moved their eyes from bottom to top. Also, it can be noted that at zero in the y axis, the collected data points are in a slanted position towards about 400 mm in the x axis while heading towards about 5000 mm in the z axis. This slant created is indicative of the head being downward and looking up.

Participant 4 had an x mean value of 61 mm, which means that it is 29 mm outside of tolerance. After reviewing Figures A.4, 4.4a, and Table 4.2, it can be determined that the participant was looking at the top of the bottle with their head tilted downward, same as Participant 2. Figure A.4 shows the same trend as A.2.

Participant 5 had a x mean value of 80 mm, which means that it is 48 mm outside of tolerance. After reviewing Figures A.4, 4.4a, and Table 4.2, it can be determined that there might have been hardware error as the readings start at about 2000 mm in z axis.

The y mean in Table 4.3 has a variance of 9 mm to 199 mm with one outlier at

977 mm. For six out of the seven y mean values, if the height of the object of interest is considered, then the values would be on target. The anomaly comes from data collected from Participant 4. After reviewing Figures A.4, 4.4a, and Table 4.2, it can be determined that the participant was looking at the top of the bottle with their head tilted downward same as Participant 2. This caused y values that range from 0 mm to about 1900 mm.

The z mean in Table 4.4 has a variance of 640 mm to 3159 mm. It can be noted that four out of seven, or 57 % of the data, will be less than the 1524 mm z value goal and three out of seven, or about 43 % of the data, will be greater than the 1524 mm goal. For the z axis the robot arm with a reach of 355 mm was taken into account for the tolerance. With the tolerance added, one out of the seven z values will be on target.

Three different plots are used as a visual representation of the collected data at 2134 mm from the object of interest. Tables 4.6-4.8 show the mean for the x, y, and z coordinates. For the x mean at 2134 mm it can observed that there is a deviation of 1 mm to as much as 127 mm. For this research, a bottle with a radius of 32 mm was utilized as the object on interest for all participants. If the radius is used as a tolerance, then three out of the seven, or about 43 % of mean values, would be on target. The remaining four mean values have deviations ranging from 5 mm to 96 mm.

Participant 2 had a x mean value of 128 mm, which means that it is 96 mm outside of tolerance. After analyzing Figures A.2, 4.2a, and Table 4.6, it can be determined that the participant started the test looking to the left then moved his gaze to the right towards the object of interest. This caused the x range to go from about -254 mm to 0 mm generating the 127 mm deviation.

Participant 3 had a variance of 37 mm in the x mean. After analyzing Figures A.3, 4.3a, and Table 4.6, it can be determined that the glasses might have moved on the participant's nose. This can be seen in Figure A.3 in the x axis where the collected data points start at zero and then skips until getting to about 45 mm. The separation in data points is indicative of the glasses moving.

Participant 5 had a variance of 57 mm in the x mean. After analyzing Figures A.5, 4.5a, and Table 4.6, it can be determined that the participant may have been off center from the object of interest. Participant 7 had a variance of 71 mm in the x mean. After analyzing Figures A.7, 4.7a, and Table 4.6, it can be determined the chair might not have been centered in front of the object of interest. This observation was made due to Figure A.5 having a 3D plot with the collected data points in a straight vertical configuration and only being between 40 mm and 57 mm in the x axis.

The y mean in Table 4.7 has a variance of -2 mm to 331 mm. For five out of the seven y mean values, if the height of the object of interest is considered, then the values would be on target. Participant 4 had a variance of 331 mm in the y mean. After reviewing Figures A.11, 4.11a, and Table 4.7, it can be determined that the participant was looking at the top of the bottle. This caused y values that range from 0 mm to about 700 mm. Participant 7 had a variance of 303 mm in the y mean. After reviewing Figures A.14, 4.14a, and Table 4.7, it can be determined that the participant was looking at the top of the bottle. The empty space above the bottle might have caused y values to range from 0 mm to about 700 mm.

The z mean in Table 4.8 has a variance of 602 mm to 2910 mm. It can be noted that six out of seven, or 86 % of the data, will be less than the 2134 mm z value goal and one out of seven, or about 14 % of the data, will be greater than the 2134 mm goal. For the z axis the robot arm with a reach of 355 mm was taken into account for the tolerance. With the tolerance added one out of the seven z values will be within 20 mm from the target.

Three different plots were used as a visual representation of the collected data at 3048 mm from the object of interest. Tables 4.10-4.12 show the mean for the x, y, and z coordinates. For the x mean at 3048 mm it can observed that there is a deviation of 2 mm to as much as 87 mm. For this research, a bottle with a radius of 32 mm was utilized as the object on interest for all participants. If the radius is used as a tolerance then two out of the seven, or about 29 % of mean values would be on target. The remaining five mean values have deviations ranging from 2 mm to 55 mm after the tolerance is considered.

The y mean in Table 4.7 has a variance of 33 mm to 775 mm. For four out of the seven y mean values, if the height of the object of interest is considered, then the values would be on target. After analyzing Figures A.15-4.21a, and Table 4.11, it can be determined that the distance affected the collected data. It can be noted that now three out of the seven y mean values have a variance of 106 mm to as much as 572 mm after tolerance.

The z mean in Table 4.12 has a variance of 669 mm to 2931 mm. It can be noted that six out of seven, or 86 % of the data, will be less than the 3048 mm z value goal. Also, one out of seven, or about 14 % of the data, will be target after the tolerance is considered. For the z axis the robot arm with a reach of 355 mm was taken into account for the tolerance.

5.2 Comparison with previous research

Zhiwei Zhu and Qiang Ji [13] researched eye gaze tracking techniques under natural head movement. There research shows that in the x and y coordinates the variance increases as the distance from the participant to the point of interest increases.

Lee *et al.* [14] researched 3D gaze tracking methods using the illuminative reflections on the surface of the cornea (Purkinje images) on the eye optical model and the pupil. The researchers found that in the z coordinate as the distance increased between the participant and the point of interest the variance also increased.

The data in this research also displayed the same behavier as found in [13]. The x and y coordinates displayed a variance which increased as the distance from the participant to the point of interest increased. In this research the z coordinate was consistent. The z values showed a constant variance with values primarily under the expected depth.

If the tolerance of 32 mm for the object of interest is taken into account then the following observations can be made. For the x mean values in Table 4.13 it can be seen that 57 % of time the variance is under 25 mm at 1524 mm. At 2134 mm the variance is 43 % under 25 mm. At 3038 mm 29 % of the time, the variance is under 25 mm. This is similar to the Horizontal accuracy in [13].

If the tolerance of 203 mm for the object of interest is taken into account then the following observations can be made. The y mean values in Table 4.14 show that 86 % of time the variance is between 0 mm and 203 mm at 1524 mm. At 2134 mm, the variance is 71 % between 0 mm and 203 mm. At 3038 mm 57 % of the time the variance is between 0 mm and 203 mm. This is similar to the Vertical accuracy in [13].

If the tolerance of 355 mm for the robot arm is taken into account then the following observations can be made. The z mean values in Table 4.15 show that 57 % of time the collected data is under 1524 mm. At 2134 mm the collected data is under the expected depth 86 % of the time. At 3038 mm 100 % of the time the variance is under the expected value of 3048 mm. This is similar to the Average ZGE of depth gaze estimation in [14].

Table 4.2 shows the mean values for the x-coordinate at 1524 mm depth test. At first sight, the data reflects poor results. If the 3D aspect of the object of interest were to be considered, the values make more sense. The point of interest was determined to be zero. The 3D parameters would allow a tolerance for the x and y coordinates. In the case of this test, a 16 oz cylindrical object was utilized. The object's radius was about 32 mm. This tolerance would allow for a +32 mm or -32 mm offset and still be able to reach the target considering the z coordinate was ideal. Table 4.2 shows that five out of the seven x mean value coordinates could have been considered on target if the tolerance was taken into account. This would mean that the object of interest could be reached 71% of the time in the x-coordinate.

For the y-coordinate it was noticed that there was very little variance in the results when the tolerance was taken into account. Table 4.3 shows that six out seven, or about 86 % of y mean value coordinates, would be on target. For this reason, it was not considered in the box and whisker plots.

The z-coordinates had the most variance of the three coordinates. Table 4.4 shows that one out seven, or about 14 % of time the z mean value, would be on target. For this reason the ellipse and straight line path were generated. The ellipse shows when the target

is within two standard deviations. The straight line path shows how it can be possible to follow a straight line path using another sensory device to arrive to the point of interest.

The results did not vary significantly in the 1524 mm and 2134 mm test depths for the x and y mean values. However, when dealing with the test depth of 3048 mm, it can be observed that the y mean values start to have more variance. This variance can be overcome if the robotic arm, which has a reach of about 355 mm, is taken into consideration.

Obstacle avoidance was another aspect of this research. The testing started with having the robot avoid one obstacle. The robot was able to avoid the obstacle during both passes. The robot was tested with three obstacles and was able to reach the goal and return to the origin. The director of this thesis has the videos.

5.3 Summary

In this research, it was proposed that the 3D coordinates generated from eye gaze head worn device could be used as the given input for a mobile device. Table 5.1 shows the percentage of time the target was within two standard deviations of the mean. In some instances this means it will be within the reach of the 7 axis robot arm.

Table 5.1: Percent on target per depth out of seven participants at two standard deviations

On target at 1524 (mm)	On target at 2134 (mm)	On target at 3048 (mm)
57 %	29 %	86 %

After reviewing the data and comparing the collected data to the results discussed in previous work [13] and [14], it is believed that the 3D coordinates yielded from the head worn device would not able to be used as input for the mobile robot. Equipment used in the medical environment needs to have 90 % accuracy. As can be seen in 5.1, the level of accuracy needed is not met. Even though when compared to similar work the results exhibit the same trend in all three coordinates, the depth value is not accurate. With more testing

and closer collaboration with the head worn device manufacturer, it could be possible to create an algorithm that could better predict the z-coordinate for the head worn device that could yield better results for the target application.

CHAPTER 6: CONCLUSION AND FUTURE WORK

In conclusion, the P3-DX mobile robot proved to be very capable as its testing results showed it had a tolerance of 100 mm in the x and z axis. The software was learned using the empirical method. Once the software became more familiar an algorithm was created using existing code. An algorithm capable of accepting x and z coordinates, as well as obstacle avoidance was created. The created code can be found in Appendix B.

The wearable gaze tracker was tested and proved to have reliability in the x and y coordinates. The z-coordinate requires further examination. It proved to have too much variance. There were instances where the depth was up to 900 mm below the expected coordinate of the object of interest. In other occasions, it would be as much as 1500 mm over the expected coordinate of the object of interest.

For the reasons stated above it is recommended that future work include the integration of the 7-axis robot arm for object retrieval. A LASER rangefinder can be used for 2D SLAM. The Xbox Kinect can be implemented to generate 3D SLAM or 3D object recognition. The Kinect can be added to the robot and then synced the glasses with the robot in order to have the robot turn left or right in conjunction with the participants head movement.

BIBLIOGRAPHY

[1] Maja J Matarić, Jon Eriksson, David J Feil-Seifer, and Carolee J Winstein, "Socially assistive robotics for post-stroke rehabilitation," *Journal of NeuroEngineering and Rehabilitation*, vol. 4, no. 1, pp. 5, 2007.

[2] A Tapus, MJ Mataric, and B Scassellati, "The grand challenges in socially assistive robotics. robotics and automation magazine, 14 (1), 1-7," 2007.

[3] Felipe Espinosa, Marcelo Salazar, Daniel Pizarro, and Fernando Valdés, "Electronics proposal for telerobotics operation of p3-dx units," in *Remote and Telerobotics*. InTech, 2010.

[4] Ha Manh Do, Weihua Sheng, and Meiqin Liu, "An open platform of auditory perception for home service robots," in *Intelligent Robots and Systems (IROS), 2015 IEEE/RSJ International Conference on*. IEEE, 2015, pp. 6161–6166.

[5] Zhaopeng Gu, Hong Liu, and Guodong Zhang, "Real-time indoor localization of service robots using fisheye camera and laser pointers," in *Robotics and Biomimetics (ROBIO), 2014 IEEE International Conference on*. IEEE, 2014, pp. 1410–1414.

[6] Rowel Atienza and Alexander Zelinsky, "Active gaze tracking for human-robot interaction," in *Proceedings of the 4th IEEE International Conference on Multimodal Interfaces*. IEEE Computer Society, 2002, p. 261.

[7] Martin Bohme, André Meyer, Thomas Martinetz, and Erhardt Barth, "Remote eye tracking: State of the art and directions for future development," in *Proc. of the 2006 Conference on Communication by Gaze Interaction (COGAIN)*, 2006, pp. 12–17.

[8] Thomas E Hutchinson, Christopher Lankford, and Peter Shannon, "Eye gaze direction tracker," Nov. 28 2000, US Patent 6,152,563.

[9] RJ Jacob and Keith S Karn, "Eye tracking in human-computer interaction and usability research: Ready to deliver the promises," *Mind*, vol. 2, no. 3, pp. 4, 2003.

[10] Roger Y Tsai and Reimar K Lenz, "A new technique for fully autonomous and efficient 3d robotics hand/eye calibration," *IEEE Transactions on robotics and automation*, vol. 5, no. 3, pp. 345–358, 1989.

[11] Ba Linh Nguyen, "Eye gaze tracking," in *Computing and Communication Technologies, 2009. RIVF'09. International Conference on*. IEEE, 2009, pp. 1–4.

[12] Andreas Bulling and Hans Gellersen, "Toward mobile eye-based human-computer interaction," *IEEE Pervasive Computing*, vol. 9, no. 4, pp. 8–12, 2010.

[13] Zhiwei Zhu and Qiang Ji, "Novel eye gaze tracking techniques under natural head movement," *IEEE Transactions on biomedical engineering*, vol. 54, no. 12, pp. 2246–2260, 2007.

[14] Ji Woo Lee, Chul Woo Cho, Kwang Yong Shin, Eui Chul Lee, and Kang Ryoung Park, "3d gaze tracking method using purkinje images on eye optical model and pupil," *Optics and Lasers in Engineering*, vol. 50, no. 5, pp. 736–751, 2012.

[15] Jason Zhou and Loulin Huang, "Experimental study on sensor fusion to improve real time indoor localization of a mobile robot," in *Robotics, Automation and Mechatronics (RAM), 2011 IEEE Conference on*. IEEE, 2011, pp. 258–263.

[16] MathWorks, "mean," `https://www.mathworks.com/help/matlab/ref/mean.html?searchHighlight=mean&s_tid=doc_srchtitle`, before R2006a, Accessed on 2018-03-11.

[17] MathWorks, "std," `https://www.mathworks.com/help/matlab/ref/std.html?s_tid=srchtitle`, before R2006a, Accessed on 2018-03-11.

[18] Andreas Wulff-Jensen, "Data conversion tool for tobii pro glasses 2 live data files: From. json to. txtfra. json til. txt," 2017.

Appendices

APPENDIX A: 3D PLOTS FOR COLLECTED DATA

A.1 3D plots for testing at 1524 mm

Figure A.1 shows the 3D spatial view of the participant's gaze. In this plot the green dot is the expected location. The red dot is the mean of the collected gaze data. For the x-coordinate it can be determined that the range of the x values are between 0 and 30 mm. For the y-coordinate the values go from 0 to -100 mm. The z-coordinate values are between 500 mm and 1500 mm.

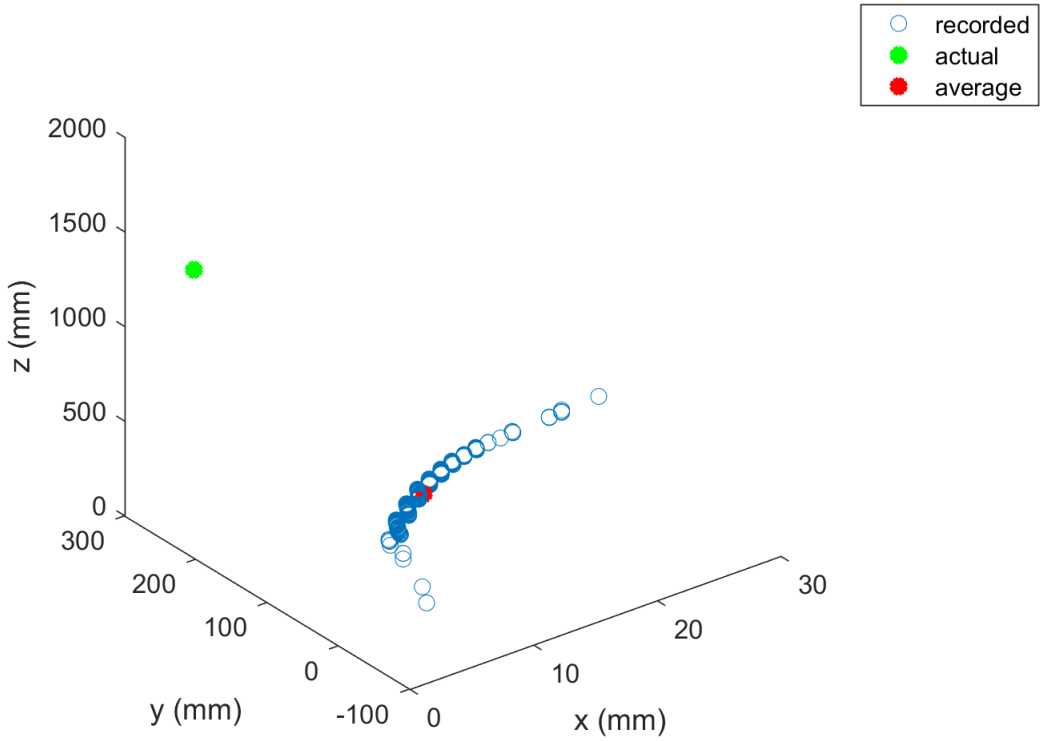

Figure A.1: 3D plot for Participant 1 at 1524 mm from object of interest

Figure A.2 shows the 3D view of the participant's gaze. In this plot the green dot is the expected location. The red dot is the mean of the collected gaze data. For the x-coordinate it can be determined that the range of the x values are between 0 and 800 mm. For the y coordinate the values go from 0 to -1500 mm. The z coordinate values are between 0 mm and 15000 mm.

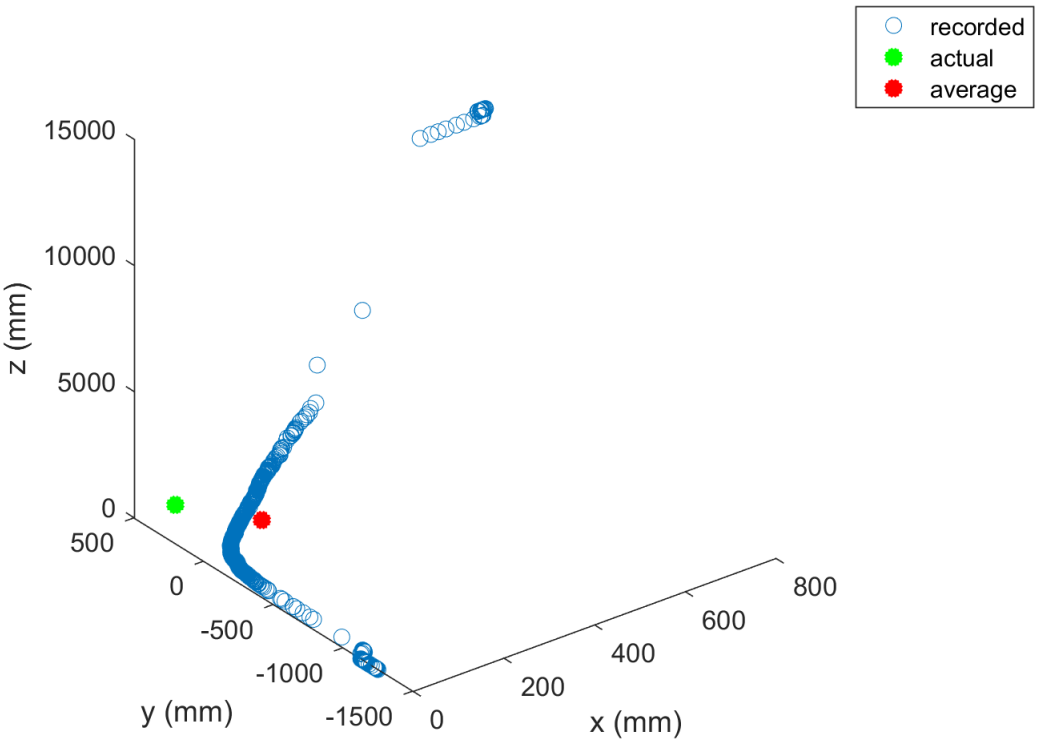

Figure A.2: 3D plot for Participant 2 at 1524 mm from object of interest

Figure A.3 shows the 3D spacial view of the participant's gaze. In this plot the green dot is the expected location. The red dot is the mean of the collected gaze data. For the x coordinate it can be determined that the range of the x values are between 0 and 60 mm. For the y-coordinate the values go from 0 to -400 mm. The z-coordinate values are between 0 mm and 2000 mm.

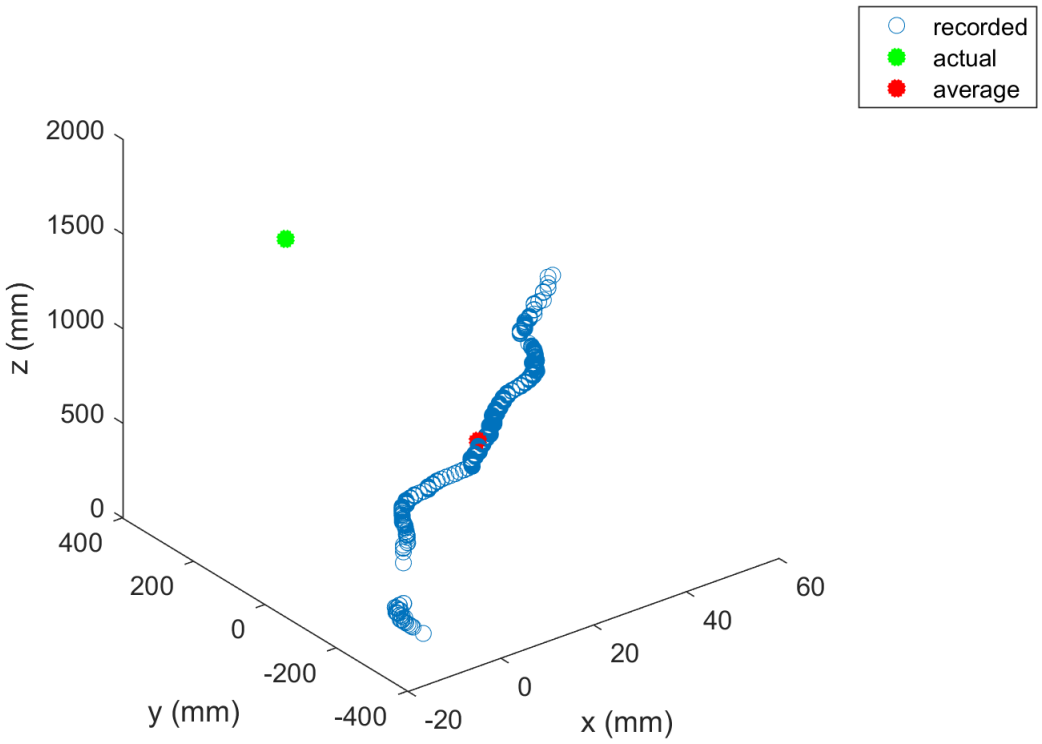

Figure A.3: 3D plot for Participant 3 at 1524 mm from object of interest

Figure A.4 shows the 3D spacial view of the participant's gaze. In this plot the green dot is the expected location. The red dot is the mean of the collected gaze data. For the x-coordinate it can be determined that the range of the x values are between -400 and 0 mm. For the y-coordinate the values go from 0 to 6000 mm. The z-coordinate values are between 0 mm and 15000 mm.

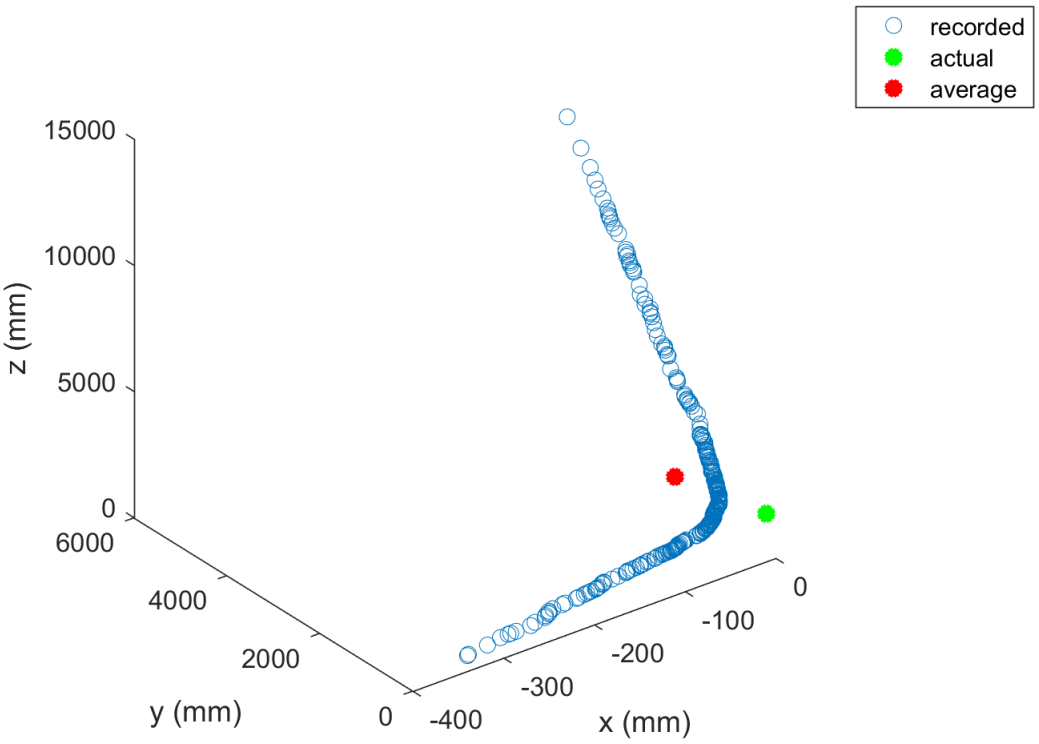

Figure A.4: 3D plot for Participant 4 at 1524 mm from object of interest

Figure A.5 shows the 3D spacial view of the participant's gaze. In this plot the green dot is the expected location. The red dot is the mean of the collected gaze data. For the x-coordinate it can be determined that the range of the x values are between 0 and 150 mm. For the y-coordinate the values go from 0 to -200 mm. The z-coordinate values are between 0 mm and 4500 mm.

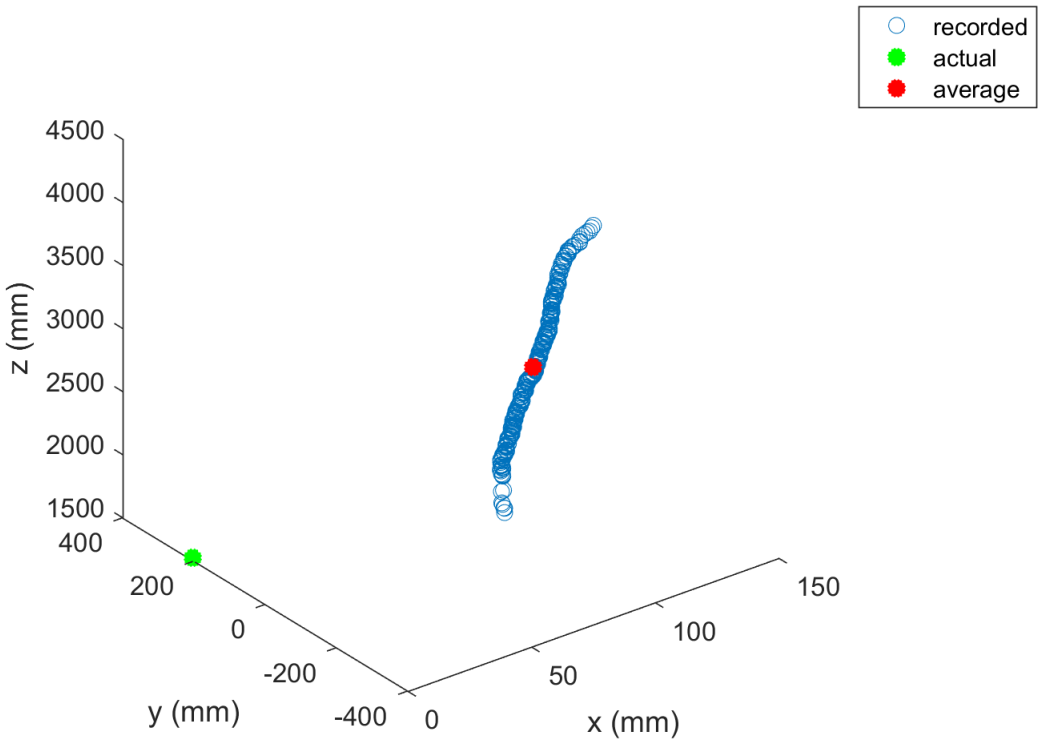

Figure A.5: 3D plot for Participant 5 at 1524 mm from object of interest

Figure A.6 shows the 3D spacial view of the participant's gaze. In this plot the green dot is the expected location. The red dot is the mean of the collected gaze data. For the x coordinate it can be determined that the range of the x values are between -150 and 50 mm. For the y-coordinate the values go from 500 to -500 mm. The z-coordinate values are between 0 mm and 4000 mm.

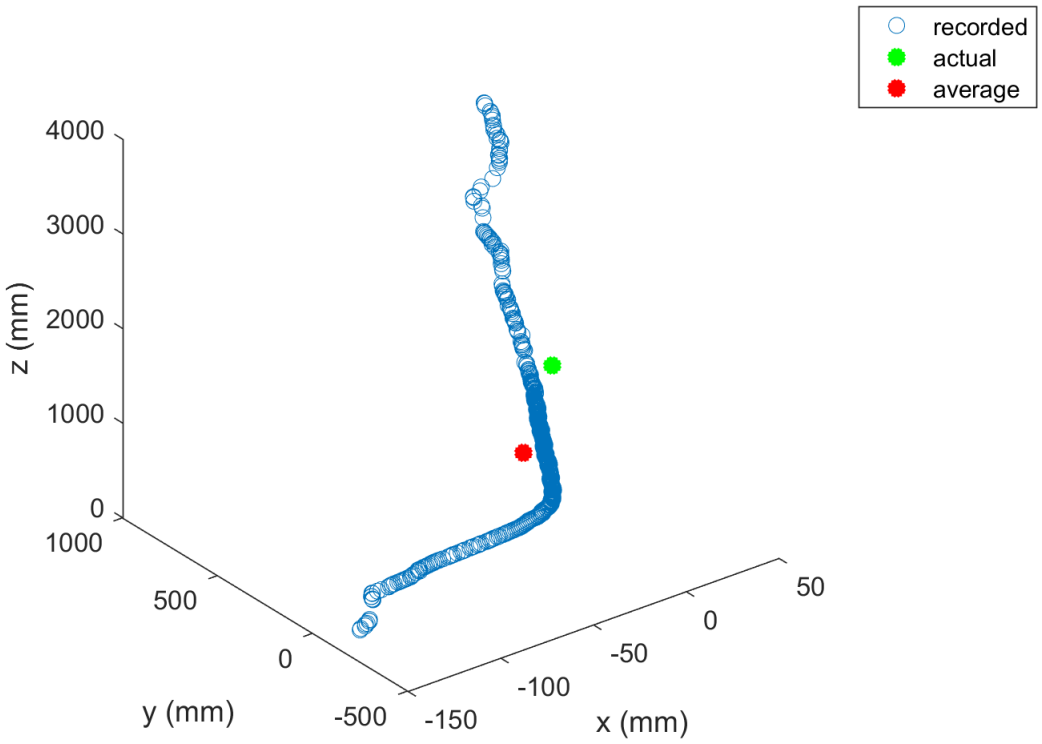

Figure A.6: 3D plot for Participant 6 at 1524 mm from object of interest

Figure A.7 shows the 3D spacial view of the participant's gaze. In this plot the green dot is the expected location. The red dot is the mean of the collected gaze data. For the x-coordinate it can be determined that the range of the x values are between 50 and 100 mm. For the y-coordinate the values go from 0 to 600 mm. The z-coordinate values are between 0 mm and 3000 mm.

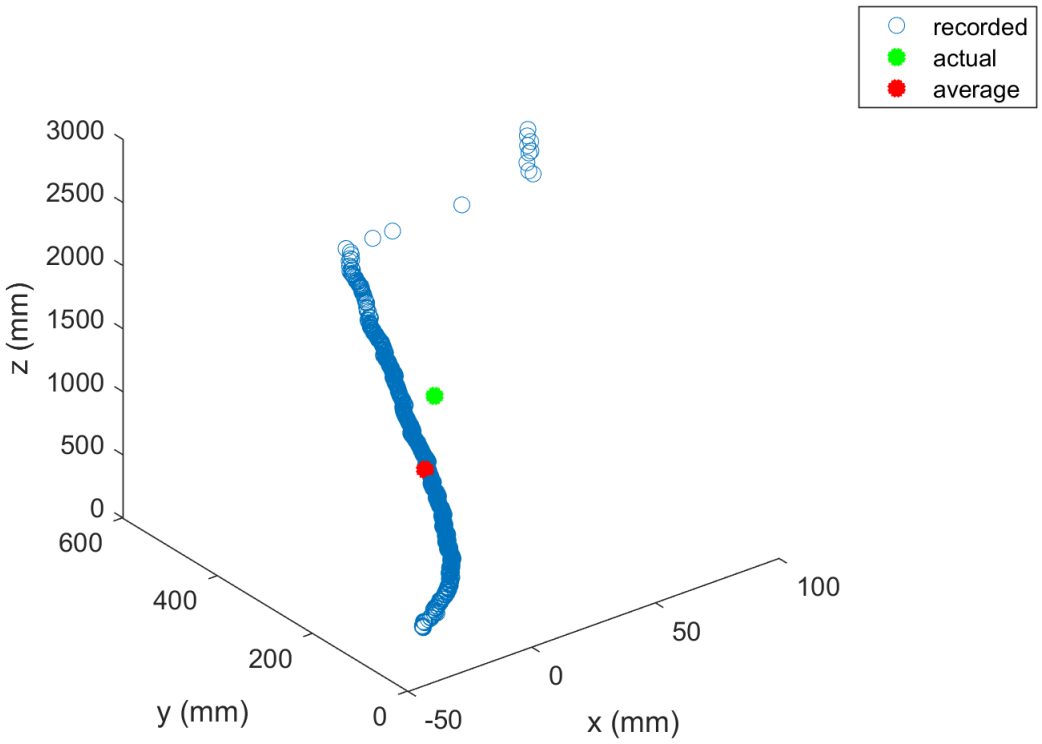

Figure A.7: 3D plot for Participant 7 at 1524 mm from object of interest

A.2 3D plots for testing at 2134 mm

Figure A.8 shows the 3D spacial view of the participant's gaze. In this plot the green dot is the expected location. The red dot is the mean of the collected gaze data. For the x-coordinate it can be determined that the range of the x values are between 5 and 15 mm. For the y-coordinate the values go from 0 to -100 mm. The z-coordinate values are between 500 mm and 1500 mm.

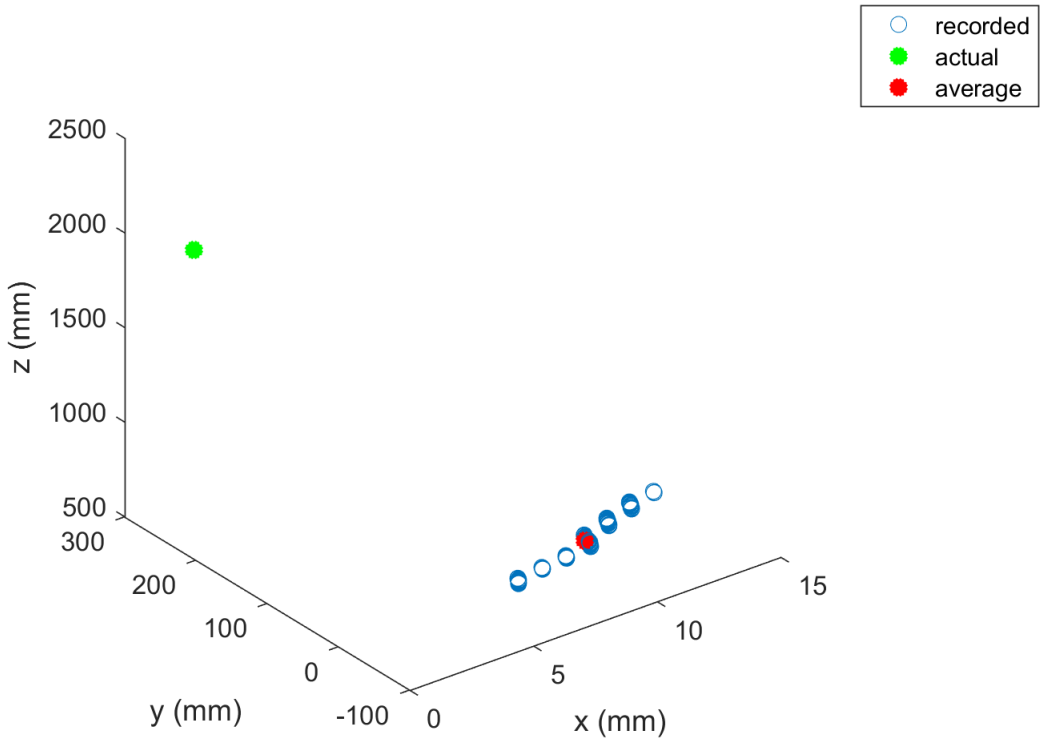

Figure A.8: 3D plot for Participant 1 at 2134 mm from object of interest

Figure A.9 shows the 3D spacial view of the participant's gaze. In this plot the green dot is the expected location. The red dot is the mean of the collected gaze data. For the x-coordinate it can be determined that the range of the x values are between 0 and -300 mm. For the y-coordinate the values go from 0 to -100 mm. The z-coordinate values are between 0 mm and 2500 mm.

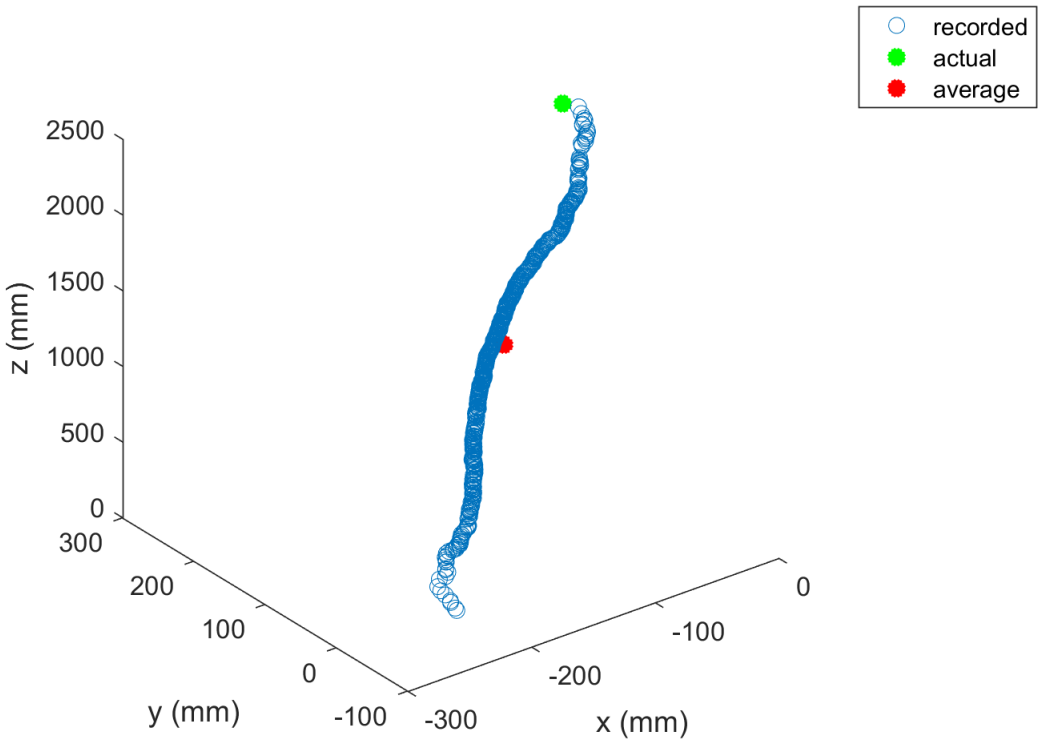

Figure A.9: 3D plot for Participant 2 at 2134 mm from object of interest

Figure A.10 shows the 3D spacial view of the participant's gaze. In this plot the green dot is the expected location. The red dot is the mean of the collected gaze data. For the x coordinate it can be determined that the range of the x values are between -50 and 100 mm. For the y-coordinate the values go from -200 to 0 mm. The z-coordinate values are between 0 mm and 2500 mm.

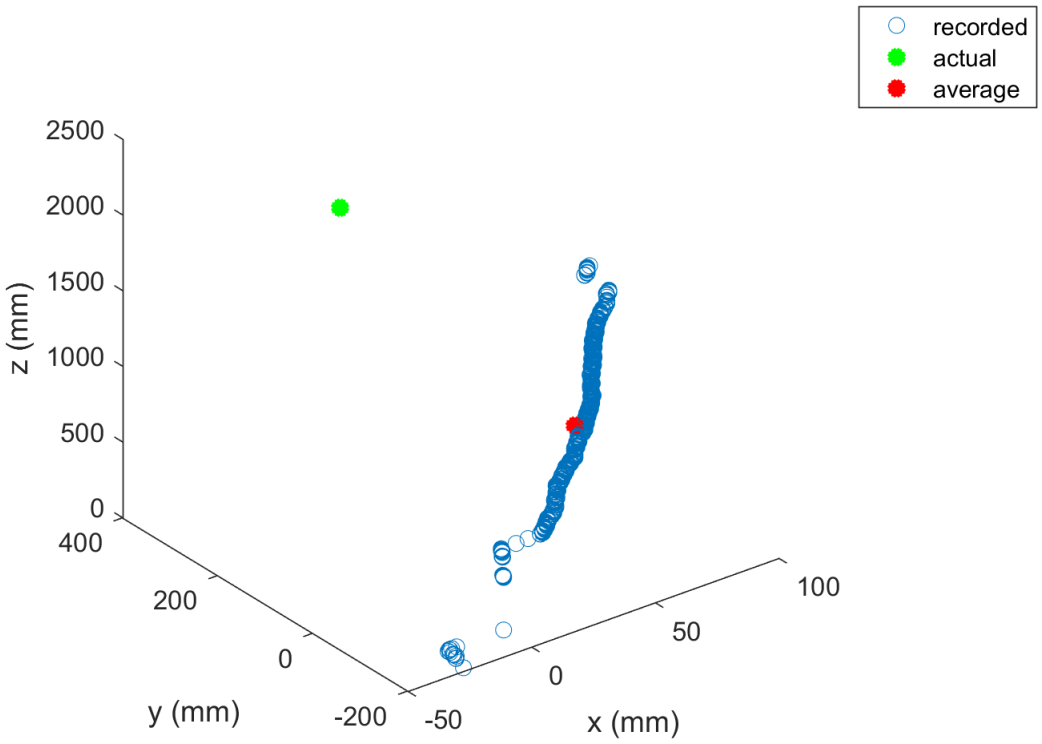

Figure A.10: 3D plot for Participant 3 at 2134 mm from object of interest

Figure A.11 shows the 3D spacial view of the participant's gaze. In this plot the green dot is the expected location. The red dot is the mean of the collected gaze data. For the x-coordinate it can be determined that the range of the x values are between -20 and 0 mm. For the y-coordinate the values go from 0 to 500 mm. The z-coordinate values are between 0 mm and 4000 mm.

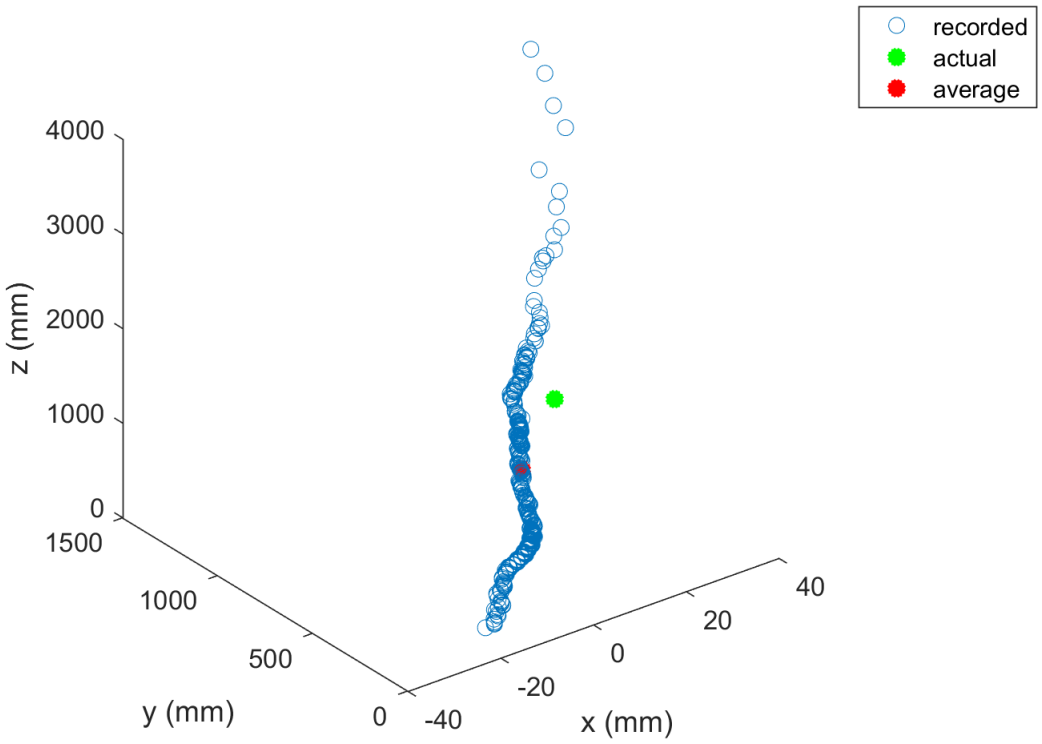

Figure A.11: 3D plot for Participant 4 at 2134 mm from object of interest

Figure A.12 shows the 3D spacial view of the participant's gaze. In this plot the green dot is the expected location. The red dot is the mean of the collected gaze data. For the x-coordinate it can be determined that the range of the x values are between 0 and 50 mm. For the y-coordinate the values go from -200 to 0 mm. The z-coordinate values are between 2000 mm and 5000 mm.

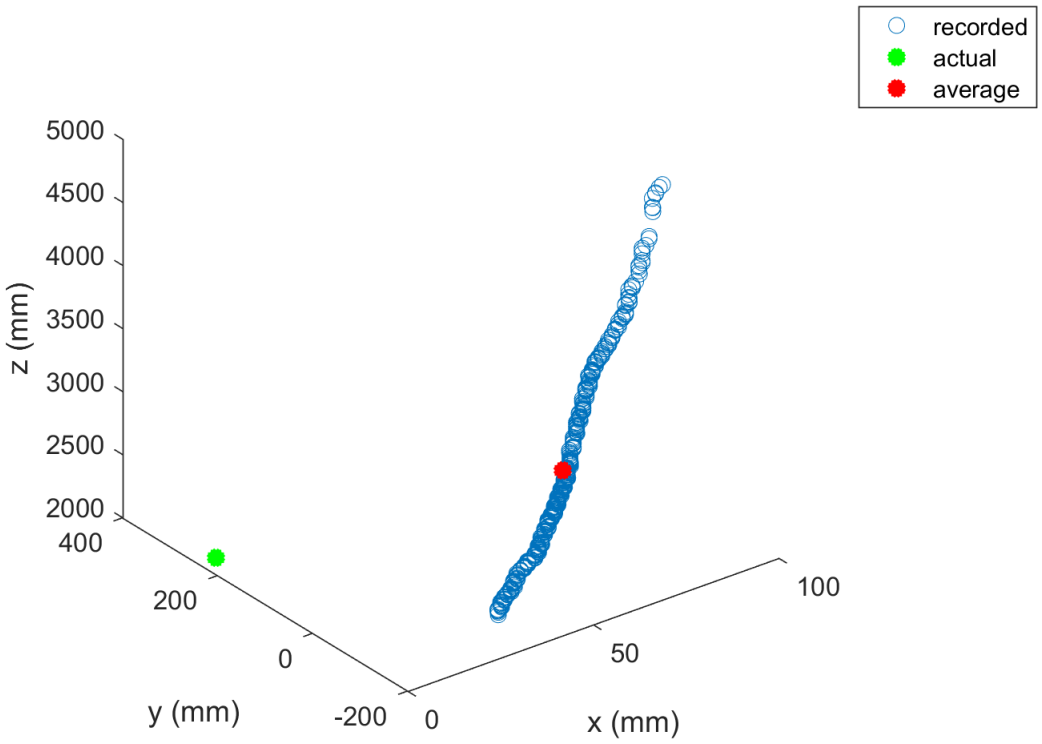

Figure A.12: 3D plot for Participant 5 at 2134 mm from object of interest

Figure A.13 shows the 3D spacial view of the participant's gaze. In this plot the green dot is the expected location. The red dot is the mean of the collected gaze data. For the x-coordinate it can be determined that the range of the x values are between 0 and 40 mm. For the y-coordinate the values go from 100 to 200 mm. The z-coordinate values are between 0 mm and 2500 mm.

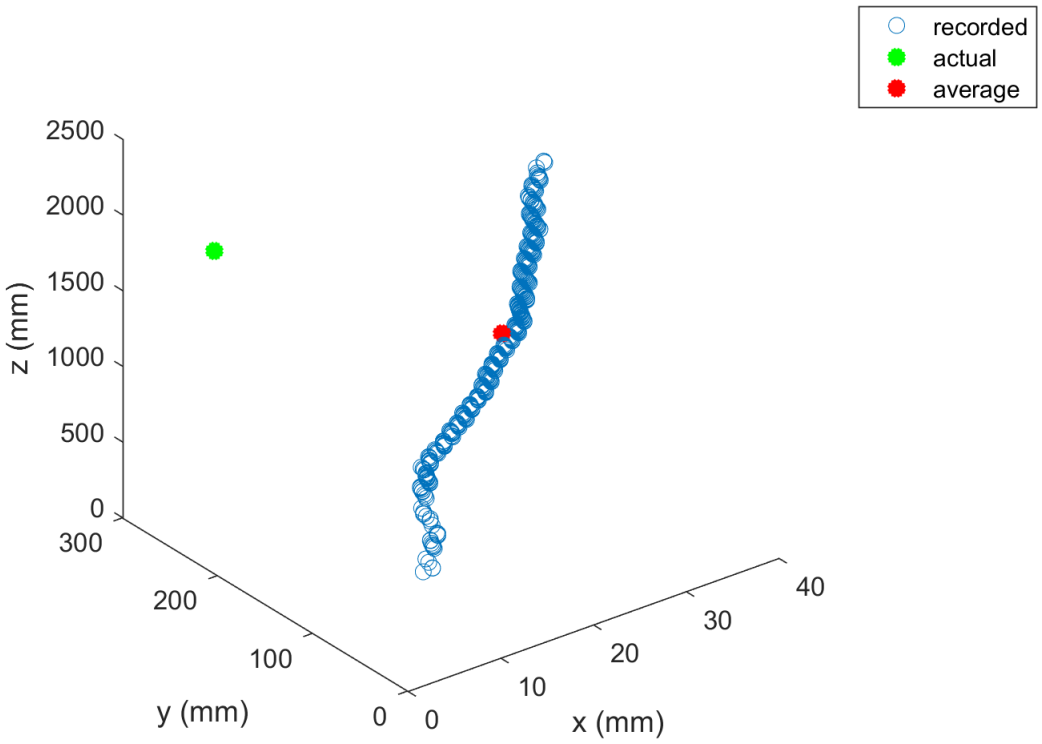

Figure A.13: 3D plot for Participant 6 at 2134 mm from object of interest

Figure A.14 shows the 3D spacial view of the participant's gaze. In this plot the green dot is the expected location. The red dot is the mean of the collected gaze data. For the x-coordinate it can be determined that the range of the x values are between 0 and 100 mm. For the y-coordinate the values go from 200 to 400 mm. The z-coordinate values are between 0 mm and 5000 mm.

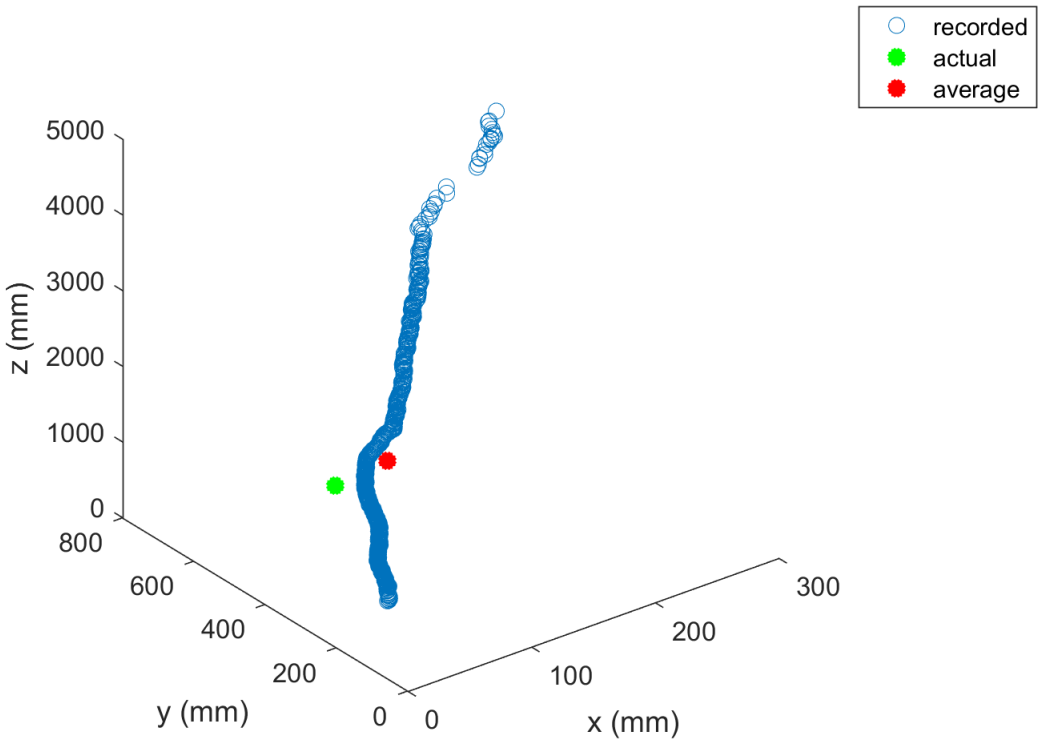

Figure A.14: 3D plot for Participant 7 at 2134 mm from object of interest

A.3 3D plots for testing at 3048 mm

Figure A.15 shows the 3D spacial view of the participant's gaze. In this plot the green dot is the expected location. The red dot is the mean of the collected gaze data. For the x-coordinate it can be determined that the range of the x values are between 50 and 100 mm. For the y-coordinate the values go from 0 to 300 mm. The z-coordinate values are between 0 mm and 5000 mm.

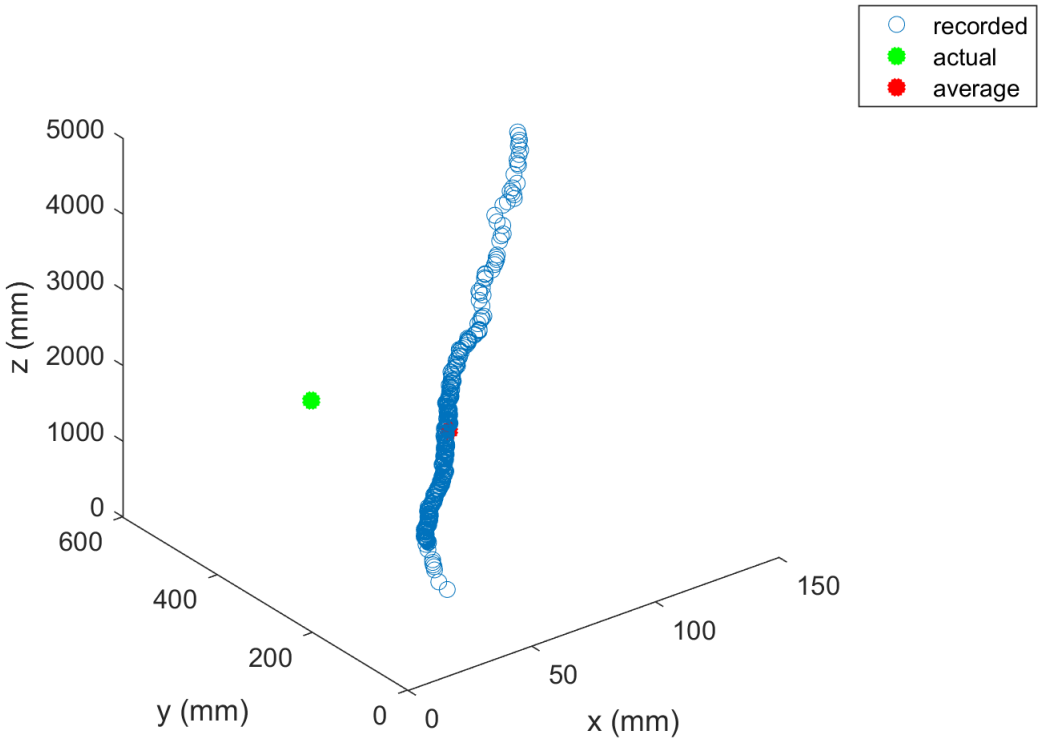

Figure A.15: 3D plot for Participant 1 at 3048 mm from object of interest

Figure A.16 shows the 3D spacial view of the participant's gaze. In this plot the green dot is the expected location. The red dot is the mean of the collected gaze data. For the x-coordinate it can be determined that the range of the x values are between -100 and 0 mm. For the y-coordinate the values go from -200 to 0 mm. The z-coordinate values are between 0 mm and 2000 mm.

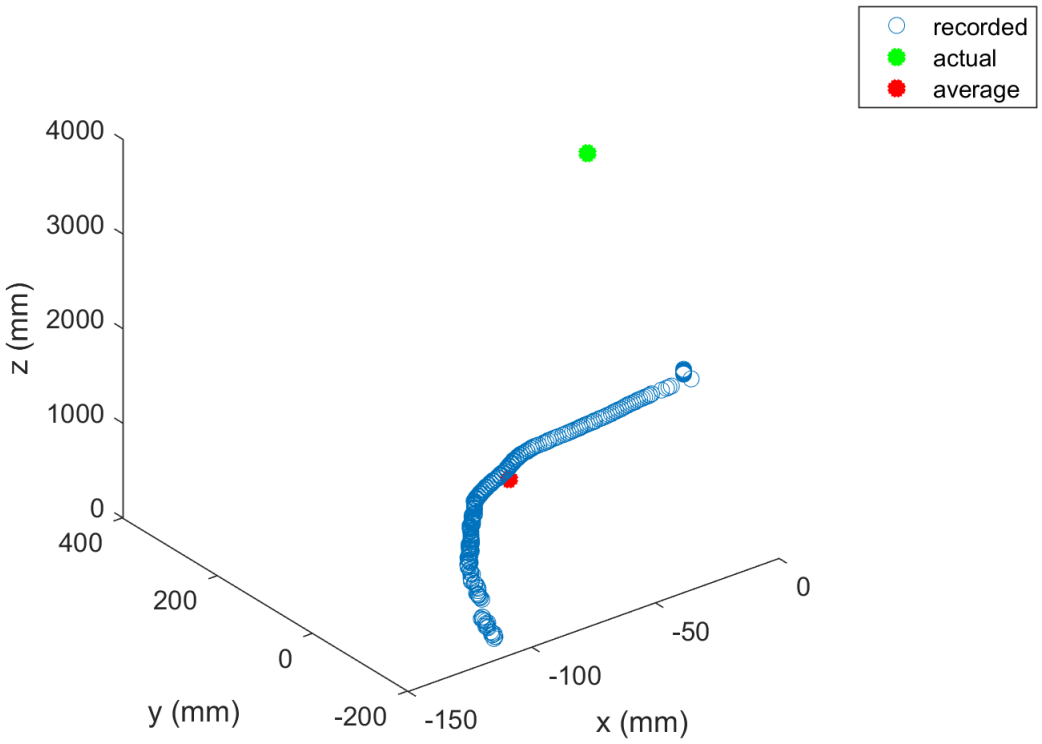

Figure A.16: 3Dl plot for Participant 2 at 3048 mm from object of interest

Figure A.17 shows the 3D spacial view of the participant's gaze. In this plot the green dot is the expected location. The red dot is the mean of the collected gaze data. For the x-coordinate it can be determined that the range of the x values are between 0 and 300 mm. For the y-coordinate the values go from -200 to 0 mm. The z-coordinate values are between 0 mm and 6000 mm.

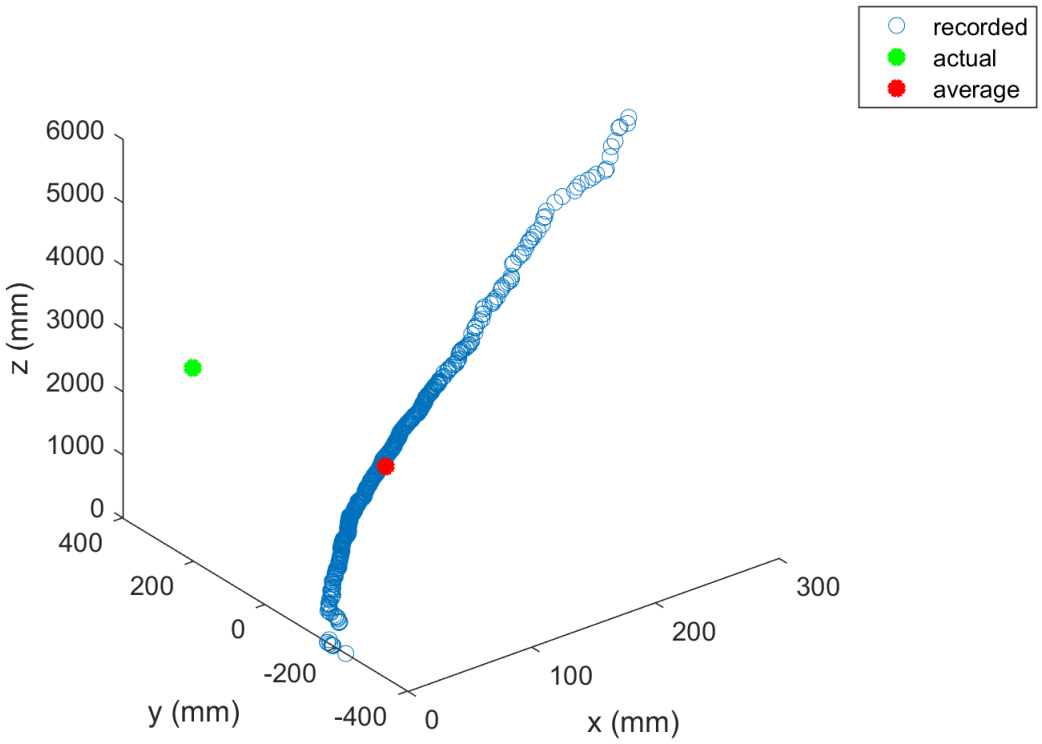

Figure A.17: 3D plot for Participant 3 at 3048 mm from object of interest

Figure A.18 shows the 3D spacial view of the participant's gaze. In this plot the green dot is the expected location. The red dot is the mean of the collected gaze data. For the x-coordinate it can be determined that the range of the x values are between -50 and 50 mm. For the y-coordinate the values go from 0 to 2100 mm. The z-coordinate values are between 0 mm and 8000 mm.

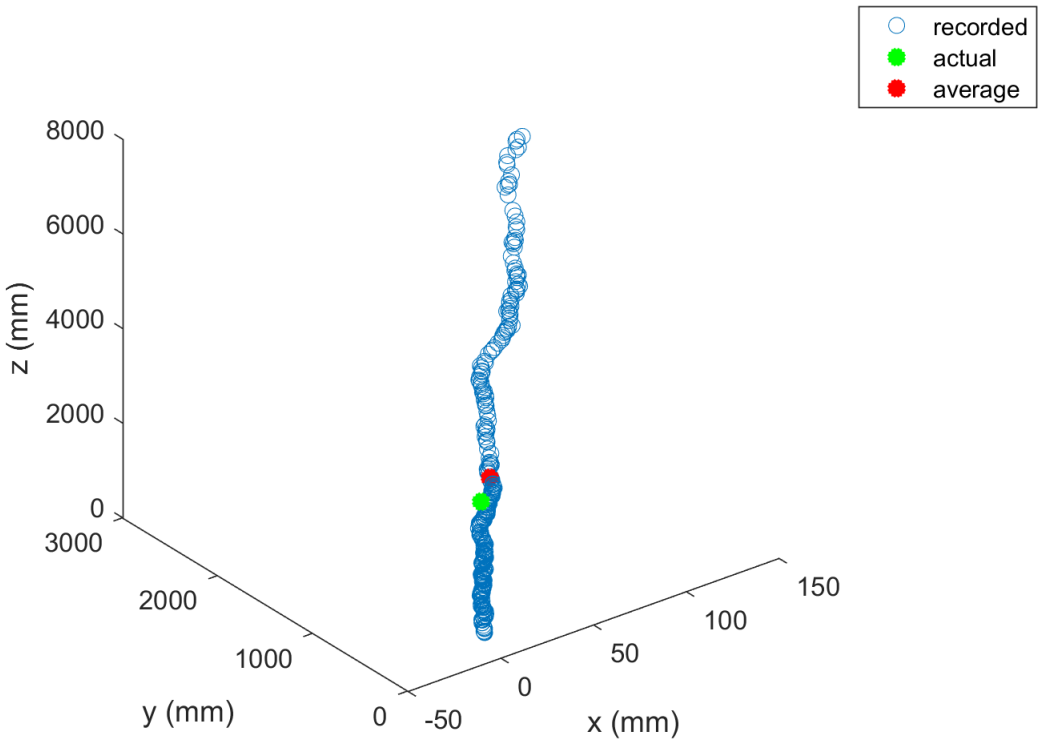

Figure A.18: 3D plot for Participant 4 at 3048 mm from object of interest

Figure A.19 shows the 3D spacial view of the participant's gaze. In this plot the green dot is the expected location. The red dot is the mean of the collected gaze data. For the x-coordinate it can be determined that the range of the x values are between -50 and 50 mm. For the y-coordinate the values go from 100 to 200 mm. The z-coordinate values are between 1000 mm and 5000 mm.

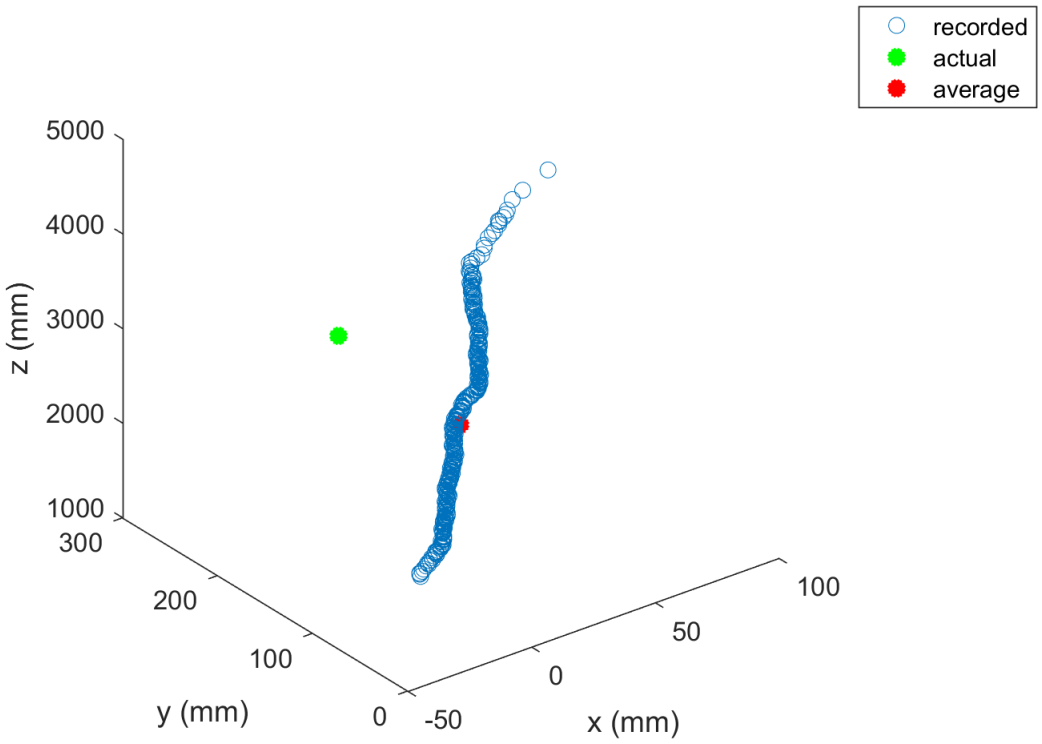

Figure A.19: 3D plot for Participant 5 at 3048 mm from object of interest

Figure A.20 shows the 3D spacial view of the participant's gaze. In this plot the green dot is the expected location. The red dot is the mean of the collected gaze data. For the x-coordinate it can be determined that the range of the x values are between 0 and 50 mm. For the y-coordinate the values go from 0 to 500 mm. The z-coordinate values are between 0 mm and 5000 mm.

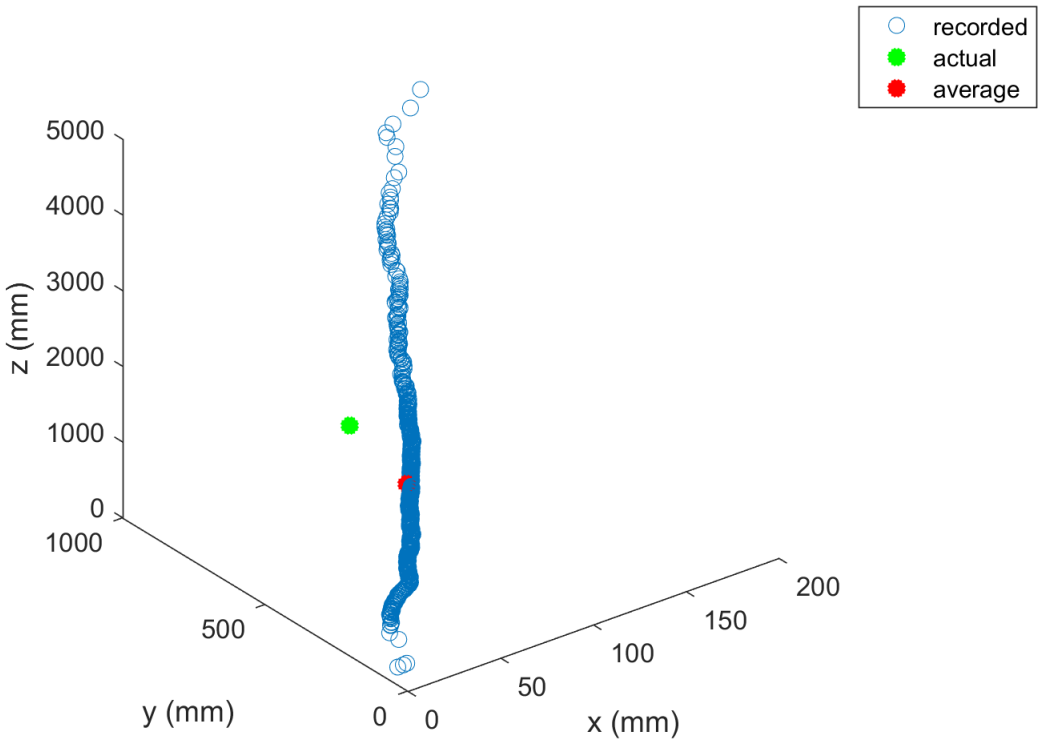

Figure A.20: 3D plot for Participant 6 at 3048 mm from object of interest

Figure A.21 shows the 3D spacial view of the participant's gaze. In this plot the green dot is the expected location. The red dot is the mean of the collected gaze data. For the x-coordinate it can be determined that the range of the x values are between -50 and 0 mm. For the y-coordinate the values go from 0 to 500 mm. The z-coordinate values are between 0 mm and 8000 mm.

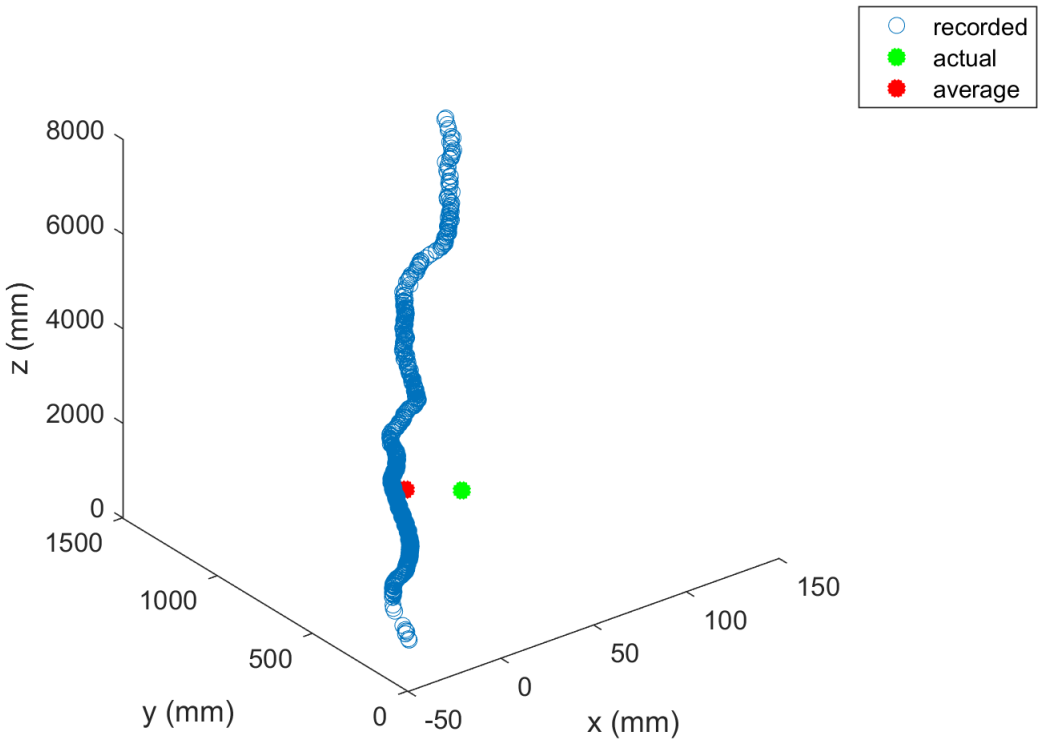

Figure A.21: 3D plot for Participant 7 at 3048 mm from object of interest

APPENDIX B: SOURCE CODE

```
1 /*
2 Adept MobileRobots Robotics Interface for Applications (ARIA)
3 Copyright (C) 2004-2005 ActivMedia Robotics LLC
4 Copyright (C) 2006-2010 MobileRobots Inc.
5 Copyright (C) 2011-2015 Adept Technology, Inc.
6 Copyright (C) 2016 Omron Adept Technologies, Inc.
7
8     This program is free software; you can redistribute it and/or
    modify
9     it under the terms of the GNU General Public License as
    published by
10    the Free Software Foundation; either version 2 of the License,
    or
11    (at your option) any later version.
12
13    This program is distributed in the hope that it will be useful,
14    but WITHOUT ANY WARRANTY; without even the implied warranty of
15    MERCHANTABILITY or FITNESS FOR A PARTICULAR PURPOSE.  See the
16    GNU General Public License for more details.
17
18    You should have received a copy of the GNU General Public
    License
19    along with this program; if not, write to the Free Software
20    Foundation, Inc., 59 Temple Place, Suite 330, Boston, MA
    02111-1307  USA
21
22 If you wish to redistribute ARIA under different terms, contact
23 Adept MobileRobots for information about a commercial version of ARIA
     at
24 robots@mobilerobots.com or
25 Adept MobileRobots, 10 Columbia Drive, Amherst, NH 03031;
    +1-603-881-7960
26 */
27 #include "Aria.h"
28 #include <iostream>
29 #include <fstream>
30 #include <math.h>
31
32 using namespace std;
33
34 /** @example gotoActionExample.cpp Uses ArActionGoto to drive the
    robot in a square
35
36  This program will make the robot drive in a 2.5x2.5 meter square by
```

```
37   setting each corner in turn as the goal for an ArActionGoto action.
38   It also uses speed limiting actions to avoid collisions. After some
39   time, it cancels the goal (and the robot stops due to a stopping
      action)
40   and exits.
41
42   Press escape to shut down Aria and exit.
43 */
44
45 ArActionGroup *ToggleActionGroup = NULL;
46 bool ToggleActionGroupActive = false;
47 void toggleaction(int signal)
48 {
49   ArLog::log(ArLog::Normal, "%s action group.",
      ToggleActionGroupActive?"Deactivating":"Activating");
50   if(ToggleActionGroupActive)
51   {
52     ToggleActionGroup->deactivate();
53     ToggleActionGroupActive = false;
54   }
55   else
56   {
57     ToggleActionGroup->activate();
58     ToggleActionGroupActive = true;
59   }
60 }
61
62 int main(int argc, char **argv)
63 {
64   std::string str;
65   Aria::init();
66   ArArgumentParser parser(&argc, argv);
67   parser.loadDefaultArguments();
68   ArRobot robot;
69   ArAnalogGyro gyro(&robot);
70   ArSonarDevice sonar;
71   ArRobotConnector robotConnector(&parser, &robot);
72   ArLaserConnector laserConnector(&parser, &robot, &robotConnector);
73
74   ArPose pose;
75   // Connect to the robot, get some initial data from it such as type
       and name,
76   // and then load parameter files for this robot.
77   if(!robotConnector.connectRobot())
78   {
79     ArLog::log(ArLog::Terse, "gotoActionExample: Could not connect to
       the robot.");
```

```
80      if(parser.checkHelpAndWarnUnparsed())
81      {
82          // -help not given
83          Aria::logOptions();
84          Aria::exit(1);
85      }
86    }
87
88    if (!Aria::parseArgs() || !parser.checkHelpAndWarnUnparsed())
89    {
90      Aria::logOptions();
91      Aria::exit(1);
92    }
93
94    ArLog::log(ArLog::Normal, "gotoActionExample: Connected to robot.")
       ;
95
96    robot.addRangeDevice(&sonar);
97    robot.runAsync(true);
98
99    // Make a key handler, so that escape will shut down the program
100   // cleanly
101   ArKeyHandler keyHandler;
102   Aria::setKeyHandler(&keyHandler);
103   robot.attachKeyHandler(&keyHandler);
104   printf("You may press escape to exit\n");
105
106
107   //Collision avoidance actions at higher priority
108   //ArActionLimiterForwards limiterAction("speed limiter near", 600,
       600, 100);
109   //ArActionLimiterForwards limiterFarAction("speed limiter far",
       600, 1100, 100);
110
111 //ArActionAvoidFront avoidFrontNearAct("Avoid Front Near", 225,
      100,10);  // OG
112 //ArActionAvoidFront avoidFrontFarAct;
       // OG
113 ArActionAvoidFront avoidFrontNearAct("avoid front obstacles", 450,
      200, 15,true);
114   //ArActionAvoidSide avoidSideAct("Avoid Side", 100, 50);;
         // OG
115
116   //ArActionConstantVelocity constantVelocityAct("Constant Velocity",
      400);  // OG
117   //ArActionLimiterTableSensor tableLimiterAction;
118   //robot.addAction(&tableLimiterAction, 95);
```

```
119   //robot.addAction(&limiterAction, 100);
120  // robot.addAction(&limiterFarAction, 90);
121
122   robot.addAction(&avoidFrontNearAct,80);
123   //robot.addAction(&avoidFrontFarAct,80);
124  // robot.addAction(&avoidSideAct,75);
125
126   // Goto action at lower priority
127   ArActionGoto gotoPoseAction("goto");
128   robot.addAction(&gotoPoseAction, 70);
129
130   // Stop action at lower priority, so the robot stops if it has no
       goal
131   ArActionStop stopAction("stop");
132   robot.addAction(&stopAction, 40);
133
134
135   // turn on the motors, turn off amigobot sounds
136   robot.enableMotors();
137   robot.comInt(ArCommands::SOUNDTOG, 0);
138
139   const int duration = 80000; //msec
140   ArLog::log(ArLog::Normal, "Going to two goals in turn for %d
       seconds, then cancelling goal and exiting.", duration/1000);
141
142   bool first = true;
143   int goalNum = 0;
144   ArTime start;
145
146   ofstream myfile;
147   myfile.open ("robotpath.txt");
148
149   start.setToNow();
150   while (Aria::getRunning())
151   {
152     robot.lock();
153     myfile << robot.getTh() << "\t"<<robot.getX()<<"\t"<<robot.getY()
       <<"\n";
154
155     // Choose a new goal if this is the first loop iteration, or if
       we
156     // achieved the previous goal.
157     if (first || gotoPoseAction.haveAchievedGoal())
158     {
159       myfile << robot.getTh() << "\t"<<robot.getX()<<"\t"<<robot.getY
       ()<<"\n";
160       first = false;
```

```
161       goalNum++;
162       if (goalNum > 2)
163     break;
164 
165       //goalNum = 1; // start again at goal #1
166       // set our positions for the different goals
167       if (goalNum == 1){
168         gotoPoseAction.setGoal(ArPose(3048,0,0));
169         myfile << robot.getTh() << "\t"<<robot.getX()<<"\t"<<robot.
    getY()<<"\n";}
170 
171       else if (goalNum == 2){
172         gotoPoseAction.setGoal(ArPose(0, 0, 0));
173         //pose.setTh(0);
174         ArLog::log(ArLog::Normal, "Going to next goal at %.0f %.0f
    %.0f",
175     gotoPoseAction.getGoal().getX(), gotoPoseAction.getGoal().getY(),
     gotoPoseAction.getGoal().getTh());
176         myfile << robot.getTh() << "\t"<<robot.getX()<<"\t"<<robot.
    getY()<<"\n";}
177 
178     }
179 
180     if(start.mSecSince() >= duration) {
181       ArLog::log(ArLog::Normal, "%d seconds have elapsed. Cancelling
    current goal, waiting 3 seconds, and exiting.", duration/1000);
182       gotoPoseAction.cancelGoal();
183 
184      // printf("theta_g: %10g getTh: %10g error1: %10g\n", u_x, u_y,
    error1);
185 
186       robot.unlock();
187 
188       ArUtil::sleep(3000);
189       break;
190     }
191 
192     robot.unlock();
193     ArUtil::sleep(3000);
194   }
195   myfile.close();
196   // Robot disconnected or time elapsed, shut down
197   Aria::exit(0);
198   return 0;
199 }
```